Patch to Landscape and Back Again: Three Case Studies of Land System Architecture Change and Environmental Consequences from the Local to Global Scale

by

Michelle Faye Stuhlmacher

A Dissertation Presented in Partial Fulfillment
of the Requirements for the Degree
Doctor of Philosophy

Approved April 2020 by the
Graduate Supervisory Committee:

Billie Lee Turner, II, Co-Chair
Matei Georgescu, Co-Chair
Amy Frazier
Yushim Kim

ARIZONA STATE UNIVERSITY

May 2020

ABSTRACT

Humans have modified land systems for centuries in pursuit of a wide range of social and ecological benefits. Recent decades have seen an increase in the magnitude and scale of land system modification (e.g., the Anthropocene) but also a growing recognition and interest in generating land systems that balance environmental and human well-being. This dissertation focused on three case studies operating at distinctive spatial scales in which broad socio-economic or political-institutional drivers affected land systems, with consequences for the environmental conditions of that system. Employing a land system architecture (LSA) framework and using landscape metrics to quantify landscape composition and configuration from satellite imagery, each case linked these drivers to changes in LSA and environmental outcomes.

The first paper of this dissertation found that divergent design intentions lead to unique trajectories for LSA, the urban heat island effect, and bird community at two urban riparian sites in the Phoenix metropolitan area. The second paper examined institutional shifts that occurred during Cuba's "special period in time of peace" and found that the resulting land tenure changes both modified and maintained the LSA of the country, changing cropland but preserving forest land. The third paper found that globalized forces may be contributing to the homogenizing urban form of large, populous cities in China, India, and the United States—especially for the ten largest cities in each country—with implications for surface urban heat island intensity. Expanding knowledge on social drivers of land system and environmental change provides insights on designing landscapes that optimize for a range of social and ecological trade-offs.

DEDICATION

I once heard it observed that the fight against climate change (and global environmental change more broadly) is not a fight to protect life on Earth because in all likelihood some form of life will persist. Instead, it is a fight to protect humankind on Earth. I dedicate this dissertation to my favorite humankind, my family.

ACKNOWLEDGMENTS

Writing a dissertation, while at points very solitary work, is an activity that cannot be undertake alone. I am indebted to many people for their support throughout the process, several of whom I would like to thank here. First, I am incredibly grateful to my committee members, Billie Lee Turner II, Matei Georgescu, Amy Frazier, and Yushim Kim for their constant support in advancing and improving my research. Dr. Turner taught me how to frame questions, engage with theory, and build a foundation for future research. He is an incredible advocate for all his students, something which I have grown to understand and appreciate more and more since the first semester of my first year when he came into the graduate student office space I was working in and told me that I needed to stop by his office more often. I thank Dr. Georgescu for the many doors he has opened for me to engage in interdisciplinary, multi-institutional research and his continual push to produce high quality research. I may have alarmed Dr. Frazier with my enthusiasm in adding her to my committee when she arrived at SGSUP in 2018. My enthusiasm has been justified many times over by her insightful perspectives on research, funding, and the academic job market. I thank Dr. Kim for her patience in teaching me about the fascinating world of public policy and helping me integrate it into my research when possible. I deeply appreciate our conversations on making sure that academic life is working for me, not the other way around.

Additionally, I thank the co-authors of my dissertation chapters—Ran Goldblatt, Riley Andrade, Nick Clinton, Sarthak Gupta, Yina Hu, Jessica Leffel, Bob Balling, and Wenwen Li–for the valuable contributions they have made to this and other research we have collaborated on. I am grateful for the interdisciplinary network of graduate students and faculty of Central Arizona Phoenix Long-Term Ecological Research (CAP LTER), Urban Resilience to Extremes Sustainability Research Network (UREx SRN), Graduates

in Integrative Society & Environment Research (GISER), the Urban Climate Research Center (UCRC), and the Environmental Justice and Policy Initiative (EJPI) who have enriched my time at ASU and broadened my disciplinary horizons.

I want to acknowledge the incredible support of my family and friends. Through many happy hours, pizza nights, hiking trips, bike rides, camping weekends, game nights, and bonfires—the community of graduate students at ASU have truly made Arizona feel like home. I thank (and apologize to) all my friends living in different parts of the country for my rambling phone conversation on the highs and lows of graduate school. I am grateful for the innumerable ways my family has supported me on my academic journey (still using the backpack you bought for my first day of kindergarten) and their wisdom and encouragement to pursue the work that aligns with my values. And last, I thank my fiancé for his intellectual and emotional contributions to my degree and tireless support of my career more broadly.

This work was made possible via support from the CAP LTER graduate student grant (NSF Grant DEB-1637590), the Lattie and Elva Coor Building Great Communities Graduate Fellowship, and the School of Sustainability's Global Intensive Experience Scholarship. I thank the Gilbert F. White Scholarship, the Emeritus Faculty Fellowship, and the ASU Graduate College Completion Fellowship for funding over the course of my graduate program. In addition, I am grateful for travel assistance from the National Science Foundation Sustainability Research Network (SRN) Cooperative Agreement 1444758 Urban Water Innovation Network (UWIN), several GPSA Travel Grants, and ASU Graduate College Travel Fellowships.

TABLE OF CONTENTS

Page

APPENDIX Page

LIST OF TABLES

Table Page

LIST OF FIGURES

Figure Page

CHAPTER 1

LAND SYSTEM COMPOSITION AND CONFIGURATION: AN INTRODUCTION

1.1.Introduction

Land is both a driver and consequence of global environmental change (Steffen et al. 2015; 2011). Land systems effect local to global processes such as the movement of biologically active nitrogen, habitat loss and fragmentation, greenhouse gas emission and absorption, and the hydrologic cycle (de Chazal and Rounsevell 2009; Lambin et al. 2001; Ruddiman 2013). To provide an example of the magnitude of land's influence—agriculture, forestry, and other land uses are the second largest emitter of greenhouse gases by economic sector (IPCC 2014). These lands accounts for 24% of total greenhouse gas emissions, while the largest emitter—electricity and heat production—accounts for 25% (IPCC 2014). Moreover, land's contributions become greater than electricity and heat production, if buildings are included in the definition of land (31%) (IPCC 2014).

Transformations and modifications made to just one aspect of land systems, such increasing the amount of urban agriculture in cities, can dramatically alter the amount of greenhouse gas emitted globally. If urban agriculture were added to cities around the world, energy consumption for heating and cooling is estimated to decrease by 13 to 15 billion kWh (Clinton et al. 2018). This is equivalent to the annual electricity used by air conditioners for approximately 9 million U.S. households (Clinton et al. 2018).

As demonstrated with this urban agriculture example, the composition and configuration of land systems are dominate factors in determining the influence of land. Composition is the amount of land and configuration is the spatial arrangement of land units. The composition and configuration of land systems has been linked to impacts on water quality (Alberti et al. 2007), carbon storage (Brinck et al. 2017), urban heat island (Connors, Galletti, and Chow 2013; Li et al. 2016), biodiversity (Dunning et al. 1995;

Hager et al. 2015), and the rates of plant and animal phonology change (Alberti et al. 2017). As such, human alterations to the composition and configuration of land systems profoundly affect the environmental benefits and burdens that land systems can provide (Osborne and Kovacic 1993).

Humans have intentionally (and unintentionally) altered land systems for centuries, but the current magnitude and scale are critical to the existence of the Anthropocene (Ruddiman 2013). With the recognition of the Anthropocene has come an interest in generating landscapes that optimize ecological and social trade-offs to balance environmental and human well-being (Nassauer and Opdam 2008; Turner et al. 2013). Part and parcel to this work is expanding knowledge on the implications of landscape composition and configuration on a variety of socio-environmental outcomes. Early work in this arena has considered the effects of landscape changes on one or two outcome variables (Connors, Galletti, and Chow 2013; Zhang, Murray, and Turner 2017; Zheng, Myint, and Fan 2014), but more work is needed on considering the impacts for multiple social and environmental benefits (Bennett, Peterson, and Gordon 2009; Lamy et al. 2016). Even as new insights are generated, this work will remain ongoing because land systems—as a coupled-human-environment system—are complex and dynamic, requiring continuous observation and adaptive management strategies (Holling 2001).

1.2 Research Background

This dissertation draws from land system science (LSS) (Verburg et al. 2013), and its recent subfield—land system architecture (LSA) (Turner et al. 2013). Within the frameworks of LSS and LSA, this research employed three case studies to examine the impact of broad social drivers on landscape composition and configuration with links to the environmental consequences of the resultant land system change. The composition and configuration of landscapes were measured via landscape metrics drawn from

disciplines such as ecology, spatial statistics, and mathematics (Frazier and Kedron 2017). Which metrics are suitable for use, and at what scale, was also a focus of this dissertation. Cross-case study conclusions about metrics will be drawn in the final chapter.

1.2.1 Land System Science

Land-use is the intersection of human activity and the environment. The mosaic of land uses and land cover (LULC) generates land systems, and land system science (LSS) is the examination of land systems with a particular emphasis on the socio-environmental drivers and consequences (Verburg et al. 2013). LSS joins together remote sensing, social science, and environmental sciences to capture coupled human-environment dynamics (Turner, Lambin, and Reenberg 2007). These considerations—especially in regards to the resulting sustainability, vulnerability, or resilience of a landscape—are often shared with sustainability science and similar fields (Meerow, Newell, and Stults 2016; Turner, Lambin, and Reenberg 2007).

Land systems are axiomatically social-ecological systems (SESs) and LSS treats LULC as a SES—an ontologically real phenomenon for which theory and models can be developed (Meyfroidt et al. 2018; Turner, Lambin, and Reenberg 2007). While the development of LSS theory has been slow, as it has for all SESs, major advances have been made in understanding land-use and land-cover dynamics (Aspinall and Staiano 2019; Gutman et al. 2004; Munroe and McSweeney 2019), the social and environmental underpinnings of these dynamics (Lambin et al. 2001; McSweeney et al. 2017), and modeling land systems (Filatova et al. 2013; Robinson et al. 2018; Veldkamp and Lambin 2001; Verburg et al. 2019).

1.2.2 Land System Architecture

LSA—an outgrowth from LSS—explores the role of the composition (relative size and total area) and configuration (shape, distribution, and connectivity) of land units in relation to the system's socio-environmental dynamics (Turner et al. 2013). LSA shares problems and approaches with work in landscape and urban ecology (Forman 1995; Wu 2013), urban morphology in urban climatology (Golany 1996), landscape architecture (Collinge 1996), and geodesign (Goodchild 2010; McHarg 1992). LSA seeks to quantify the impacts of land composition and configuration on the environment and livelihoods, ultimately, identifying tradeoffs or potential "win-win" solutions that enhance resilience (Turner et al. 2013). Most LSA research to date has been focused on urban sustainability—foremost extreme heat and associated issues (Li et al. 2011; Turner 2016; Zhou, Wang, and Cadenasso 2017)—with the aim of designing and implementing landscape (i.e., "cityscape") changes that improve urban sustainability (Childers et al. 2015; McPhearson et al. 2016).

1.2.3 Landscape Metrics

Landscape metrics are algorithms that quantify the spatial structure of land-cover patches in order to represent the biophysical structure and function of interacting land-cover patches (Forman and Godron 1986; Frazier 2019). For example, in some habitats, fragmentation can be detrimental to biodiversity and landscape metrics provide a means to quantify fragmentation (McGarigal and Marks 1995). With numerical quantification of fragmentation, assessments can be made about the impacts on diversity and assist in management decisions, such as aggregating land uses by maintaining undeveloped corridors through developed areas (Forman 1995).

A limitation to LSA research—and cognate fields—is the disparate and disjointed means of measuring landscape change. Metrics have been developed by a variety of

research communities to measure the configuration of landscape mosaics (e.g., landscape ecology), the spatial dimensions of phenomena (e.g., spatial science), to explore land systems (e.g., land system science), and design urban or regional configuration (e.g., geodesign). While there are overlaps in the goals and motivations of these research communities, each draws from different theoretical foundations to address different aspects of land dynamics, commonly focused on different spatial scales of analysis. When metrics developed by different communities are applied to the same question, however, they have been shown to result in different answers (Li et al. 2016; Zhou, Wang, and Cadenasso 2017; Zhou, Huang, and Cadenasso 2011).

This dissertation begins to address this limitation by employing landscape metrics from a variety of research communities to measure composition and configuration in each of the LSA case studies. Within the categories of composition and configuration, LSA is concerned with size, shape, connectivity, and distribution. Size is the relative extent or area of a particular LULC type. Shape is the form of an area of a particular LULC, connectivity the linking between areas of the same LULC type, and distribution is the spatial arrangement of areas of the same LULC. Table 1 presents the landscape metrics used for each case study.

Table 1. Names, definitions, and equations of the landscape metrics used for each chapter of the dissertation. Aspects of composition and configuration are in the left column with corresponding metrics in columns to the right.

	CHAPTER 2	**CHAPTER 3**	**CHAPTER 4**
SIZE (composition)	Percentage of Landscape Proportional abundance of each class type in the landscape. Calculated: $\frac{\sum_{j=i}^{n} a_{ij} \times 900}{Z}$	Patch Area Sum of all pixels in a given patch. Calculated in hectares: $a_{ij} \times 250$	Class Area Sum of the area of all pixels within the urban extent classified as built-up. Calculated in km²: $\sum_{j=i}^{n} a_{ij} \times 0.0009$

SHAPE (configuration)	Median Shape Index Median value of each patch in a given class' shape complexity as defined by: $\left(\frac{p_{ij}}{\min p_{ij}}\right)_{50\%}$	Fractal Dimension Index Measure of shape complexity computed with a patch's area and perimeter: $\frac{2 \times \ln(0.25(p_{ij} \times 500))}{\ln(a_{ij} \times 250{,}000)}$	Edge Density Measure of edge complexity by computing the ratio of the length of edge to the total area: $\frac{\sum_{k=1}^{m} e_{ik}}{A}$ (10000) Reock Score Ratio of class area to its minimum bounding circle: $\frac{A}{C}$
CONNECTIVITY (configuration)	Median Euclidean Nearest-Neighbor Index Median value of the distance each patch to the nearest patch of the same class. Equation is represented as: $h_{ij_{50\%}}$	Contiguity Index Assess spatial connectedness of pixels in the same patch: $\frac{\left[\frac{\sum_{r=1}^{z} c_{ijr}}{a_{ij}}\right] - 1}{v - 1}$	Patch Cohesion Index Measure of connectedness defined by the area and perimeter of groups of connected built-up pixels: $\left[1 - \frac{\sum_{j=1}^{n} p_{ij}}{\sum_{j=1}^{n} p_{ij}\sqrt{a}_{ij}}\right] \times \left[1 - \frac{1}{\sqrt{Z}}\right]^{-1} \times 100$
DISTRIBUTION (configuration)	Interspersion and Juxtaposition Index Ratio of observed interspersion over maximum possible interspersion: $\frac{-\sum_{k=1}^{m}\left[\left(\frac{e_{ik}}{\sum_{k=1}^{m} e_{ik}}\right)\ln\left(\frac{e_{ik}}{\sum_{k=1}^{m} e_{ik}}\right)\right]}{\ln(m-1)} \times 100$	Euclidean Nearest Neighbor Index Distance of each patch to the nearest patch of the same class. Equation represented as: h_{ij}	Percentage of Like Adjacencies Calculates the number of built-up pixels that are adjacent to built-up pixels divided by the total number of pixel adjacencies: $\left(\frac{g_{ii}}{\sum_{k=1}^{m} g_{ik}}\right)(100)$

WHERE:
$a_{ij} = area\ in\ terms\ of\ number\ of\ cells,$
$A =\ total\ class/landscape\ area\ (m^2),$
$e_{ik} = total\ length\ (m)\ of\ edge\ involving\ class\ i\ and\ k,$
$p_{ij} = perimeter\ of\ patch\ ij\ in\ terms\ of\ number\ of\ cell\ surfaces,$
$Z = total\ number\ of\ cells\ in\ the\ landscape,$
$g_{ii} = number\ of\ like\ adjacencies\ between\ pixels\ of\ class\ i,$
$g_{ik} = number\ of\ like\ adjacencies\ between\ pixels\ of\ classes\ i\ \&\ k,$
$c_{ijr} = contiguity\ value\ for\ pixel\ r\ in\ patch\ ij,$
$v = size\ of\ filter\ matrix,$
$h_{ij} = distance\ to\ the\ nearest\ neighboring\ patch\ of\ the\ same\ class\ i\ (m),$
$m = number\ of\ classes\ present\ in\ the\ landscape,$
$C = area\ of\ class'\ minimum\ bounding\ circle$

These metrics were selected from a larger set of metrics based on their relevance to the research question and data of each case study. Chapter 5.2 presents this table again and reviews each metric and the reason it was selected.

1.3. Dissertation Organization

The component works of this dissertation advance understanding on how broad social, political, and economic drivers shape LSA and the resultant environmental consequences at a variety of scales. Scale is defined as the extent in space, the unit of analysis (i.e., patch, class, landscape), and grain size—consistent with Wu and Qi (2000). Patches are groupings of pixels of the same or similar LULC type that are different from their surroundings. This is the smallest unit of analysis for most landscape metrics (McGarigal, Cushman, and Ene 2012). Classes are all patches of the same LULC type in a land system, and a landscape is the bounding unit for a mosaic of different LULC types (Frazier 2019; McGarigal, Cushman, and Ene 2012).

Each chapter is a case study which engages the causes and consequences of LSA change at differing scales (Table 2). The chapter are each a published or to be submitted research paper.[1]

Table 2. Location and spatial scale of analysis for each dissertation chapter. Scale is defined in terms of extent, the land unit used for analysis, and the grain (i.e., pixel size) of the LULC data.

CHAPTER	LOCATION	SCALE		
		Extent	Land Unit	Grain
Chapter 2	Phoenix Metropolitan Area, Arizona, United States	Local	Class	30 m
Chapter 3	Republic of Cuba	National	Patch	500 m
Chapter 4	India, China, & United States	Multi-national	Class	30 m

Chapter 2 examined different development trajectories of two urban riparian areas in the Phoenix metropolitan area, their resulting LSA, and consequences for bird biota, vegetation, and the urban heat island effect. It was previously published in Land Use Policy (Stuhlmacher et al. 2020). Chapter 3 related LSA and environmental changes to the broad institutional shifts and policy changes made in Cuba during the "special period in time of peace", the period after the 1991 collapse the Soviet Union (a major trade partner of the country). Chapter 4 tested for homogeneity in urbanization across global cities in China, India, and the United States and examined the surface urban heat island impacts of this urban pattern change.

[1] The dissertation author is the lead author on the three papers, but all are co-authored works. For this reason, references to the case studies throughout the dissertation may use "we" as opposed to "I". Permission for the use of co-authored work was granted from all co-authors, see Appendix A.

1.3.1 Urban Development: Rio Salado and New River

The first case study was at the local level and used class as the unit of analysis (Table 2). In the Phoenix, Arizona (USA) metropolitan area, efforts to better utilize the Rio Salado riverfront began fifty years ago (Elmore 1995), with substantial attention to design and planning but minimal action along the 200-mile riverfront. The exception is the city of Tempe's channelization of a portion of the Rio Salado to the north of its downtown, known as Tempe Town Lake (Elmore 1995). Subsequent development around the lake included Tempe Beach Park, a riverfront trail, and mixed-use development (Elmore 1995). Inspired by the vibrancy Tempe Town Lake's development has brought to Arizona's central valley, the late Senator John McCain made the redevelopment of the Rio Salado riverbed—stretching from Buckeye to Mesa—his legacy project. With considerations for the next redevelopment that may be underway, we evaluated how the LSA of the riverfront area in Tempe changed from 1985 to 2010 in comparison to a similar riparian site (New River) that underwent the more typical developer-lead development over the same period. Specifically, we evaluated:

1. Given the different design intentions of the Rio Salado and New River sites, how does their LSA differ?
2. How does the land surface temperature and vegetation abundance differ between the sites? Which LSA modifications—size, shape, distribution, or connectivity—have the greatest impact on land surface temperature and vegetation?
3. How do the bird communities differ between the two sites? What role does LSA play in the bird community differences between the sites?

1.3.2 Institutional Shifts: Cuba

The second case study is at the national level, with patch as the unit of analysis (Table 2). This research examined the LSA changes in the Republic of Cuba triggered by

the collapse of the Soviet Union and Cuba's subsequent institutional changes. The Republic of Cuba's rapid institutional transition make it a unique testbed for advancing research on the influence of institutional change on LSA change. After the collapse of the Soviet Union in 1991, the country began what the government termed the "special period in time of peace" (Maal-Bared 2006). Profound changes followed, including privatization of land, an opening of the agriculture commodity market, as well as several initiatives to diversify and turn production inward (Wright 2009). Employing a quasi-experimental design approach (Shadish, Cook, and Campbell 2002), we asked:

1. How did the composition and configuration (land system architecture) of Cuba's land system change as a result of the institutional shifts caused by the collapse of the Soviet Union?
2. How are the land system architecture and environmental outcomes temporally linked to the policy changes in the "special period"?

1.3.3 Homogenization of Urban Form: China, India and the United States

The third case study was at the multi-national level with class as the unit of analysis (Table 2). The class of interest is built-up lands in China, India, and the United States. Built-up land (i.e., urban areas) now house over 50% of the worlds' population and the way in which they are growing (i.e., form or morphology) influences a variety of socio-ecological processes (Alberti 2005; Bettencourt et al. 2007; Forman 2014; Georgescu et al. 2013; Seto et al. 2012; Turner et al. 2013; United Nations 2018a). The high spatial and temporal resolution classifications needed to study these processes, however, are few in number (Goldblatt et al. 2018). Employing Landsat and nighttime light satellite imagery from 1995-2015, we classified urbanization in five-year time-steps using machine learning and transfer learning methods. There is some evidence that the urban form of global cities is homogenizing (Jenerette and Potere 2010; Seto and

Fragkias 2005) and potential homogenization could have important consequences for global environmental change and how cities respond. With this time-series dataset we evaluated:

1. Are large cities around the world homogenizing in terms of the configuration of their built-up land footprint?
2. How do the rates of growth in terms of size, shape, distribution, and connectivity influence the potential homogenization?
3. How does homogenization, if detected, affect the surface urban heat island?

1.4 Dissertation Contributions

This dissertation's three main contributions are: 1) expanded applications of the LSA approach, 2) results with implications for landscape design for each case study, and 3) insights from the cross-case synthesis on the selection and use of landscape metrics in LSA research. Each of these contributions will be discussed in greater detail in the concluding chapter (5.4).

CHAPTER 2

ENVIRONMENTAL OUTCOMES OF URBAN LAND SYSTEM CHANGE: COMPARING RIPARIAN DESIGN APPROACHES IN THE PHOENIX METROPOLITAN AREA

2.1 Abstract

In the face of climate change and other environmental challenges, an increasing number of cities are turning to land design to enhance urban sustainability. Land system architecture (LSA)—which examines the role of size, shape, distribution, and connectivity of land units in relation to the system's social-environmental dynamics—can be a useful perspective for examining how land contributes to the social and environmental aspects of urban sustainability. There are two gaps, however, that prevent LSA from fully contributing to urban sustainability dialogues. First, it is not well understood how urban design goals, as expressed by urban planners and other practitioners, relate to LSA and environmental outcomes. Second, most LSA work focuses on individual environmental outcomes, such as the urban heat island effect, instead of considering the broader suite of outcomes that LSA changes impact. Here, we undertake an integrated assessment of LSA impacts on surface urban heat island (based on land surface temperature), vegetation presence/health (based on NDVI), and bird biota at two riparian sites with different design intentions in the Phoenix, Arizona metropolitan area. The Rio Salado in Tempe underwent a city-led, infill redevelopment that mixed economic, recreational, and flood control design goals. The New River in Peoria experienced a more typical developer-driven urbanization. The contexts and design goals of the sites generated differences in their LSA, but only a few of these differences were sufficiently unique to contribute to divergent environmental outcomes. These differences reside in (1) the greater distribution of recreational land-covers and (2) increased surface water at the Rio Salado site compared to the New River site. Both

changes are linked to land-cover patches becoming greener and cooler as well as a greater presence of waterbird and warbler species at the Rio Salado site. The distinctions between the sites provide insight for crafting design goals for redeveloping or restoring urban riparian landscapes in the Phoenix metropolitan area grounded in LSA. With the incorporation of additional relevant variables, especially socioeconomic ones, the research approach employed in this study provides a foundation for the assessment of other urban land system change.

2.2 Introduction

Urban areas cover approximately one percent of the world's land surface, house over half of the world's population, and consume seventy-five percent of the world's resources (Harrison and Pearce 2000; Z. Liu et al. 2014; United Nations 2018b). Their continued growth raises concerns about urban sustainability (Childers et al. 2014; Grimm et al. 2008; Seto et al. 2012; Wu 2014) and the ways in which cities can adapt to and mitigate for the range of consequences from global environmental change, foremost climate change (Chhetri, Stuhlmacher, and Ishtiaque 2019; Martin and McTarnaghan 2018; Rosenzweig and Solecki 2015). Urban land design—intentional modifications to the size and pattern of a cityscape—affects the structure and function of the environment (henceforth environmental outcomes) and is one means to mitigate and adapt to local and global environmental changes (Grimm et al. 2015; Turner et al. 2013).

As such, urban land design is increasingly of interest to research fields such as urban climatology (Golany 1996), landscape architecture (Collinge 1996), landscape ecology (Forman 1995; Wu 2013), geodesign (Goodchild 2010; McHarg 1992), and land system science. Each of these research fields approach design and urban sustainability with different queries, theories, and methods, but all are concerned with how design

impacts the urban environment (Leemans and Groot 2003; Roy Chowdhury and Turner 2019). Each fields' incorporation of urban land design is briefly reviewed below.

Urban climatology examines the effects of the morphology of built structures and vegetation to better understand how the design of urban areas impact microscale and mesoscale climate (Oke 1988). Urban climate research also integrates findings, such as those on air quality and the urban heat island, with the planning and design process (e.g. Coseo and Larsen, 2015; Oke, 1984; Stewart and Oke, 2012).

Landscape architecture has long examined urban design in terms of the cultural landscape, with recent attention on sustainability and design linkages to urban ecosystems (Collinge 1996; Wines 2000). Landscape ecology, in turn, has traditionally examined the impacts of landscape mosaics, or the composition and configuration of land units (i.e., patches), on ecosystem structure and function (Dramstad, Olson, and Forman 1996). These two fields have found synergies over the past several decades (Forman 2008; Wu 2019), with planned and designed landscapes providing field experiments to test landscape ecology hypotheses (Golley and Bellot 1991). Nassauer and Opdam (2008) further solidified design as a central component of landscape ecology in their pattern-process-design framework. Urban ecology has followed suit (Grimm et al. 2008) by assessing the role of urban landscape mosaics on environmental outcomes (Cadenasso et al. 2013; Forman 2014; S. T. Pickett and Cadenasso 2008). Landscape architecture, landscape ecology, and urban ecology now call for transdisciplinary inclusion of design in research and practice (Ahern 2013; Cadenasso and Pickett 2013; Childers et al. 2015; Dramstad, Olson, and Forman 1996; Nassauer 2012; Nassauer and Opdam 2008; Pickett, Cadenasso, and Grove 2004; Steiner 2014).

Sharing this focus, but largely associated with spatial science, the emerging field of geodesign provides a platform for linking various landscape and land system

approaches to sustainability (Huang et al. 2019; Wu 2019). Geodesign emphasizes inclusive and iterative design in a framework that incorporates spatial technologies (i.e., models and simulations) with real-time stakeholder feedback (Steinitz 2012).

Lastly, land system architecture (LSA) is an outgrowth from land system science (LSS) and its interest in sustainability, vulnerability, and resilience (Verburg et al. 2013). LSA examines the composition (size/area of a land cover type) and configuration (shape, distribution, connectivity of a land-cover type) of built landscapes as a result of formal and informal design—typically with a lens on its social-environmental consequences (Turner 2010; Turner et al. 2013). LSA has many synergies with landscape ecology (Frazier et al. 2019; Vadjunec et al. 2018) and, in some cases, LSA and landscape ecology are indistinguishable in methods (Huang and Cadenasso 2016; Li et al. 2011). Additionally, sharing concerns with morphology in urban climate research, recent LSA research has incorporated the vertical dimension of land-covers (e.g. building or tree height) (Zhang, Middel, and Turner 2019). We designate LSA as the variety of work across several fields of research loosely affiliated with land system science, especially urban land systems.

Emergent LSA research has largely focused on the built environment's effect on land surface temperature (LST) at a fine-grain level: cases in which 1-30 m resolution remote sensing data can be matched to the composition of land units. The composition of urban land units have been found to be the dominant driver of LST, but configuration has also proven to be significant, and joined with composition, increases the explained variance of LST (Li et al. 2016; Li et al. 2012; Zhou, Wang, and Cadenasso 2017; Zhou, Huang, and Cadenasso 2011).

Less is known about how urban design and configuration impact environmental outcomes beyond LST, such as flora and fauna abundance and diversity. Additionally,

there is increasing interest in evaluating how composition and configuration affect multiple ecosystem services (e.g. Bennett et al., 2009; Lamy et al., 2016) especially using remotely sensed data (Clinton et al. 2018; Wang et al. 2018). Few assessments, however, have addressed the LSA of formally designed landscapes and their multiple environmental impacts in an urban context or undertaken a comparison of these impacts between developments with different design intentions (but see Turner and Galletti, 2015). Our study seeks to fill these gaps through a comparison of two urban riparian corridors that were constructed with different design intentions in the Phoenix, Arizona metropolitan area. The first landscape consists of a riverfront area in the City of Tempe that was designed to enhance community use and economic development near the historic city center. The second landscape consists of a more common, developer-led design of commercial and residential expansion in Peoria. Both sites are similar in terms of geography, environment, and climate; and they differ primarily in the role design played in their development. The overarching query of this research concerns the urban LSA and environmental outcomes generated by the design distinctions.

These concerns are addressed through three questions:

1. Given the different design intentions of the two sites, how does their LSA differ?
2. How does the land surface temperature and vegetation abundance differ between the sites? Which LSA modifications—size, shape, distribution, or connectivity—have the greatest impact on land surface temperature and vegetation?
3. How do the bird communities differ between the two sites? What role does LSA play in the bird community differences between the sites?

2.3 Case Study

The Phoenix metropolis is situated in the arid Sonoran Desert and is characterized by a sprawling, low-density urban form. Municipal economic growth has

long been driven by annexing surrounding unincorporated land (Gerszewski et al. 2014). More recently, however, older municipalities in the center of the metropolitan area have become "land-locked" (i.e., minimal or no new land to incorporate), and their focus has turned to infill development to increase the density of economic and recreational opportunities (Gerszewski et al. 2014). In contrast, newer cities on the metropolitan fringe have the capacity to convert agricultural and vacant land for urban development. The two study sites—Rio Salado in Tempe and New River in Peoria—capture these divergent approaches to urbanization within the "land-locked" city of Tempe and along the urban fringe in the city of Peoria.

2.3.1 Rio Salado: Tempe, AZ

Tempe, Arizona is located approximately 14 km southeast of downtown Phoenix, has a population of over 185,000 permanent residents, and is home to the main campus of Arizona State University (ASU). Incorporated in 1894, Tempe is one of the older municipalities in the region. The Rio Salado (Salt River) flows immediately north of Tempe's downtown and the ASU campus (Fig. 1). A series of upstream reservoirs has rendered the riverbed dry for most of its extent through the metro-area; water only flows during heavy rains and when reservoirs release water.

Historically, the majority of the Rio Salado riverfront has been underdeveloped for community use, commonly serving as a site for dumping, quarrying, or industrial activities. In the 1982 Rio Salado Plan, the city of Tempe enumerated several overarching goals to develop the Rio Salado riverfront relevant to design: (1) "Encourage the optimum development of land along the Salt River"; (2) "Promote the development of outdoor recreational facilities"; and (3) "Combine the flood control with environmental design in a manner that will achieve the greatest social and economic benefits for the citizens of Tempe" (City of Tempe, 1982: 11-13). Guiding these design goals was an

interest in transforming the Rio Salado from an eyesore to an economically viable and signature urban environment and, in doing so, investing in Tempe's downtown.

In the 1990s, the city of Tempe channelized the portion of the Rio Salado within the city limits to create Tempe Town Lake and established Tempe Beach Park along the new waterfront (Elmore 1995). The river and the riverfront park are now used for multiple social and cultural events, such as concerts, festivals, major races and triathlon competitions. Within the park are multi-use paths that stretch along the riverfront into neighboring municipalities. Significant development, foremost high-rise commercial office buildings and apartment-condo units, continue to be built around the lake today in concert with the development of ASU, which possesses a large portion of the river's south bank.

2.3.2 New River: Peoria, AZ

Peoria, Arizona is located approximately 22 km northwest of downtown Phoenix. It is situated on the western most edge of Maricopa county (the county in which much of the Phoenix metropolitan area resides) with a small portion of the city boundaries extending west into Yavapai county. Peoria was incorporated in 1954 and has a current population of over 168,000 people. The city has seen rapid population growth since the 1990s and is expected to continue growing faster than both the Phoenix area and the state averages (City of Peoria 2014). The New River crosses the southeastern portion of Peoria and is an intermittent stream that flows only during heavy rains. Just outside of Peoria's boundaries it joins the Aqua Fria River (also intermittent), which enters the Gila River just west of the Rio Salado-Gila connection on the southwest side of the Phoenix metropolitan area (Fig. 1).

The New River development in Peoria, led by commercial developers, constitutes a common, contemporary use of riparian space. The aim was to expand the commercial

and housing areas of Peoria, while protecting this development from intermittent flood events. The area directly around the riverbed (60-150 m on either side) remains largely undeveloped (i.e., desert soil and native vegetation) or contains green infrastructure resistant to flood impacts. A paved pedestrian and biking trail run along the banks of the dry riverbed. At the north end of the study area is Rio Vista Community Park. At 54 acres it is the third largest park in Peoria (City of Peoria 2014). It has recreational fields, picnic areas, a playground, and a community recreation building (City of Peoria 2014).

2.4 Methods

2.4.1 Site Selection

The portion of the Rio Salado riverfront examined in this study constitutes an area 1.5 km on either side of the former perineal river and extends 7 km east-west across northern Tempe (Fig. 1). The 1.5 km buffer to the north and south of the river includes a previously established bird survey site—part of the Central Arizona-Phoenix Long-Term Ecological Research (CAP LTER) network (Bateman et al. 2017)—and was delineated to capture both the built and unbuilt parts of the region. The eastern and western bounds of the study area are demarcated by the limits of the city of Tempe, as only land within the jurisdiction of the city of Tempe's development project is included in the analysis. The boundary of the New River study area is 3 km wide and 6.5 km in length to match the approximate dimensions and area of the Rio Salado site. Within the 1.5 km buffer from the New River's banks is a second CAP LTER bird site as well as both built and unbuilt lands.

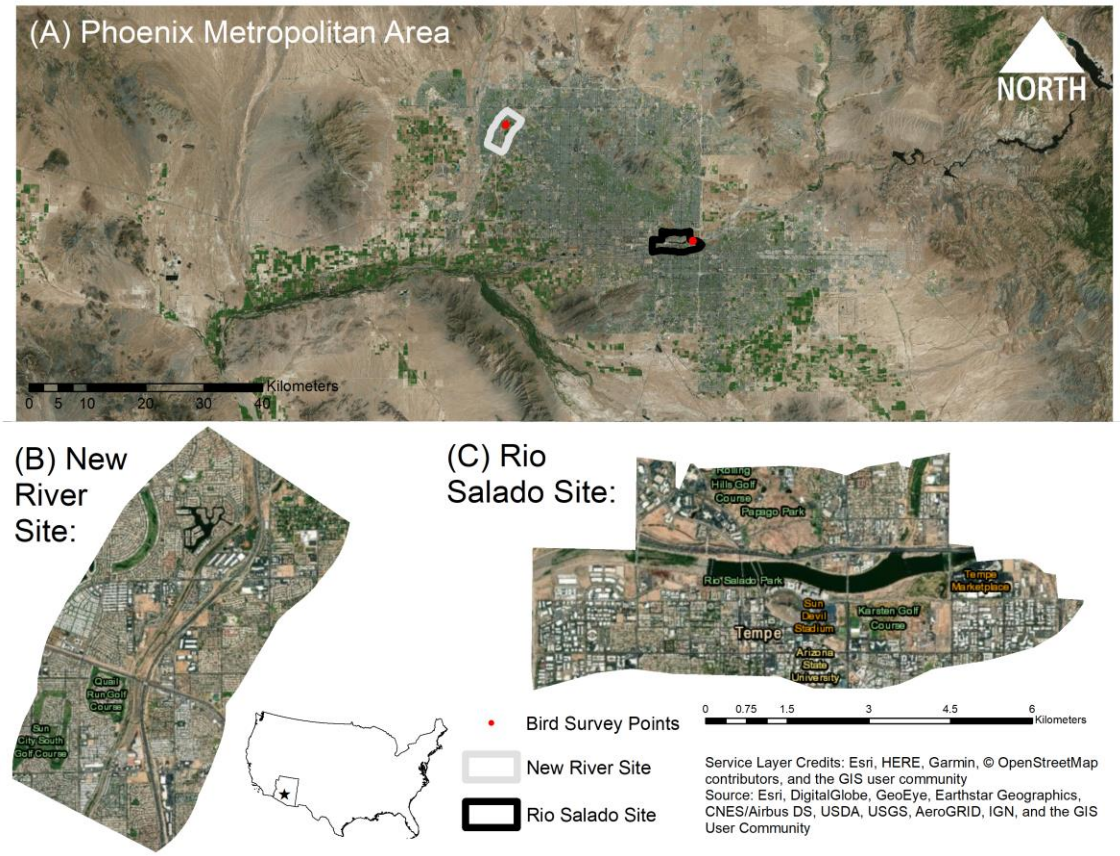

Figure 1. (A) Study sites and location of bird surveys in the Phoenix Metropolitan area, Arizona, USA. 2019 land cover from high resolution imagery at (B) New River and (C) Rio Salado sites.

2.4.2 Base Data and Variables.

Three principal data sources were employed to generate the variables in this study: Landsat 5 satellite images, land use/land cover (LULC) classifications, and bird community surveys from CAP LTER (Fig. 2).

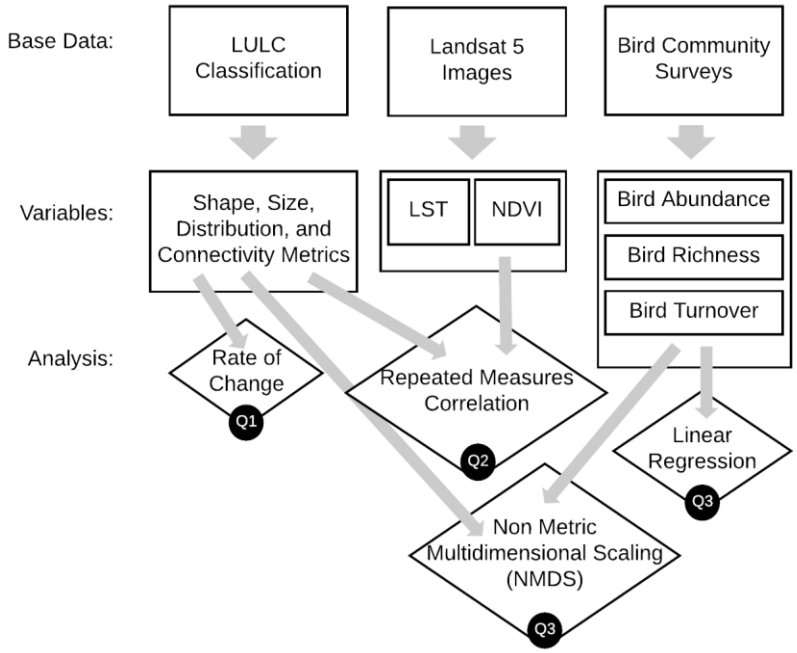

Figure 2. Methodological workflow. Input data are represented in boxes along the top row, intermediate data processing in boxes in the middle row, and analysis in the diamonds along the bottom. Black circles at the bottom of the diamonds denotes the corresponding research question.

2.4.2.1 Land Use/Land Cover (LULC) Classification and Landscape Metrics

The land-cover data used to quantify LSA change are based on 30 m classifications of Landsat TM 5 imagery (Zhang and Li 2017). Every five-year increment from 1985 to 2010 was classified using change vector analysis from the supervised object-based classification of the 2010 image (see Zhang and Li, 2017 for full details), resulting in six sets of land cover classifications (n=6). The overall accuracy of the classification is 92.1%. The original eleven classes have been aggregated to five—water, built-up, crop, vegetation, and desert/bare soil.

Landscape metrics were calculated for each of the five land cover classes. Landscape metrics are algorithms that quantify the spatial structure of land-cover patterns—primarily composition and configuration—within a geographic area (Frazier 2019). Landscape metrics typically rely on land units, referred to hereafter as patches, as

the fundamental building blocks for computation. Patches represent relatively homogenous areas of land-cover that differ from their surroundings (McGarigal, Cushman, and Ene 2012). We use patches as our unit of assessment (as opposed to larger parcel boundaries) because in urban areas, patches tend to be small and heterogeneous within parcel boundaries.

A suite of landscape metrics was selected to quantify land-cover composition and configuration based on correspondence with the four components of LSA: size, shape, distribution and connectivity (Turner et al., 2013). Size is the relative extent of an area of a particular land cover. Shape is the form of an area of a particular land cover (i.e., elliptical, rectilinear) and also considers the complexity of the land cover's boundaries (Connors et al., 2013). Distribution is the spatial arrangement (adjacency) of land-cover types, such as random, aggregated, or uniform (Gustafson, 1998). Connectivity is the linking, or lack thereof, between land covers of similar ecological or social significance (Schumaker, 1996).

Four class-level landscape metrics were computed in the software program FRAGSTATS (McGarigal et al., 2012) to capture each of the four components of LSA. Percentage of Landscape (PLAND) quantifies the proportional abundance of each patch type in the landscape and represents the area or size of each land-cover class (e.g., built-up, vegetation). The median Shape Index (SHAPE_MD) is used to quantify shape. This index measures shape compactness where a value of one constitutes a square patch and higher values represent increasing complexity in shape. SHAPE_MD is calculated by taking the median of all patch-level Shape Index values for a given class (i.e., the median of the Shape Index for all vegetation patches). The Interspersion and Juxtaposition Index (IJI) is used to measure distribution. Higher values mean a proportionate distribution of patch type adjacencies (i.e., equal adjacency); a value of zero means a

patch type is poorly interspersed. Lastly, the median Euclidean Nearest-Neighbor (ENN_MD) is used to measure connectivity. It is calculated by measuring the straight-line distance between the center of a patch and the nearest neighboring land unit of the same class. Since the study sites are small, we are using this distance between patches as a proxy for connectivity. Like the Shape Index, ENN_MD is a class-level metric that is computed by taking the median value of all patches in a land-cover class. Increasing values constitute increasingly dispersed patterns of patches of the same class. These four metrics were chosen for their direct relationships to the components of configuration, their intuitiveness and ease of interpretation for non-experts, as well as their use in previous scholarship linking environmental outcomes to land system composition and configuration (Connors, Galletti, and Chow 2013; Li et al. 2012) and measuring landscape change over time (Smiraglia et al. 2015). To calculate the metrics, the land-cover maps for each year were cropped to the study area with a 30 m (1 pixel) exterior buffer added to decrease edge effects (McGarigal and Marks, 1995).

2.4.2.2 Land Surface Temperature (LST) and Normalized Difference Vegetation Index (NDVI).

The average LST and the Normalized Difference Vegetation Index (NDVI)—an indicator of vegetation vigor—were calculated using the same cloud-less, summer time Landsat 5 Tier 1 Surface Reflectance imagery as the LULC classification. LST is regularly used to capture facets of urban climate and studies of urban landscapes (Li et al. 2016; Myint et al. 2015; Zhang, Murray, and Turner 2017). NDVI is used in a range of studies to measure the rudimentary character of vegetation (Fan and Myint 2014; Qin et al. 2017), and here NDVI is used to signify the density and quality (greenness) of vegetation cover. LST was emissivity corrected using NDVI (Shen et al. 2016). To control for daily and monthly variations in temperature, relative class-level NDVI and LST values are

used (i.e., water is 5° C cooler than the study area average). Relative values were computed by taking the difference between the average class value and the average value for the entire study area on a given day. The relative NDVI value for a given class is the difference between the average NDVI of the study area and the average NDVI for all patches in a given class. The relative LST value for a given class is the difference between average LST of the study area and the average LST for all patches in a given class.

2.4.2.3 Bird Community Surveys.

The bird survey data at the Rio Salado and New River sites (Fig. 1) contains observations of birds seen or heard for a 40-m fixed radius (fixed-radius point count) at a 15 minute interval (Bateman et al., 2017). Surveys were completed within four hours of sunrise twice annually, once during the winter (December-February) and once during the spring (March-May). One bird survey site is located near the Rio Salado and one at the New River site (Fig. 1). Observations began in 2001 and are ongoing; we used the publicly available data for 2001-2015 for our analysis (n = 14). Community-level metrics, including annual bird abundance, richness, and turnover were calculated for each of the survey sites (Banville et al., 2017). Annual abundance is calculated as the greatest number of individuals of each species observed at the site during the survey year. Annual species richness is the number of unique species found at the site during the survey period. Turnover is the percentage of species in the community that were lost or gained compared to the previous survey. Community metrics were organized and calculated using the tidyverse package in R (Wickham 2017).

2.4.3 Analyses

Research question one was examined descriptively because of the small number of years for which there is LULC data (n = 6). The slopes (i.e., rate of change) of the landscape metrics for size, shape, distribution and connectivity were calculated and

compared between sites across the six years of data. Both magnitude and direction of change were examined.

To answer research question two, repeated measures correlations were used to determine the relationship between the class-level landscape metrics and the class-level NDVI and LST values (rmcorr package, Bakdash and Marusich, 2017). Repeated measures correlations are preferred over a simple regression or correlation because the yearly landscape metrics and environmental outcome variables are non-independent observations (Bakdash and Marusich 2017). For the repeated measures correlation, the association of one landscape metric with one environmental outcome is calculated with each year of data acting as the repeated measure.

For research question three, a general linear regression was used to determine how the bird community changed over time and between sites for abundance (n = 14), richness (n = 14) and turnover (n = 13), followed by an ordination of sites in species space to compare the community composition between sites and years. Abundance, richness, and turnover are the dependent variables while time and sites are the independent variables. We tested for normalcy using a Q-Q plot as well as plotted residuals and did not note heteroscedasticity. Given the small number of samples, we determined that a linear regression was appropriate to test the general trend over time.

Temporal and spatial differences in bird community composition were tested using nonmetric multidimensional scaling (NMDS) with a square-root transformation fitted to two dimensions (vegan package, Oksanen et al., 2018). NMDS is a visualization of sites in species space by maximizing the rank correlation between the distance matrix; for our analysis we used Bray-Curtis distance and the plotted distances (Clarke 1993). Rare species—those observed in less than 10 percent of the total surveys—were removed from analysis (McCune and Grace 2002). Dispersion ellipses were calculated based on

the standard deviation of weighted averages for the three LSA survey periods (Time Period 1: 2001-2004, Time Period 2: 2005-2009, and Time Period 3: 2010-2015) and the two sites (Rio Salado and New River). We then fit the landscape metrics onto the bird community ordination to calculate the correlation and significance of each metric with the bird community. All code and documentation for the analysis is available in a GitHub repository: https://github.com/MStuhlmacher/phx-lsa.

2.5 Results

2.5.1 Question 1: Change in Land System Architecture

Research question one examines the changes in composition and configuration of land-cover patches at the sites and their resultant land covers. Despite different locations in the Phoenix metropolitan area (i.e., center vs. fringe), both sites started with a similar level of built-up land (Fig. 3, 4). By 2010, the New River site has 18% more built-up area.

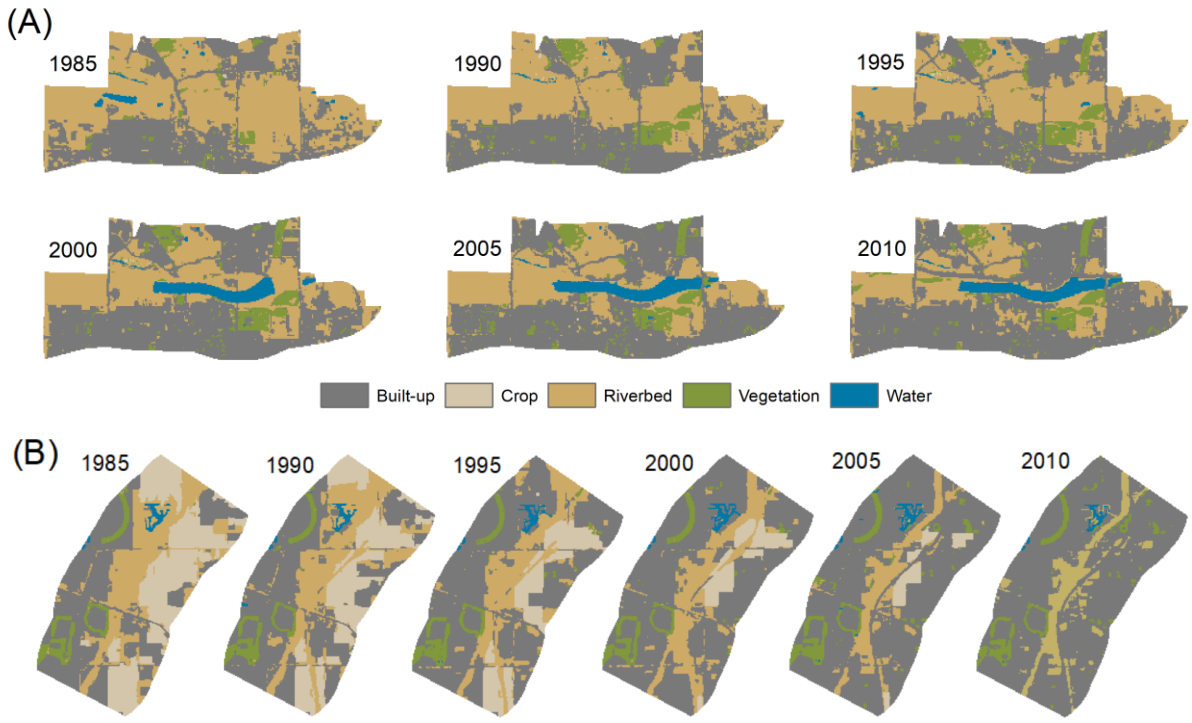

Figure 3. Land use/land cover maps for the (A) Rio Salado and (B) New River sites.

Cropland at the New River site was almost entirely urbanized and, at both sites, desert land also made up a large portion of what was eventually urbanized. A greater proportion of desert land was developed at the Rio Salado site, but approximately 26% of it was maintained, largely in desert parklands adjacent to the river (Fig. 3, 4). The amount of vegetated land cover increased at both sites, but the Rio Salado gained more in terms of both vegetation and water.

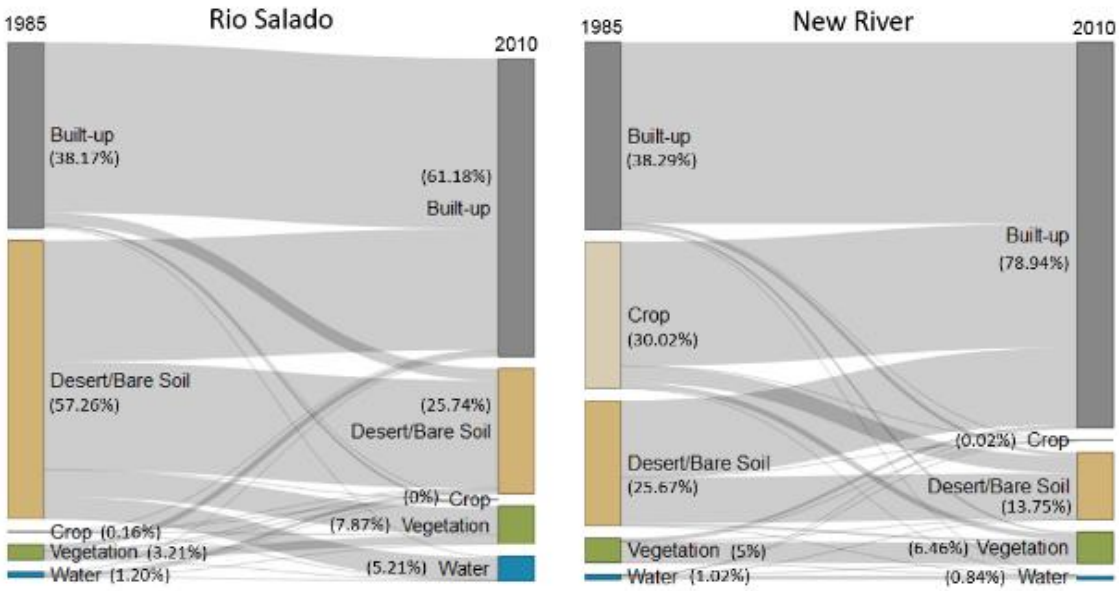

Figure 4. Land-cover class conversion between 1985 and 2010 at the Rio Salado and New River sites. Values in parenthesis are the percentage of land a given class covers in the study area.

The shape of the land covers at the Rio Salado site underwent little change and largely remained compact, with a notable exception of the addition of water in the elongated lake (Table 1). In contrast, the land-cover classes at the New River site were less compact to start and became marginally more compact as development consolidated patches of different land-cover types. Shape compactness for the crop class increases at both sites, likely a function of the decreasing amount of cropland and the consolidation of the few remaining crop patches (Fig. 3).

Table 1. Change in size, shape, distribution, and connectivity at the Rio Salado and New River sites by land-cover class. Values in parenthesis are the rate of change (slope) of the landscape metrics between 1985 and 2010.

		Built-up	Desert/ Bare Soil	Crop	Vegetation	Water
Size (PLAND)	Rio Salado	Increasing (0.805)	Decreasing (-1.182)	Decreasing (-0.005)	Increasing (0.152)	Increasing (0.230)
	New River	Increasing (1.704)	Decreasing (-0.567)	Decreasing (-1.213)	Increasing (0.077)	No Change (0)
Shape (SHAPE_MD)	Rio Salado	No Change (0)	No Change (0)	More Compact (-0.008)	No Change (0)	Less Compact (0.013)
	New River	More Compact (-0.012)	More Compact (-0.004)	More Compact (-0.005)	More Compact (-0.004)	More Compact (-0.001)
Distribution (IJI)	Rio Salado	More Interspersed (0.892)	More Interspersed (0.296)	Less Interspersed (-2.085)	More Interspersed (0.054)	More Interspersed (1.581)
	New River	Less Interspersed (-0.385)	Less Interspersed (-2.049)	More Interspersed (0.137)	Less Interspersed (-0.327)	More Interspersed (0.472)
Connectivity (ENN_MD)	Rio Salado	More Isolated (0.460)	More Isolated (0.619)	More Isolated (22.589)	More Isolated (0.228)	Less Isolated (-0.560)
	New River	Less Isolated (-1.467)	More Isolated (0.705)	More Isolated (2.892)	Less Isolated (-6.269)	Less Isolated (-3.372)

Distribution values show the largest differences between the sites: built-up, desert, crop, and vegetation classes have opposite trends at the two sites (Table 1). Land covers within the Rio Salado site became more interspersed, and land covers within the New River site became less interspersed. Water, the one class with agreement, became more interspersed at both sites.

Desert and cropland became more isolated at both sites—likely a function of the decreasing amounts of those classes as well as the increasing interspersion of built-up lands. Water, on the other hand, was less isolated at both sites and was the only class at the Rio Salado that did not become more isolated. The built-up and vegetation land-

covers increased in connectivity for the New River site, while these two land-cover classes at the Rio Salado site did not.

The contrasting design goals of the sites led to two distinctive differences. First, the city of Tempe's goal of encouraging development balanced with the goal of creating outdoor recreational spaces which led to less built-up land and more vegetation and desert land at the Rio Salado site compared to the New River site. The "recreational" (i.e., desert and vegetation) and built-up land-covers became more isolated and dispersed. Conversely, at the New River site, almost all classes became less interspersed as the development consolidated land-cover patches. Second, the creation of Tempe Town Lake to meet flood control goals constituted a major difference in land-cover composition between the two sites. The more typical means for ensuring flood-control in the Phoenix metropolitan area—in which the area in and around a riverbed is left undeveloped or only developed with land covers that are resilient to flooding (i.e. playgrounds and playing fields)—was employed at the New River site. The distinctive lake created by channelizing the Rio Salado is a function of the way in which the city tied flood control to "achieving the greatest social and economic benefits for the citizens of Tempe" (City of Tempe, 1982: 11-13). The Rio Salado in Tempe now serves as a focal point for tourism and large-scale community events.

2.5.2 Question 2: Land Surface Temperature, Vegetation Abundance, and LSA Change.

Research question two examines the differences between NDVI and LST at the two sites and asks which LSA modification—size, shape, distribution, and connectivity—had the greatest impact on NDVI and LST. Figure 5 and 6 present NDVI and LST values from two Landsat scenes in early August in 1985 and 2010 in order to visualize the spatial distribution of these values within the study sites. August 8th, 1985 and August

13th, 2010 were selected from the available cloudless summer images based on their proximity in date and because they are similar to the monthly average minimum and maximum temperatures for the area according to the Global Historical Climatology Network Daily Database (Menne, Durre, Vose, et al. 2012; Menne, Durre, Korzeniewski, et al. 2012).

Overall, NDVI increased at the Rio Salado site and decreased at the New River site (Fig. 5). The New River site had higher NDVI values in 1985 due to the presence of large tracts of farmland, but NDVI declined by 2010 as those tracts urbanized. Both sites see pockets of greater NDVI with the addition of small, verdant parks and residential landscapes.

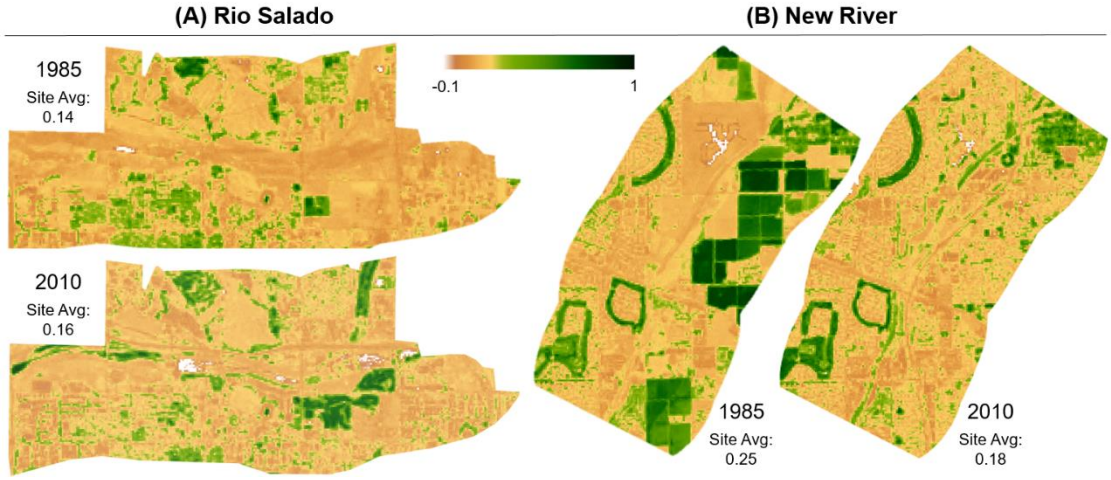

Figure 5. Normalized Difference Vegetation Index (NDVI) maps for the (A) Rio Salado and (B) New River sites in August 1985 and 2010. Average NDVI for the whole study area is presented below the year label. Agricultural lands, as well as golf courses and traditional (mesic) residential landscaping have the highest values while water has negative values.

LST increased at both sites between 1985 and 2010, and the average August daytime LST reached approximately 46° C in 2010 at both sites (Fig. 6). The increase in temperature at both sites can be attributed to the overall urbanization occurring within and outside the study area boundaries (i.e., urban heat island effect) and, perhaps,

climate change. In 1985 and 2010, areas with water and vegetation were cooler at both sites, and built-up areas had the highest LST. The New River site was cooler in 1985 and experienced a much greater increase in temperature than the Rio Salado site—partially attributable to the loss of cropland and gain in built-up area.

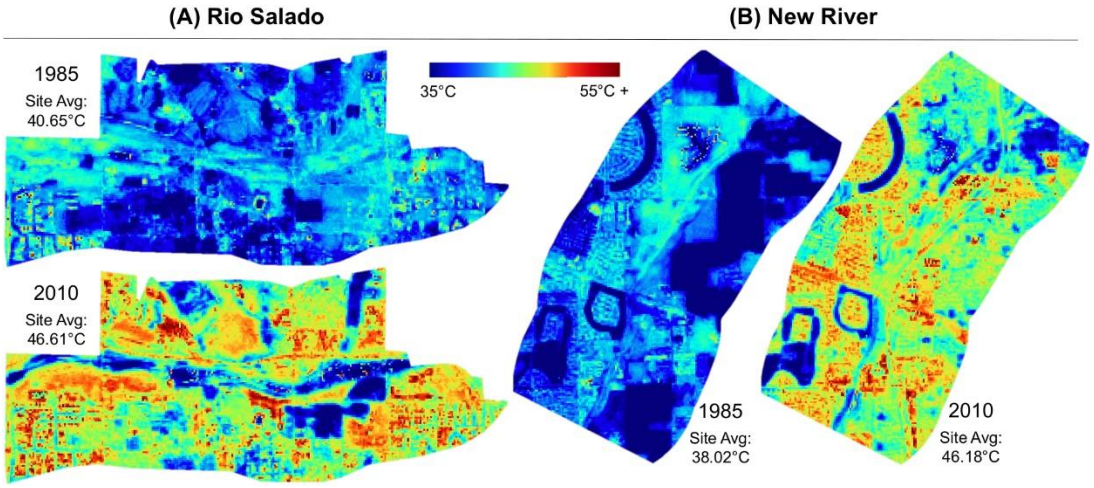

Figure 6. Land Surface Temperature (LST) maps for the (A) Rio Salado and (B) New River sites in August 1985 and 2010. Average LST for the whole study area is presented below the year label. Color palette was determined by stretching the values within 2.5 standard deviations of the Rio Salado 2010 mean (SD = 4.7° C). Agricultural lands, as well as golf courses and water bodies, are cool while built up surfaces, especially in 2010, are hot.

Examining the impact of configuration on NDVI and LST, we find that only shape and distribution had statistically significant relationships with these two environmental variables (Fig. 7). Size and connectivity did not have statistically significant relationships with NDVI and LST so are not presented here.

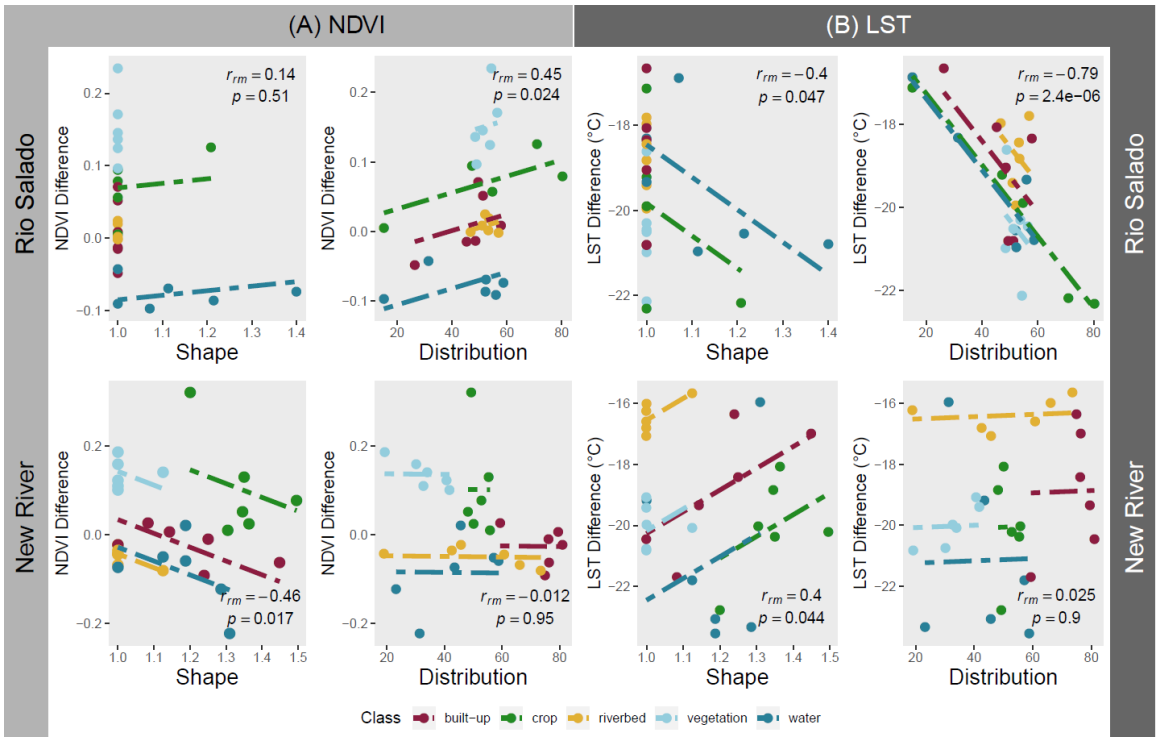

Figure 7. Repeated Measures Correlation graphs for the class-level landscape metric values and environmental variables at the Rio Salado and New River sites. Each point represents one year of data, and the colors denote the classes. (A) is the relationship between class NDVI difference (y-axis) and class shape or distribution values (x-axis). Class NDVI difference is the difference between the average NDVI of the site and the average NDVI for all patches in a given class. Positive y-axis values indicate greater greenness compared to site average. (B) is the relationship between class LST difference (y-axis) and class shape or distribution values (x-axis). Class LST difference is the difference between the average LST of the site and the class average LST. Negative y-axis values indicate that the patches in a given class were cooler than the site average.

At the Rio Salado site, patches that were interspersed were greener (r_{rm} = 0.45, p = 0.024) and cooler (r_{rm} = -0.79, p = 2.4e-06) compared to the site average. This relationship was determined considering all land classes but was largely driven by the built-up, crop, and water classes (Fig. 7). At the New River site, patches that were more compact were greener (r_{rm} = 0.46, p = 0.017) and cooler (r_{rm} = 0.4, p = 0.044) compared to the average. Overall, the statistically significant relationships were most often driven by the built-up, crop, and water classes with riverbed and vegetation having a smaller range of values. Shape and LST had the opposite relationship at the two sites. There was

very little change in the shape of patches at the Rio Salado site, so the relationship was largely driven by the only land-cover classes that did change (water and the crop). Thus, more weight should be given to the New River shape result—that more compact patches are cooler—because it has a greater number of non-zero values.

Overall, there were moderate differences between the sites in terms of NDVI and LST. NDVI at the Rio Salado site increased marginally, while NDVI at the New River site decreased dramatically (largely owing to the urbanization of cropland). LST for both sites rose, ending at approximately the same average temperature. The New River site experienced a larger increase in temperature, but it was approximately 2.5°C cooler than Tempe in 1985. The repeated measures correlation indicates that shape and distribution have a statically significant relationship with NDVI and LST, while size and connectivity do not. The small number of years examined in this assessment limit the conclusions we can draw with the repeated measures correlation, but the results provide context about the effect of landscape metrics as well as the classes that drive the relationships between landscape metrics and NDVI/LST. Water, for example, is a driver in all of the correlations presented.

2.5.3 Question 3: Bird Community and LSA Change.

Research question three evaluates bird community differences between the two sites and the role that LSA played in these differences. Bird community abundance, richness, and turnover declined at both sites (Fig. 8), but abundance is the only metric for which there was a statistically significant difference between the two sites (F= 4.36, P=0.04).

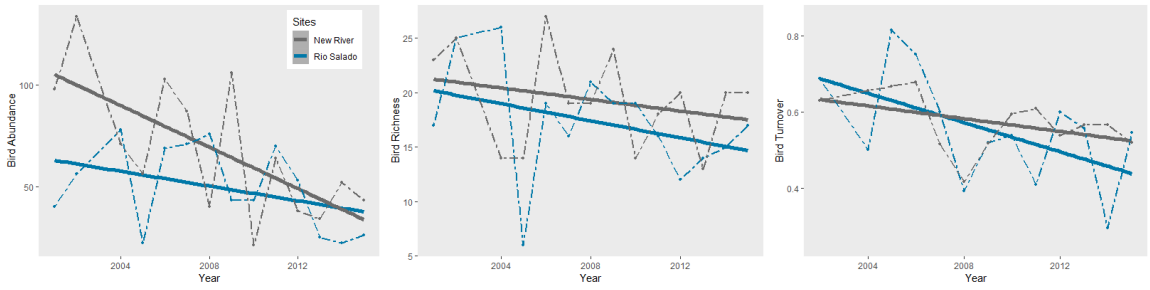

Figure 8. Bird Community Metrics. The dashed lines are the raw data, the solid lines represent the linear regression slope for the community metric (abundance, richness, turnover) at the given site from 2001 to 2015.

Abundance values started higher at the New River site, likely a function of the nearby undeveloped desert and agricultural land. The steep decline in abundance, from approximately 100 to approximately 40 over the course of fourteen years, is attributable to accumulative effects of rapid land-use change and urbanization on the urban fringe. The Rio Salado site, in the urban center, had lower abundance in 2001 but was more stable, potentially due to the addition of water and vegetation classes, which could provide consistent resources to the bird community there. The two sites appear to be nearing similar levels of abundance over time, following a larger trend in the Phoenix metro area where riparian bird communities are shifting toward urban dwelling species (Banville et al. 2017).

Differences between site type and temporal shifts in the bird community (Non-metric multidimensional scaling - NMDS stress= 0.23; fit R^2=0.95) is evidenced in the unconstrained ordination of sites in species space (Fig. 9). Temporal shifts are displayed on the x-axis, with lower x-values representing earlier survey years (R^2=0.32, P= 0.001). Over time, the species composition at the sites became more similar. Site differences are displayed on the y-axis, with negative y-values representing the New River site and positive y-values representing the Rio Salado site (R^2=0.36, P= 0.0001). We found that the Rio Salado supported a different bird community than it might have if it followed an

urbanization trajectory similar to the New River site (Fig. 9). The Rio Salado site supported bird species that require aquatic habitat, as well as warbler species, likely due to the prevalence of semi-restored, perennial riparian habitat (H. L. Bateman et al. 2015). Conversely, terrestrial bird species and desert specialist species were more prevalent at the New River site. Appendix B contains a table with the four-letter alpha code, common name, and scientific name for all bird species in our analysis.

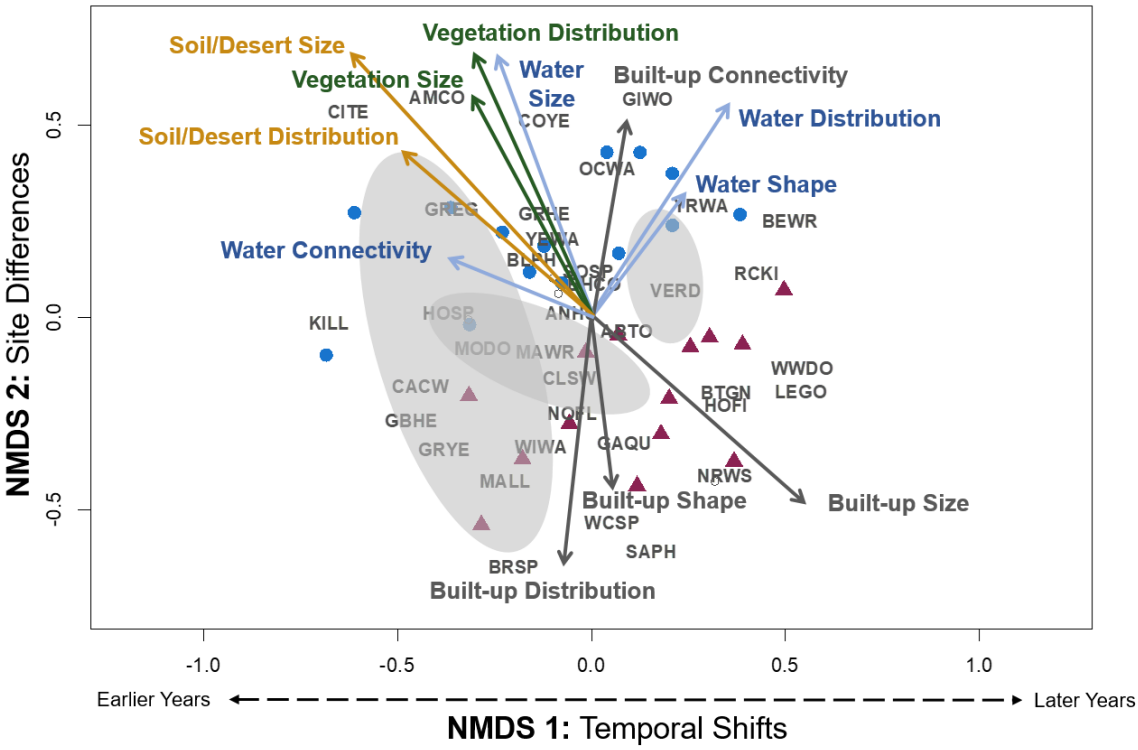

Figure 9. Non-metric multidimensional scaling (NMDS) visualizing the temporal and spatial relationship between bird species, and the LSA components of size, shape, distribution, and connectivity. The blue circles (Rio Salado) and maroon triangles (New River) are the sites over time, arranged in species-space with bird-species labeled by their 4-letter alpha codes. See Appendix B for corresponding species names. Vectors reflect the strength and direction of the LSA components; only statistically significant ($P< 0.05$) vectors are presented. Site differences are reflected by the y-axis; vectors related to Rio Salado are in the upper portion (positive numbers), vectors related to the New River site are in the lower portion (negative numbers). Grey ellipses represent centroids for the three time periods (Time Period 1: 2001-2004, Time Period 2: 2005-2009, and Time Period 3: 2010-2015) along the x-axis. Positive x-axis numbers refer to earlier time periods beginning in 2001, while negative numbers refer to later time periods ending in 2015.

Water was one of the most important land-cover classes separating the sites in terms of habitat. All landscape metrics for the water class were significantly related to the bird community at the Rio Salado: water size (R^2=0.73, P= 0.001), water connectivity (R^2=0.24, P= 0.022), water shape (R^2=0.28, P= 0.025), and water distribution (R^2=0.52, P= 0.001).Conversely, built-up patches were emphasized in relationship to the bird community at the New River site: built-up size (R^2=0.71, P= 0.001), built-up shape (R^2=0.34, P= 0.007), and built-up distribution (R^2=0.63, P= 0.001). Built-up connectivity was positively and significantly related to the Rio Salado bird community (R^2=0.44, P= 0.003). Consistent with the role of urbanization in the convergence of the bird community make-up over time, built-up lands are more significant in the later years of the analysis, while the soil/desert and vegetation classes are significant for earlier years. Two of the four vegetation landscape metrics were significantly related to the bird community at the Rio Salado site: vegetation size (R^2=0.48, P= 0.002), and vegetation distribution (R^2=0.52, P= 0.001) along with soil/desert size (R^2=0.74, P= 0.001) and distribution (R^2=0.52, P= 0.001).

In answer to research question three, only the bird abundance trend was statistically different between the two sites. Bird abundance at the New River site was higher to begin with but appears to be nearing similar levels to that of the Rio Salado over time. The abundance trend at the Rio Salado was more stable, but still in decline. In terms of the role that LSA plays in the bird community differences between the sites, the interspersed patches of desert and vegetation noted above were also found to be significant in their relationship with the bird community at the Rio Salado.

The bird community's relationship with water and built-up land was even more pronounced; size, shape, distribution and connectivity were all significant for the water and built-up classes at the Rio Salado site. The differences in the sites' bird communities

is attributable to the presence of desert, vegetated areas, and water at the Rio Salado site (more water bird species) and built-up areas at the New River site (more terrestrial species). Despite these differences, the bird communities' species composition at both sites—depicted by the three grey ellipses—became more similar over time, a trend mirrored in the larger metro-area (Banville et al. 2017).

2.6 Discussion

The distinctive design goals of Rio Salado generated various differences in LSA compared to the developer-led urban expansion at the New River site. Only two LSA differences, however, were sufficiently unique to lead to divergent outcomes for the environmental variables examined. First is the difference between the sites in terms of configuration—specifically the distribution of recreational land-cover classes. Second is the large composition change caused by the addition of Tempe Town Lake at the Rio Salado site.

2.6.1 Configuration

Among the four components of LSA—size, shape, distribution and connectivity—the differences in the trajectories of the two sites were greatest in terms of distribution (i.e., the interspersion or adjacency of patches of the same class among other classes). The Rio Salado's built-up, vegetation, and desert land-cover patches became more interspersed as the area developed (Table 1), which had implications for the site's surface temperature, greenness, and the bird community. The repeated measures correlations and NMDS indicate that distribution has a statistically significant relationship with each of the examined environmental outcomes: greater interspersion was related to greener and cooler conditions (Fig. 7) and the distribution of desert, vegetation, and water patches were related to the bird community at the Rio Salado site (Fig. 9).

The importance of land-cover distribution in distinguishing the Rio Salado site has potential planning implications. Developers, planners, and other land design professionals must consider the surrounding context of the land covers with which they are working (Connors, Galletti, and Chow 2013). The value of considering the composition and configuration of landscapes as a whole is well understood (Huang et al. 2019; Nassauer and Opdam 2008; Steinitz 2012; Turner 2016; Vadjunec et al. 2018), and our findings on the importance of distribution highlight this further. Distribution, of all the components of LSA, is a measure of configuration strongly tied to the surrounding landscape.

Notably, our findings about the primacy of distribution are counter to much of the previous LSA literature that has found composition to be the primary driver of LST (Li et al. 2017; Li et al. 2012; Zhou, Wang, and Cadenasso 2017; Zhou, Huang, and Cadenasso 2011), although at least one LST study (Li et al., 2016) also found configuration to be more important than composition. Additionally, the finding that interspersed patches are greener and cooler is contrary to some previous findings on pattern and LST (Fan, Myint, and Zheng 2015; Li et al. 2017; Li et al. 2012; Myint et al. 2015). Configuration relationships, however, have been found to vary in magnitude, significance, or direction based on the location of the case study (Zhou, Wang, and Cadenasso 2017), the scale (Connors, Galletti, and Chow 2013) and the land-cover class evaluated (Myint et al. 2015). The variation in scale may partly be explained by the Phoenix metro-area findings that clustered green space enhances local cooling but interspersed patches lead to greater regional cooling (Zhang, Murray, and Turner 2017).

Our findings on the role of distribution may be influenced by our methodology. The majority of previous research has examined one class (i.e., greenspace or impervious surface) at a time (Fan, Myint, and Zheng 2015; Li et al. 2012; Zhang, Murray, and

Turner 2017). We chose to use a repeated measures correlation, which considers the relationship between NDVI and LST with all land-cover classes together but also identifies which classes drive the relationship. Methodologically, this mirrors the need for thinking about and planning land-cover change in context. The repeated measures correlation may be more appropriate than examining one class in isolation because land-cover classes co-exist in a landscape, and any environmental impacts are a response to a mosaic of heterogeneous land covers. This is especially the case in urban green spaces, which are functional components of urban ecosystems that interact spatially with surrounding land-covers (Noss 1987; Tian et al. 2011).

2.6.2 Composition

The addition of Tempe Town Lake—a major change of land composition—allowed the Rio Salado site to support waterbird and warbler species. The New River site, with its greater amount of built-up land cover, supported more terrestrial bird species (Fig. 9). This aligns with multi-site evaluations in central Arizona which have found land-change to be a dominate factor in changes in species composition over time, leading to more unique species between land-use types (Allen et al. 2019). Water was also one of the most influential classes in determining the relationships of the repeated measures correlations (Fig. 7).

Additionally, abundance declined less precipitously at the Rio Salado site (Fig. 8), which may be attributable to the lower levels of abundance to begin with or the addition of water. In the Phoenix metro-area, abundant surface water can lead to higher levels of bird diversity than the outlying desert (Andrade et al. 2018). The lake creation may have slowed the decline of bird diversity at the Rio Salado, but diversity and abundance at the two sites seem to be converging. These trends reflects the larger, regional scale shifts in which the riparian bird community is shifting toward urban dwelling, resident species

(Banville et al. 2017) along with a decline of desert species in the southwest (Iknayan and Beissinger 2018; Warren et al. 2019) and the broader North American avifauna decline (Rosenberg et al. 2019).

2.6.3 Summary

In summation, despite distinctive design goals and corresponding differences in the LSA of the two sites, only moderate differences in the environmental outcomes were identified. Our findings are consistent with Turner and Galletti (2015), who also found modest improvements in the environmental performance of an urban development that employed purposeful environmental design. It follows that one of the major policy and planning implications of our study is that existing methods from LSA (and similar landscape design fields) can inform sustainable urbanization by providing quantifiable metrics for measuring a range of environmental outcomes (Turner 2016; Turner et al. 2013; Turner and Galletti 2015; Wu 2019). There is more to be done, however, before LSA methods are regularly operationalized in land-based decision making. In this study, we focused on environmental consequences, but recognize that the inclusion of the social dimensions of LSA (e.g., housing costs or proximity to recreation spaces) would alter our results. Future LSA work requires collaboration with government officials, policy makers, planners, developers, and other stakeholders to identify and monitor relevant socio-environmental desired outcome variables and frame them in terms of their contribution to neighborhood, city, or regional sustainability goals (Aragon et al. 2019; Groffman et al. 2017).

2.6.4 Limitations

One limitation of this study is the effect that the selection and the extent of the two case study sites may have on the results. The Rio Salado's urbanization is an infill development, while the New River site urbanized the fringe of the metropolitan area.

These contrasting sites were chosen to ensure divergent design intentions, systematic bird survey data, and riparian locations. The initial differences in the land systems of the two sites, however, confounds our ability to assess environmental change because they do not begin with similar bird communities, NDVI, or LST values. Moreover, while the boundaries of each site were selected to be similar in area and inclusive of surrounding land-covers, the extent of the study areas influences the LSA, NDVI, and LST results.

Another limitation involves the 2010 end date of the systematically classified LULC data for the Phoenix metropolitan area. High resolution Google Earth imagery shows that land changes between 2010 and 2015 are minimal at the New River site. The Rio Salado site, however, continues to be developed, including large, commercial, and residential buildings along the eastern portions of Tempe Town Lake. This development would not likely change the composition trajectories identified from the 1985-2010 data, but it may have an impact on the configuration results of our study.

Finally, the disparate and disjointed means of measuring urban landscape composition and configuration is a limitation of this study and all LSA research. Many of the most commonly employed landscape metrics were developed for traditional ecological questions, and it is not clear how robust they may be for heterogeneous urban contexts. Inconsistencies may emerge in urban landscapes because the patterns and processes of urban areas differ from the non-urban settings. As an example, the urban heat island effect is a local climatological process unique to urban areas (Oke et al. 2017), and changing the metrics applied to LSA and temperature have yielded different outcomes (Li et al. 2016; Zhou, Wang, and Cadenasso 2017; Zhou, Huang, and Cadenasso 2011). The research community has yet to systematically address this issue.

2.7 Conclusion

Our research investigated how the divergent design intentions of the Rio Salado and New River sites affected the areas' LSA and explored some environmental outcomes of this change. The findings indicate that few LSA changes were sufficiently unique to contribute to divergent environmental outcomes, but those that did had an outsized role in shaping the differences between sites. The design goals of the Rio Salado resulted in the interspersion of built-up, vegetation, and desert patches. Distribution (the interspersion of patches) was found to be statistically significant in terms of all analyzed environmental outcomes. The distribution of non-built (vegetation, water, and soil/desert) land cover was related to the Rio Salado bird community, and greater interspersion was related to cooler land surface temperature and higher vegetation presence/health at the Rio Salado site. The channelization of the Rio Salado into Tempe Town Lake allowed the site to support more waterbird and warbler species. In contrast, with less surface water and greater built-up area, the New River site supported mostly terrestrial species.

Advancing understanding about the relationship between LSA and environmental outcomes is important for a range of research fields—landscape and urban ecology, landscape architecture, urban climatology, geodesign, and LSS—and to urban planning. Many cities are developing or redeveloping their urban structure, especially in riparian areas. The composition and configuration changes cities make in these waterfront development projects will affect the areas' environmental outcomes. We encourage using (and improving) LSA's quantitative geospatial methods to plan land-cover change contextualized by the surrounding landscape as well as environmental, social, and economic goals. Our queries and findings are the beginning of a line of

research that will provide insights on design goals and their impacts on composition, configuration, and environmental outcomes.

2.8 Acknowledgements

We thank the anonymous reviewers for the journal Land Use Policy for their perspective and corresponding improvement of this research as well as Yushim Kim, Jordan P. Smith, and Lance Watkins for their insights. This material is based upon work supported by the National Science Foundation under grant number DEB-1832016, Central Arizona-Phoenix Long-Term Ecological Research Program (CAP LTER) and was carried out in the Environmental Remote Sensing and Geoinformatics Lab at Arizona State University.

CHAPTER 3

INSTITUTIONAL SHIFTS AND ENVIRONMENTAL CHANGE: A LAND SYSTEM ARCHITECTURE CASE STUDY FROM THE REPUBLIC OF CUBA DURING THE PERÍODO ESPECIAL

3.1 Abstract

Policy plays a key role in where, how, and when land systems are modified. While the role of policy in governing land systems is commonly acknowledged, it is often under-addressed due to difficulties isolating the effect of policy or data availability. We begin to fill this gap by examining the landscape modifications in Cuba brought about by the collapse of the Soviet Union and the resulting El Período Especial en Tiempos de Paz ("The Special Period in Time of Peace"). Employing a time-series of satellite imagery, we compared the land system and environmental variables before and after the collapse of the Soviet Union. We found that the Cuban landscape underwent statistically significant change that can be linked to the institutional shift that occurred in this period. In particular, concentrated policy efforts to transform agricultural production and protect forest lands corresponded to landscape composition and configuration change (or, in the case of protected forest lands, a lack of change). The landscape and environmental change resulting from the Período Especial's institutional shifts became visible in the landscape in as quickly as a few years or as slowly as a few decades.

3.2 Introduction

With global populations expected to increase by an additional two billion over the next thirty years (United Nations 2019) and over 75% of the Earth's ice-free land (terrestrial surface) already modified by humans (Verburg et al. 2013), it is increasingly important to understand how land systems contribute to environmental change locally and globally. Governance is an acknowledged but commonly under-addressed aspects of

land systems (Verburg et al. 2015) or other socio-environmental systems (Ostrom 2009). Governance is the coordination and control of actors leading to the creation of institutions (Lebel et al. 2006). Institutions are the rules constraining and prescribing actors' interactions such as formal rules (i.e., policy) and informal norms (Crawford and Ostrom 1995). With the exception of research on the commons (e.g., Ostrom et al., 2007) and recent attention to illicit land changes (e.g., McSweeney et al., 2017; Tellman et al., 2020), much of land system governance research is focused on formal institutions such as policies. In the context of land systems, policy can take many forms, such as zoning, establishment of protected areas, treaties, taxation, regulation, and permitting.

Global level examinations of the role of institutions grouped countries by broad institutional structures (i.e., democracy, communism) and compared environmental outcomes by group. Corresponding to the mix of economic development levels, resource availability, and institutional structures of countries around the world, conclusions of this research were mixed. Democracies were found to establish more protected lands, were more likely to regulate domestic environmental outputs, and support global efforts of environmental regulation (Congleton 1992; Midlarsky 1998; Neumayer 2002). Some, but not all, types of pollution decreased with an increase of political freedoms (Barrett and Graddy 2000). Namely, democracies produced more methane (Congleton 1992) and were also correlated with higher rates of deforestation, carbon dioxide emissions, and soil erosion (Midlarsky 1998).

The role of institutional changes on land systems and environmental outcomes can also be examined within countries that have undergone broad institutional change which holds some country level variables constant. The dissolution of the Soviet Union (USSR) provided several case studies as Soviet bloc countries transitioned to different institutional structures. For instance, broad land system change analysis in southern

central Siberian Russia, found that deforestation due to logging decreased, reforestation occurred, and the extent of agricultural lands decreased (Bergen et al. 2008; Peterson et al. 2009).

The Republic of Cuba is a good candidate for research that furthers the unresolved debate about institutions and environmental protection. Cuba has undergone profound institutional transitions over the course of several decades, especially those stemming from the Cuban revolution in 1959 and the dissolution of the USSR in 1991. Moreover, these changes took place within an archipelago holding the highest endemism of all the West Indies and Antillean islands; 90% of the amphibians, 85% of the reptiles, 50% of the flowering plants, and 32% of the vertebrates are only found in Cuba (Santana 1991).

After the 1959 Cuban revolution, the island's agriculture (and broader) economy became structured almost entirely around capital investments and trade relations with the USSR (Choy et al. 2005; Diaz-Briquets and Pérez-López 2000). Sugar was the keystone crop, through protected trade with Russia, sugar funded a highly mechanized state agricultural program reliant on Soviet machinery and fossil fuels (Choy et al. 2005). Indeed, Cuba is said to have had the most tractors per arable unit of land of any country in the world during this time (Choy et al. 2005). When the USSR dissolved in 1991, Cuba lost its main trade partner, industrial agricultural in the country came to a standstill, and an economic crisis followed (Castro and Ramonet 2008; Choy et al. 2005).

The government termed this economic crisis the "special period in time of peace" ("Período Especial en Tiempos de Paz", often shortened to "Período Especial"). The period (1991-2000) brought profound changes in land tenure, including privatization of land, an opening of the agricultural commodity market, as well as several initiatives to diversify and turn agricultural production inward (Wright 2009). These institutional

changes have been subject to a mix of condemnation and praise in regard to the country's sustainability (Maal-Bared 2006; Machado 2017; Pope and Finn 2017; Stricker 2010). For example, mining and tourism—activities controlled by the government—have been found to be the greatest threat to water quality because of their contributions to Cuba's already burdened wastewater system (Maal-Bared 2006). On the other hand, initiatives such as the government's push for low-input, subsistence agriculture in both urban and rural areas, have been praised as exemplars of sustainability and food sovereignty (McKibben 2005; Wright 2009).

What impact did these institutional changes have on the Cuban land system and environment? We pose this question through the lens of land system architecture—examining the composition and configuration of land-use, land-covers, and their change (Turner, Lambin, and Reenberg 2007; Turner et al. 2013). Land system architecture affects processes including the movement of biologically active nitrogen, habitat loss, greenhouse gas emission and absorption, and the hydrologic cycles (Hager et al. 2015; Lambin et al. 2001). Reliable data, especially time-series data, is often difficult to access as US-Cuba relations fluctuate with each new administration (Biegon 2020; Cohn 2010; Pope and Finn 2017). Satellite imagery, however, provides unbiased systemic source of data on land system and can improve understanding on the processes that influence land-based outcomes, even when other data are scarce (Tellman et al. 2020).

Employing a time series of Landsat imagery (1985-2010) as well as other remotely sensed data sources, we evaluated the linkages between institutional changes and land system changes as a result of the Período Especial using a quasi-experimental design approach. Specifically, we asked:

1. How did the composition and configuration (land system architecture) of Cuba's land system change as a result of the institutional shifts caused by the collapse of the Soviet Union?
2. How are the land system architecture and environmental outcomes temporally linked to the policy changes in the Período Especial?

3.3 Data and Methods

3.3.1 Study Area

The Cuban archipelago comprises approximately 1600 islands; the largest island of the archipelago (hereafter the main island) is about 104,000 km^2 in area. Cuba's population was ~10,098,000 in 1985 and ~11,226,000 in 2010 (United Nations 2018a). Historically, Cuba's economy has been centered around the production of sugar cane, tobacco, and rum (Alvarez 2004). These still make up a substantial portion of the country's exports—sugar (34%), rolled tobacco (19%), rum (7.3%)—along with nickel and other minerals (10%) (Hausmann et al. 2012).

The biomes of Cuba's main island include: tropical/subtropical moist/dry broadleaf forests, mangroves, and flooded grasslands and savannas (Dinerstein et al. 2017). We focused our analysis on the main island because the 30m resolution of Landsat imagery cannot adequately capture many of the smaller islands of the archipelago which are a kilometer or less in area.

3.3.2 Research Design

Figure 1 visualizes the research design. Remotely sensed imagery from each year was used to calculate land system and environmental variables. Values from pre and post the dissolution of the USSR were compared via statistical tests and linked to the policy changes that occurred during the period.

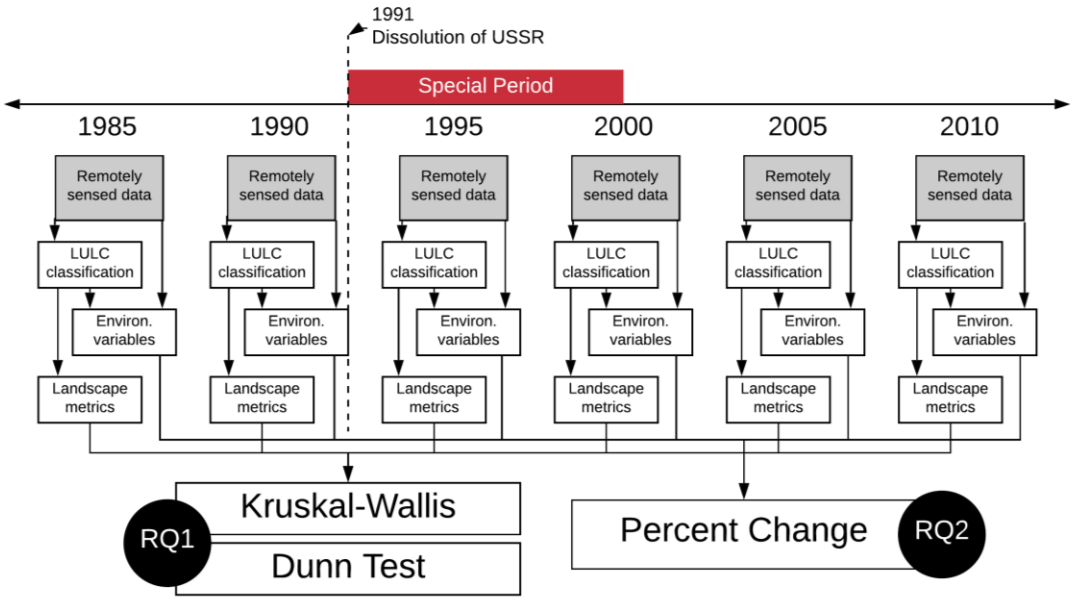

Figure 1. Research design diagram. Timeline along the top shows the years analyzed and the major events related to institutional change. Input data from remotely sensed sources represented in grey, with intermediary data below. Statistical tests which compare the two periods (1985-1990 vs. 1995-2010) are labeled with circles corresponding to the research question.

3.3.3 Cuban Policy Documents

We collected Cuban policy documents from 1963 to 2012 at the Law Library archives at the United States Library of Congress. In advance of the visit to the archives, a list was made of all potentially relevant primary source policy documents visible in the online catalogue. While at the archive, primary source documents as well as additional secondary source documents were scanned. Scanned documents were then ordered by year of enactment and summarized. Those that were deemed potentially relevant were translated and coded according to the LULC class they may affect. Five types of policy documents were collected: leyes (laws by the National Assembly of People's Power—Cuba's largest legislative body), decreto leyes (decree-laws by the Council of State—the smaller legislative body), decretos (decrees by the Council of Ministers), and instrucciónes (instructions by Cuba's judicial body). It should be noted that all

documents related to land and environment available in the archive were scanned but, because of tenuous relations between the two countries, may not reflect the full set of Cuban policies instituted in this era.

3.3.4 Land and Environmental Data

Landsat 5 Thematic Mapper (TM) served as the main data source for the land use/land cover (LULC) classifications and computing environmental variables (Fig. 1). Landsat 5 was launched mid-1984 and decommissioned in 2013. Our analysis used satellite imagery from 1985, 1990, 1995, 2000, 2005 and 2010 to provide two sets of datapoints before the fall of the USSR and four after to examine short and long-term impacts.

3.3.4.1 Land use/land cover classification

The LULC classification used a combination of Landsat 5 TM Tier 1 imagery, the Shuttle Radar Topography Mission (SRTM) 30m digital elevation model (Farr et al. 2007), and Global Radiance-Calibrated Nighttime Lights Version 4, Defense Meteorological Program Operational Linescan System (DMSP-OLS) imagery when available. A cloud-free Landsat 5 composite was created for each year, pulling from surrounding years when a complete cloud-free coverage was not attainable from one year. All of the Landsat bands were included along with the Normalized Difference Spectral Vector (NDSV), the Enhanced Vegetation Index (EVI), and texture computed from each band's gray level co-occurence matrix (Haralick, Shanmugam, and Dinstein 1973). NDSV is a stack of indices that is computed by taking the normalize difference of every band with each other (Trianni et al. 2015). We used NDSV over a smaller subset of normalized difference calculations (such as NDVI and NDWI) because including all has been shown to increase classification accuracy (Goldblatt et al. 2018).

A random forest classification was used to identify 1) cropland, 2) barren, grasslands and shrublands, 3) built-up, 4) forest, and 5) water LULC classes. The classification was run in Google Earth Engine with 30 trees, because average accuracy often levels off between 10 and 50 trees (Goldblatt et al. 2016). Two random forest classifiers were trained, one for 1985 and 1990 (the years for which there is not DMSP-OLS data) and one for 1995 and 2000 (which included the DMSP-OLS nighttime lights imagery).

Each classifier was trained with 760 labels and each classification was validated with 100 labels. The training and validation data was generated by randomly distributing samples according to the proportional presence of that land cover in each year (determined via the 2000 MODIS MCD12Q1.51 Land Cover Type classification) (Foody 2017; Wulder et al. 2006). Samples were hand labeled using high resolution imagery for 2005 and 2010. Landsat imagery was used for the remaining years because high-resolution, cloud-free imagery was not accessible. In the original validation and training set, each label was agreed upon by at least two hand labelers. 160 more labels were added to improve the accuracy for a total of 760 training labels for each classifier.

In order to have a greater number of training labels and predictor data for each classifier, we combined training labels and predictors from two years. This resulted in using 760 labels for each classifier instead of running each year separately with 380 labels per year. The 1985/1990 combined classifier was used to classify imagery from 1985 and 1990 separately. The 1995/2000 combined classifier was used to classify imagery from 1995, 2000, 2005 and 2010 separately.

3.3.4.2 Classification accuracy assessment

For each year, 100 validation samples were used to calculate the accuracy results for the land cover classification. We computed overall accuracy, as well as precision and recall by class.

$$Overall\ accuracy = \frac{TP + TN}{TP + TN + FP + FN}$$

$$Precision\ (a.k.a.user'accuracy) = \frac{TP}{TP + FP}$$

$$Recall\ (a.k.a.sensivity\ or\ producer's\ accuracy) = \frac{TP}{TP + FN}$$

where TP = true positive, TN = true negative, FN = false negative & FP = false positive.

3.3.5 Measures

3.3.5.1 Landscape metrics

The LULC classifications were used to calculate landscape metrics. Landscape metrics are algorithms that quantify the composition and configuration of relatively homogeneous patches of land within a geographic area (Frazier 2019; McGarigal, Cushman, and Ene 2012). Composition is the proportionate area of land patches and configuration is their spatial arrangement. Table 1 presents the metrics used to measure composition (size) and configuration (shape, connectivity, and distance between patches), which together constitute land system architecture (Turner et al. 2013).

Table 1. Patch-level metrics used to quantify size, shape, and connectivity at the patch level. Equations are derived from FRAGSTATS (McGarigal, Cushman, and Ene 2012).

	Metric Name	Description	Equation
SIZE (composition)	Patch Area	Sum of all pixels in a given patch. Calculated in hectares.	$a_{ij} \times 250$
SHAPE (configuration)	Fractal Dimension Index	Measure of shape complexity computed with a patch's area and perimeter.	$\frac{2 \times \ln(0.25(p_{ij} \times 500))}{\ln(a_{ij} \times 250{,}000)}$

CONNECTIVITY (configuration)	Contiguity Index	Assess spatial connectedness of pixels in the same patch.	$\frac{\left[\frac{\sum_{r=1}^{z} c_{ijr}}{a_{ij}}\right] - 1}{v - 1}$
DISTANCE (configuration)	Euclidean Nearest Neighbor Index	Distance of each patch to the nearest patch of the same class.	h_{ij}

WHERE:
$a_{ij} = area\ in\ terms\ of\ number\ of\ cells,$
$p_{ij} = perimeter\ of\ patch\ ij\ in\ terms\ of\ number\ of\ cell\ surfaces,$
$c_{ijr} = contiguity\ value\ for\ pixel\ r\ in\ patch\ ij,$
$v = size\ of\ filter\ matrix,$
$h_{ij} = distance\ to\ the\ nearest\ neighboring\ patch\ of\ the\ same\ class\ i\ (m)$

We chose these metrics because of their use in similar research and their ease of interpretation (Li et al. 2012; Stuhlmacher et al. 2020). We computed patch level metrics using the landscapemetrics R package (Hesselbarth et al. 2019; McGarigal and Marks 1995). To reduce computation and memory loads, the LULC classification was aggregated from 30m to 500m resolution using the majority rule.

3.3.5.2 Environmental variables

We computed brightness, greenness, and wetness from the tasseled-cap transformation as proxies of environmental conditions related to the presence of bare ground/soil, vegetation, and levels of soil moisture. A tasseled-cap transformation is a linear combination of image bands, we used the coefficients computed for Landsat 5 from Crist and Cicone (1984). Brightness corresponds to the overall reflectance of the image, in particular the presence of soil or other bare areas (i.e., soil brightness), greenness identifies high levels of vegetation, and wetness corresponds to soil or surface moisture (Crist and Cicone 1984).

3.3.6 Statistical Analysis

We used Kruskal-Wallis tests to determine if the change in patch-level landscape metrics from 1985-2010 was statistically significant. The Kruskal-Wallis test was chosen

because it is non-parametric as our data did not satisfy regression assumptions. Additionally, because we were particularly interested in comparing the years before and after 1991, we employed a post-hoc analysis—the Dunn Test—to quantify which changes between years were statistically significant. The p-values for the Dunn Test results were adjusted using the Benjamini-Hochberg method. The Dunn Test is a commonly used post-hoc analysis and was appropriate for our data because the groups had an unequal number of variances (Zar 2010).

To determine how the landscape change affected environmental variables, we averaged pixel-level environmental values by class and by year. Each year's class level values were used to compute the percent change of the environmental variables using 1985 as the baseline. 1985 was used as the baseline because the USSR slowly weakened before it dissolved in 1991, and the land system architecture of Cuba may already have begun to change in response by 1990.

3.4 Results

3.4.1 Environmental Policy

A total of fifty-three policies from the Library of Congress archives were collected, with forty determined to be potentially relevant to land systems or the environment. The set of forty were subset further based on dates of enactment (1980-2012) and specific content of the policy as it related to land systems (Table 2).

Table 2. Environmental policies (laws, decrees, resolutions, and instructions) from 1980 to 2012 collected at the United States Library of Congress ordered by date of enactment. Citation column contains the policy sponsor and the year enacted.

Policy Type & No.	Name	Summary	Citation
Ley No. 27	Gran parque nacional Sierra Maestra	Establishes a national park in the Sierra Maestra	Roa García, 1980

Decreto No. 66	Reglamento de mercado libre campesino	Allows a free market for surplus agricultural products. Expands rights for urban farmers	Castro Ruz, 1980
Instrucción No. 99	Sobre la succesión de la tierra de los pequenos agricultores	Allows for small plots of land to be inherited by others who have worked the land	Edelemann, 1981
Decreto No. 106	Reglamente del mercado libre campesino	New regulations for the previously established free market for agricultural products	Castro Ruz and Villa Sosa, 1982
Ley No. 36	Cooperativas agropecuarias	Gives legal recognition to agricultural cooperatives	Pardo, 1982
Decreto Ley No. 63	Sobre la herencia de la tierra propiedad de los agricultores pequeños	Regulations on the inheritance of small agricultural plots	Castro Ruz, 1983
Decreto Ley No. 125	Regimen de posesion, propiedad y herencia de la tierra y bienes agropecuarios	Regulations on inheritance of land and agricultural goods	Castro Ruz, 1991
Decreto Ley No. 136	Del patrimonio forestal y la fauna silvestre	Protection of forests and wildlife	Castro Ruz, 1993a
Decreto Ley No. 138	De las aguas terrestres	Protection and conservation of terrestrial waters	Castro Ruz, 1993b
Decreto Ley No. 153	De las regulaciones de la sanidad vegetal	Establishes sanitation and other public health related requirements for agricultural products	Castro Ruz, 1994

Ley No. 76	Ley de minas	Establishes regulations for the protection, development, and exploitation of mineral resources	Alarcón de Quesada, 1995
Decreto No. 199	De contravenciones de las reglaciones para la protección y uso racional de los recursos hidráulicos	Defines consequences of violating the regulations of hydraulic resources	Castro Ruz et al., 1995
Ley No. 81	De medio ambiente	Comprehensive environmental law about protected areas and biodiversity	Alarcón de Quesada, 1997
Decreto No. 222	Reglamento de la ley de minas	Mining regulations	Castro Ruz et al., 1997
Ley No. 85	Ley forestal	Forest protection	Alarcón de Quesada, 1998
Decreto No. 268	Contravenciones de las regulaciones forestales	Regulation to support the forest protection law (No. 85)	Castro Ruz et al., 1999
Decreto Ley No. 201	Del sistema nacional de areas protegidas	Establishes a national system of protected areas	Castro Ruz, 1999b
Decreto Ley No. 259	Sobre la entrega de tierras ociosas en usufructo	Regulations on the use of usufruct land	Castro Ruz, 2008
Decreto No. 282	Reglamento para la implementacion de la entrega de tierras ociosas en usufructo	Regulations to support the usufruct land law (No. 259)	Castro Ruz et al., 2008

Decreto Ley No. 300	Sobre la entrega de tierras estatales ociosas en usufructo	Consolidation and simplification of regulations on the use of state lands	Castro Ruz, 2012

Policies pre and post the collapse of the Soviet Union were focused on different themes. From 1980-1991 most policies were focused on agriculture reform. After 1991, there continued to be some policy creation around agriculture, but the majority of change centered around environmental protection, particularly of forest lands. We thus hypothesized considerable change in agricultural lands as a result of the collapse of the Soviet Union but minimal change to forest lands.

3.4.1 Land and Environmental Change

3.4.1.1 LULC Classification

The LULC classification resulted in overall accuracies ranging from 85-92% (Table 3). Accuracies were lower in 2005 and 2010 because the classification was trained using earlier years and validation samples were labeled using different imagery. The barren/grass/shrubland class has the lowest precision and recall which was likely attributable to being more spectrally mixed compared to the other classes. One limitation to our research, along with most research relying on remotely sensed time-series data, was that changes observed in the LULC classification may be a function of classification errors or sensor degradation instead of on-the-ground landscape change.

Table 3. Accuracy assessment of five land cover classes for Cuba's main island for 1985, 1990, 1995, 2000, 2005 and 2010.

	1985	1990	1995	2000	2005	2010
Overall Accuracy	90.0%	92.0%	90.0%	91.0%	88.0%	86.0%
Cropland Precision	88.5%	91.7%	82.8%	79.3%	87.0%	88.9%
Barren/Grass/Shrubland Precision	55.6%	77.8%	60.0%	60.0%	44.4%	50.0%
Built-up Precision	100.0%	90.0%	100.0%	100.0%	100.0%	66.7%

Forest Precision	72.7%	81.8%	75.0%	90.9%	69.2%	90.0%
Water Precision	100.0%	97.8%	100.0%	100.0%	100.0%	100.0%
Croplands Recall	92.0%	88.0%	96.0%	92.0%	80.0%	64.0%
Barren/Grass/Shrubland Recall	50.0%	70.0%	30.0%	30.0%	40.0%	60.0%
Built-up Recall	90.0%	90.0%	90.0%	100.0%	100.0%	100.0%
Forest Recall	80.0%	90.0%	90.0%	100.0%	90.0%	90.0%
Water Recall	100.0%	100.0%	100.0%	100.0%	100.0%	100.0%

3.4.1.2 Landscape Composition and Configuration

Cuba experienced considerable change to the composition of LULC on its main island after the fall of the Soviet Union (Fig. 2).

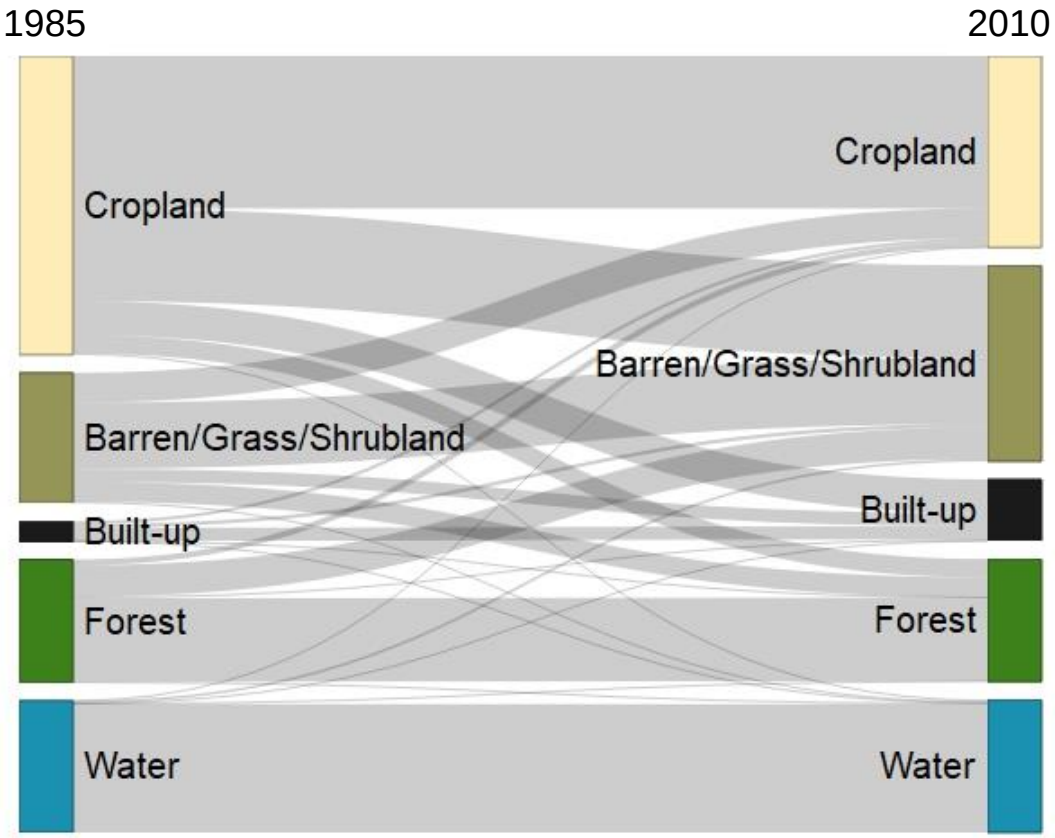

Figure 2. LULC class conversions between 1985 and 2010 in Cuba. See Table 4 for the percentage of land a given class covers each year.

Cropland, barren/grass/shrubland, and built-up lands changed the most, with the majority of their change occurring after 1991 (Fig. 2, Table 4). Cropland was

predominately converted to barren/grass/shrubland or built-up areas. Some cropland and barren/grass/shrubland also becomes forest land, causing the percentage of overall forest land to stay relatively constant, peaking in 2005 and returning 17.4% by 2010. The growth of the barren/grass/shrubland class came primarily from cropland that was left fallow but secondarily from degraded forest land.

Table 4. Proportion of LULC for each class from 1985-2010.

	1985	**1990**	**1995**	**2000**	**2005**	**2010**
Cropland	45.2%	45.1%	39.3%	38.8%	38.1%	27.2%
Barren/Grass/Shrubland	16.0%	14.0%	17.0%	18.2%	21.3%	27.8%
Built-up	2.5%	2.7%	2.4%	3.8%	5.2%	8.8%
Forest	17.4%	19.2%	22.4%	20.6%	16.7%	17.4%
Water	18.8%	19.0%	19.0%	18.6%	18.7%	18.9%

Water proportion (which includes lakes and rivers as well as the ocean boarding the main island) stayed relatively constant over the period. Maps of the LULC for each year are in Appendix C.

We quantified the composition and configuration of these landscape changes in terms of patch size, shape, connectivity, and the distance between patches of the same LULC class. Figure 3 presents the average values for each metric (i.e., class-level value) for the croplands, barren/grass/shrublands, built-up, and forest LULC classes. Water was excluded because it was relatively stable (Table 4) and was not expected to fluctuate based on policy changes.

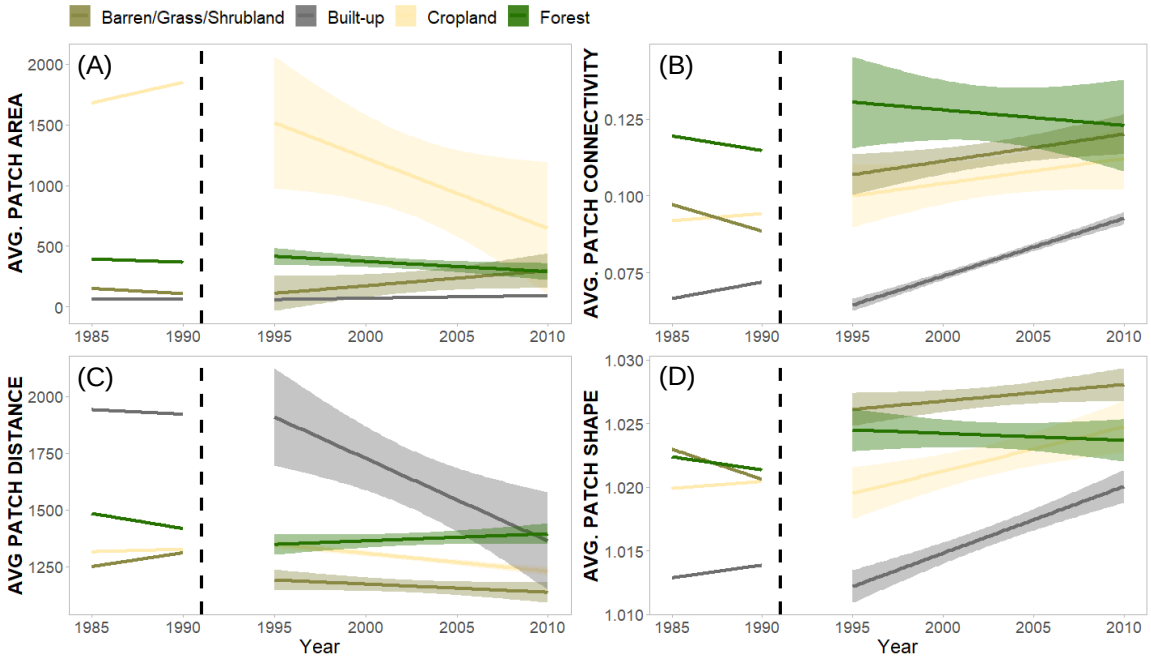

Figure 3. The average values of patch (A) area, (B) connectivity, (C) distance, and (D) shape landscape metrics by year and by class. Each plot has a vertical dotted line drawn at 1991, the year that the Soviet Union collapsed. Linear trends were calculated for datapoints before (1985-1990) and after the fall (1995-2010) of the Soviet Union, with standard errors calculated for 1995-2010 (there was insufficient data to calculate standard error for 1985-1990).

For many metrics and classes there was a change in values or trend after 1991 (Fig. 3). Croplands have some of the largest magnitudes of change, but depending on the metric, barren/grass/shrubland and built-up land also underwent substantial change. Forest experienced some change immediately after the 1991, but remained relatively constant.

Along with the overall decline in cropland, the average patch size decreased (Table 4, Fig. 3A). The croplands class experienced an increase in connectivity (Fig. 3B), a decrease in distance between patches (Fig. 3C), and increasing shape complexity (Fig. 3D). The average patch size of the barren/grass/shrublands class increased—similar to the total area (Fig. 3A, Table 4). Barren/grass/shrubland increased in patch connectivity (Fig. 3B), decreased in distance between patches (Fig. 3C), and experienced a jump in shape complexity (Fig. 3D). Consistent with the growth in built-up areas, the average patch size of built-up patches (i.e., urban areas) increased slightly (Table 4, Fig. 3A).

Patch connectivity and shape complexity also increased (Fig. 3B & 3D) while the average distance between urban patches decreased substantially (Fig. 3C). Forest patches did not change considerably in terms of size (Fig. 3A). The connectivity and shape complexity of forest patches increased post-1991 but decreased to 1985 levels by 2010 (Fig. 3B & 3D). The distance between forest patches also declined immediately after 1991 but increased from 1995 onward (Fig. 3C).

The Kruskal-Wallis test indicated that the changes in the composition and configuration of the LULC over time were statistically significant for all classes and metrics (Table 5).

Table 5. Kruskal-Wallis chi-squared values by metrics and by LULC class. All are statistically significant ($p<0.05$).

	Crop	**Barren/Grass /Shrubland**	**Built-up**	**Forest**
Size (Patch Area)	82.9	407.0	352.3	35.5
Connectivity (Contiguity Index)	79.6	412.9	321.7	35.1
Distance (Euclidean Nearest Neighbor Index)	101.5	1415.1	1869.2	105.5
Shape (Fractal Dimension Index)	82.0	342.2	356.8	30.9

The LSA change was different for each LULC class, with higher chi-squared values corresponding to a higher likelihood that the variation was not a product of chance (i.e., greater change). With the post-hoc analysis (Dunn Test), we examined the difference between 1985 and each subsequent year (Fig. 4). See Appendix C, Figs. 2-17 for the Dunn Test results for all year combinations.

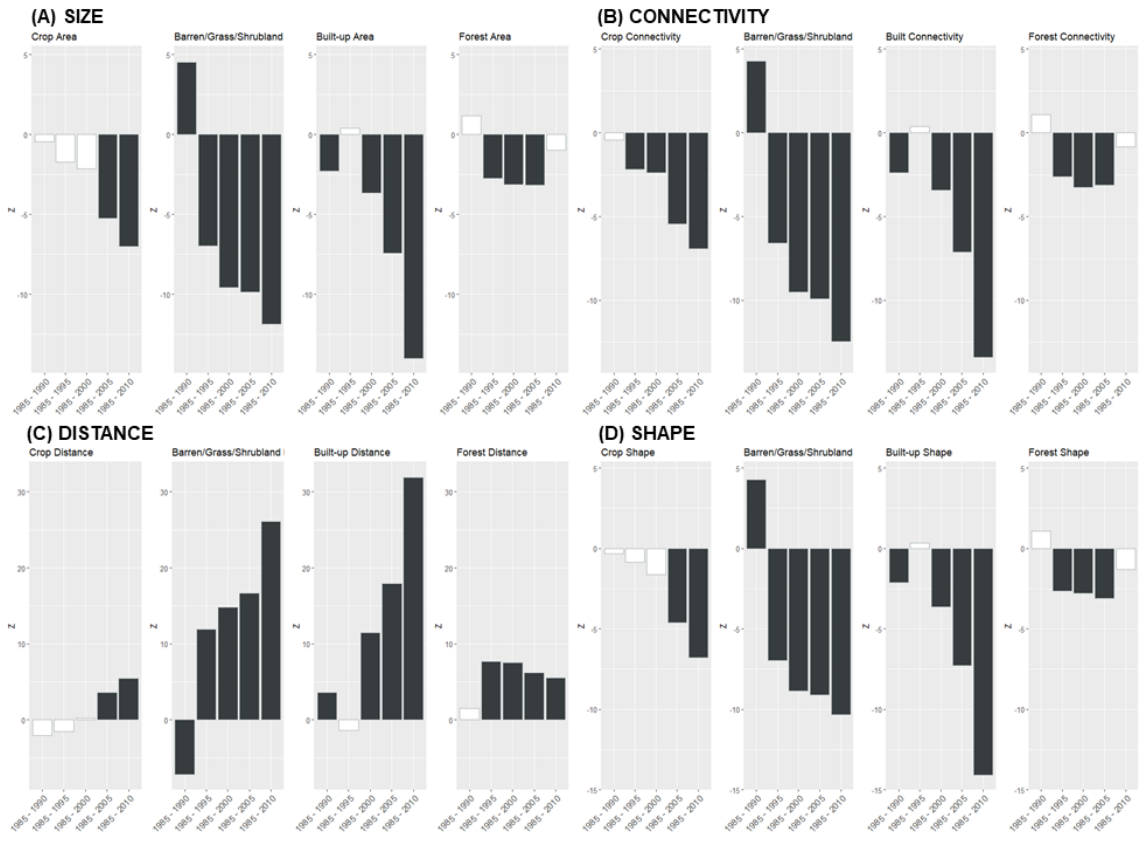

Figure 4. Bar plot of the Dunn test Z value for the comparison between 1985 and each subsequent year. Positive or negative Z values indicate the direction of the differences. Dark grey bars are statistically significant (p<0.05) and white bars are not.

The year in which the landscape metric values became statistically significantly different from 1985 varied by metric and LULC class. Barren/grass/shrubland showed a statistically significant difference immediately in 1990 and croplands took the longest to have statistically significant differences. By 2005, however, the differences were statistically significant for all metrics and LULC classes. After 2005, all classes remained significant except for forest. The forest class began to return to 1985 values in terms of size, connectivity, and shape (Fig. 4B, C, D). Forest areas also had the lowest magnitude of change for most metrics. Collectively, connectivity and distribution (measures of configuration) had a greater number of statistically significant years than size (a measure of composition).

3.4.1.2 Environmental Variables

Additionally, we examined the change over time for a selection of environmental variables calculated from satellite imagery. Table 6 presents the percent change of the environmental variables by class.

Table 6. Class average percent change between 1985 and subsequent years for each of the environmental variables.

		Brightness	Greenness	Wetness
Cropland	1985-1990	-4.7%	6.6%	-83.6%
	1985-1995	-2.3%	35.9%	-83.4%
	1985-2000	0.9%	34.5%	-53.9%
	1985-2005	1.5%	24.7%	-33.4%
	1985-2010	3.8%	2.5%	49.8%
Barren/Grass/ Shrubland	1985-1990	-4.4%	6.2%	-87.7%
	1985-1995	-4.3%	29.3%	-107.4%
	1985-2000	-1.6%	26.0%	-84.7%
	1985-2005	-1.7%	21.5%	-83.6%
	1985-2010	-2.8%	-7.2%	-13.6%
Built-up	1985-1990	-2.5%	22.2%	-40.4%
	1985-1995	-7.6%	68.1%	-69.4%
	1985-2000	-2.5%	63.8%	-38.0%
	1985-2005	-0.3%	62.3%	-22.4%
	1985-2010	-0.4%	36.8%	32.4%
Forest	1985-1990	1.0%	11.9%	-175.2%
	1985-1995	2.3%	30.6%	-205.5%
	1985-2000	2.8%	29.1%	-171.0%
	1985-2005	1.7%	28.3%	-197.6%
	1985-2010	-3.2%	9.1%	-79.5%

With a few exceptions, the absolute percent change of environmental variables peaked between 1995 and 2005. This is consistent with when the majority of landscape metrics began to show statistically significant change from pre-collapse values; 56% experienced statistically significant change in 1995, 87.5% by 2000, and 100% by 2005 (Fig. 4).

In the context of our results, brightness corresponds to the amount of bare soil or barren land in a given class. The brightness of cropland and barren/grass/shrubland decreased immediately in 1990, suggesting that a lower percentage of the crop class was

bare ground in 1990 and 1995. The percent change became positive in 2000 and was highest in 2010 which means that croplands had the highest proportion of bare soil that year. The amount of bare soil in forest lands increased until 2000, indicating perhaps some level of stress in the years before and after the collapse of the USSR which corresponds to some of the forest conversion seen in Figure 2. Brightness decreased in subsequent years and by 2010 the total amount of bare soil in the forest class was lower than 1985.

Greenness corresponds to the presence and health of vegetation in each LULC class. Of the four classes, built-up lands (i.e., urban areas) experienced the most change in vegetation, and cropland experienced the second highest change. The increase in the greenness of urban areas was likely a function of the increase in urban agriculture that occurred to meet the nutrition needs of urban residents. Correspondingly, the greenness of built-up lands peaked in 1995, immediately after the collapse of the Soviet Union and before new trade relationships were established.

Wetness—the amount of surface moisture in each class—declined for nearly all years and classes with forest lands showing the largest decline in wetness. The decline in the soil moisture of croplands could correspond to a decrease in irrigation. In other classes, which receive the majority of their moisture from rainfall, the meaning of the declining values is obscured by any year-over-year changes in precipitation.

3.5 Discussion

The land system architecture of Cuba underwent a variety of changes as a result of the Período Especial and the corresponding institutional transition. First, agricultural lands decreased in total area, patch size, and the distance between patches but increased in shape complexity and connectivity (Table 4, Fig. 3). These composition and configuration changes point to a move away from large standard plot sizes towards

smaller, irregularly sized plots. Much of the agricultural land transitioned to barren/grass/shrublands and a portion of it urbanized (Fig. 2, Table 4). There was some urbanization during this period, built-up lands increased in area, the distance between built-up patches decreased, and the average size, complexity, and connectivity increased (Table 4, Fig. 3). Finally, the composition and configuration of forest lands fluctuated somewhat with conversions to and from the barren/grass/shrubland class (Fig. 2), but by 2010 have values similar to before the Período Especial (Table 4, Fig. 3). Many of these changes are linked to policies that came into effect from 1980-2012 (Batchelder 1952; Diaz-Briquets and Pérez-López 2000; Gott 2004; Houck 2000); next, we link these policies to change in agriculture, urbanization, and forest lands/protected areas.

3.5.1 Agriculture

The Cuban government's response to the fall of the Soviet Union can be seen in several major agriculture policy changes, many of which occurred before 1991 as the USSR began to weaken. The first major change was Decreto No. 66 (1980), which established a free market for the sale of surplus agricultural projects. Second, several policies expanded legal rights and protections for agricultural cooperatives and urban farmers (Decreto No 66, 1980; Ley No. 36, 1982; Decreto Ley No. 125, 1991). Most salient to land tenure were 1) the allowances made for small plots of land to be inherited by others who have worked the lands (as opposed to a state-ownership model) (Instrucción No. 99, 1981) and 2) clarifying the use of usufruct lands (Decreto Ley No. 259, 2008).

The sequence of policies suggests that the transition from large, state-run plots to smaller, community or individually held plots was an iterative process. For example, free markets for agricultural goods were established in 1980 (Decreto No. 66), inheritance of small plots became legal in 1981 (Instrucción No. 99, 1981), and the use of usufruct land

was clarified in 2008 (Decreto Ley No. 259, 2008). Yet for many years after—in 1982, 1991, 1994, 2008 and 2012—additional regulations were added to the free market and land tenure changes (Decreto No. 106 ,1982; Decreto Ley No. 63, 1982; Decreto Ley No. 125, 1991; Decreto Ley No. 153, 1994; Decreto No. 282, 2008; Decreto Ley No. 300, 2012).

This iteration in the creation and implementation of policies may explain why the land system architecture showed impacts as quickly as five years and as late as two decades (Fig. 4, Table 6). The greatest percent change to the environmental variables computed for the cropland class occurred early in this range with absolute change peaking in 1990 for brightness and wetness and 1995 for greenness (Table 6). Similar changes are seen in the first few years of percent change of brightness, greenness, and wetness for the barren/grass/shrubland class (Table 6), which experienced an increase in area in tandem with the decline in cropland extent (Table 4, Fig. 4A).

3.5.2 Urbanization

The influence of agricultural change extended into Cuba's urban landscapes. In particular, a major consequence of the collapse of the USSR was food shortages in Cuba (Rodríguez-Ojea et al. 2002). In the early 1990s, Cuba had one of the worst per capita food production rates of any country in the Caribbean or Latin America; Cuba was dependent on imports for 90% of the fats, 55% of the calories, and 50% of the protein consumed in the country (Altieri and Funes-Monzote 2012; Koont 2011).

Partially a function of food scarcity, Cuba had significantly lower population growth than other Caribbean and Latin American countries (11.2% vs. 47.0%) between 1985 and 2010 (United Nations 2018a). The majority of population growth that did occur was in urban areas (World Bank Group 2019), and the extent of built up lands increased by 6% (Table 4). Consistent with this urbanization, the average patch size of built-up

lands (i.e., urban areas) increased (Fig. 3A), the average distance between urban patches decreased, and the connectivity and shape complexity of patches increased (Fig. 3).

The urbanization trend became statistically significant in 2000 (Fig. 4), approximately a decade after the Soviet Union's dissolution. This lag in urban growth could correspond with the time needed for Cubans to adapt and diversify their food sources (Bono and Finn 2017). With policies like Decreto No. 66 (1980), the government encouraged urban agriculture as a way to cope with the loss of Soviet subsides (Cruz and Medina 2003; Koont 2011; Premat 2012; Wright 2009). The increase in the greenness of urban areas (likely due to the increase of urban agriculture) peaked in 1995 immediately after the collapse of the Soviet Union and remained high until after the end of the Período Especial in 2000 (Table 6).

3.5.3 Forest Lands and Protected Area

Compared to the other LULC classes examined, forested lands experienced relatively little change in composition (Table 4) and a lower magnitude of configuration change (Fig. 3, 4). The relative stability of forest lands during this period of otherwise profound LULC change may be attributable to specific policy efforts made to protect forests and other natural areas in Cuba (Whittle and Santos 2006). The earliest law protecting forest land came before the collapse of the USSR, but the majority were instituted after the country had recovered from the initial economic shock of the collapse.

For example, Ley No. 27 (1980) established one of the first National Parks in the Sierra Maestra mountains. About a decade later, a comprehensive environmental law on protected areas and biodiversity was enacted (Ley No. 81, 1997), and a national system of protected areas was established (Ley No. 201, 1999). Also enacted after the collapse of the USSR were several policies aimed at protecting forests in particular (Ley No. 136,

1993; Ley No. 85, 1998; Decreto No. 268, 1999), as well as others that protected wildlife and terrestrial waters (Decreto Ley No. 138, 1993; Decreto No. 199, 1995), and regulated mineral extraction (Ley No. 76, 1995; Decreto No. 222, 1997).

The total area of forest land peaked in 1995 as did its absolute percent change in greenness and wetness (Table 4, 6). In 2010, greenness and wetness were closest to their pre-collapse values. Satellite imagery provides a very high-level assessment of environmental quality (Clinton et al. 2018; Wang et al. 2018), but these results point to some conversion, with a small peak and decline in both forest extent and vegetation quality (Fig. 2, Table 3, 5). This is corroborated by on-the-ground environmental assessments of invasive scrubland species (Perez, Noa, and Sinoga 2010), soil degradation (Medina et al. 2017) and water quality (Maal-Bared 2006) as well as research that has found that some of the keystone environmental policies were not fully implemented (Whittle and Santos 2006).

3.5.4 Land System Architecture

The combination of our lands system architecture and environmental variable results suggests that immediately after the 1991 shock, Cuban land systems underwent a transition that lasted from a few years to a few decades. Consistent with other examinations of post-shock land systems (Bergen et al. 2008; Kuemmerle et al. 2009; Munteanu et al. 2014; Peterson et al. 2009), some aspects of the land system architecture took new trajectories while others returned to pre-shock conditions (Chhetri, Stuhlmacher, and Ishtiaque 2019). Forest areas appeared to return to pre-shock values: by 2010, the total proportional cover returned to 17.4% (Table 3). Additionally, area, connectivity, and shape were no longer statistically significant in their difference from 1985 (Fig. 3A, B, D). In contrast, agriculture showed the opposite

trajectory: land tenure was fundamentally altered (Febles-González et al. 2011) with corresponding changes to composition and configuration (Table 4, Fig. 3, 4).

Previous research has largely examined the composition of LULC in Cuba (Gebelein 2012; Machado 2018). We found measures of configuration to have greater statistical significance than composition (Fig. 4) which shows the importance of considering both. We advocate for a land system architecture approach to capture greater nuisance around the role of governance in influencing land systems. Advancing understanding of this relationship also requires attention to the consequences of land system composition and configuration following more mundane institutional changes.

3.6 Conclusion

We found statistically significant changes to Cuba's land system architecture—the composition and configuration of land—which related to the policy changes made as a result of the Período Especial. Agriculture was one of the most salient ways in which the land use and cover of Cuba changed during this period. Leading up to and after the collapse of trade and subsidy relations with the USSR, the Cuban government instituted a series of policies to transition the country from large-scale, state supported mechanized agriculture to smaller, low-input farming (Cruz and Medina 2003; Premat 2012; Wright 2009). We see the likely manifestation of this change in the composition and configuration of cropland as well as the barren/grass/shrubland patches that took its place. Forest lands experienced the least amount of change, which was potentially attributable to the wide-ranging environmental protections established in this period (Whittle and Santos 2006). The largest differences from pre-collapse environmental proxy values (both positive and negative) occurred in 1995 and 2005, consistent with the timing of the majority of landscape metrics showing statistically significant change.

3.7 Acknowledgements

This research was carried out in the Environmental Remote Sensing and Geoinformatics Lab at Arizona State University (ASU). M.S. thanks the helpful staff at the Library of Congress's Law Library and the ASU School of Sustainability's Global Intensive Experience Scholarship for funding part of her trip to Cuba.

CHAPTER 4

IS URBAN FORM HOMOGENIZING IN GLOBAL CITIES?: ASSESSING GROWTH PATTERNS AND IMPLICATIONS

4.1 Abstract

In the past few decades, the world's population has become majority urban and cities are becoming increasingly globalized. Many have hypothesized that globalization will result in a homogenization of urban form in globalized cities, but this hypothesis has rarely been tested. Using satellite data and machine learning, we test the urban form homogenization hypothesis on the fifty largest cities of China, India, and the US, examining how the composition and configuration of urban areas have changed over time (1995-2015). Additionally, we quantify the impact of homogenization in terms of the temporal relationship between urban form and surface urban heat island intensity. There is some evidence of homogenization, with greater evidence for the most globalized cities in each country. Connectivity and shape show homogenization, and shape is also strongly related to both daytime and nighttime surface urban heat island intensity (with opposite relationships for day and night). Surface urban heat island is likely not the only socio-environmental impact of urban homogenization, we close with a discussion on what homogenization means for cities.

4.2 Introduction

The proportion of the world living in urban areas is growing along with the extent of urban areas (Liu et al. 2018; United Nations 2018a). In 1950, 30% of the world's population lived in urban areas, and by 2050 this proportion is expected to increase to 68% (United Nations 2018a). Urbanization has been especially dramatic in China, India, and the United States, which together contributed about 43% of the increase in urban areas globally between 1990 and 2010 (Liu et al. 2018). These profound population shifts

and corresponding urban growth have changed the form (i.e., composition and configuration) of cities. Composition is the area of a city's built footprint and configuration is the spatial arrangement—collectively these make up two-dimensional urban form (Turner et al. 2013).

The form of urban areas have a variety of socio-ecological consequences for cities and their surrounding landscapes (Eakin, Winkels, and Sendzimir 2009; Forman 2014; Seto et al. 2012; Turner et al. 2013). In terms of social impacts, the size of urban areas has been empirically related to wealth creation, innovation, and infrastructure—factors that determine the pace and quality of life for urban residents (Bettencourt et al. 2007). Environmental impacts of urban form include the alteration of hydrological networks (Hurkmans et al. 2009; McPhillips et al. 2019); energy, carbon, and nutrient flows (Chen and Chen 2015; Lin et al. 2014); and habitat availability and biodiversity (Hahs et al. 2009; Seto, Güneralp, and Hutyra 2012). In addition, the growth of urban areas contributes to an urban heat island effect which, in tandem with global climate change, has major consequences for human health and mortality in urban areas (Hondula, Georgescu, and Balling 2014; Oke et al. 2017). Prolonged extreme heat events (20 days or more per year) now affect around 30% of the world's population (Mora et al. 2017).

With the many effects that composition and configuration have on socio-environmental outcomes in cities, more work is needed on how the form of urban areas are changing and at what rate. The rapid increase in the built-up footprint of urban areas has occurred in tandem with globalization, with globalized forces likely playing a role in urban growth in the last few decades. As such, homogenization of urban form at a variety of scales has been hypothesized (Boone et al. 2012; Sassen 2008). There is limited research testing this hypothesis, but studies of a small number of cities or at coarser scales have found evidence of homogenization—as measured by changes in the

magnitude and the variation of landscape metric values over multiple years (Jenerette and Potere 2010; Seto and Fragkias 2005). If the form of global cities is homogenizing, cities will experience increasingly similar socio-ecological consequences; for example, increased intensity of the urban heat island effect.

Urban heat islands are influenced by the composition and configuration of built-up land as registered by both air and land surface temperature (Imhoff et al. 2010; Oke 1988). Land surface temperature (LST) and surface urban heat islands (SUHI), while not equivalent to air temperature, can be a useful proxy variable for studying urban heat because of its global coverage and high spatial resolution (Imhoff et al. 2010). The total area of impervious surface (i.e., composition) is often a primary predictor of SUHI intensity (Clinton and Gong 2013). Configuration also significantly contributes to LST (Kamarianakis et al. 2017; Galletti, Li, and Connors 2019). For example, a 10% increase in the spatial contiguity of built-up land has been predicted to increase urban air temperatures by 0.3-0.4°C in large US cities (Debbage and Shepherd 2015), and, in Shanghai, highly concentrated and adjacent built-up land was related to greater summer SUHI intensity (Li et al. 2011).

Increased understanding of how urban form contributes to SUHI intensity may improve mitigation efforts (Rosenzweig and Solecki 2015). For instance, small, dispersed, and oblong cities have been found to decrease urban heat island intensity (Zhou, Rybski, and Kropp 2017). A mosaic of natural land-cover classes interspersed within urban areas can provide a suite of socio-environmental benefits including decreased SUHI (Stuhlmacher et al. 2020). Star-shaped cities could keep the GHG emissions of transportation low while also avoiding some of the negative urban heat island implications of compact cities (Pierer and Creutzig 2019). In fact, commonly

employed urban adaptation strategies, may have the potential to completely counteract the urban heat island impacts of urban expansion (Georgescu et al. 2014).

In the era of globalization and global environmental change, there is a need for linking urban form changes to impacts in globalized cities around the world. If urban form is homogenizing, a multitude of socio-environmental outcomes will be affected, but there is little research examining urban homogenization and its impacts over time. We begin to fill this gap by quantifying year-over-year urban form changes of 150 global cities in China, India, and the United States, and examining the impacts on year-over-year SUHI intensity in those cities. Specifically, we ask:

1. Are large cities around the world homogenizing in terms of the configuration of their built land footprint?
2. How do the rates of growth in terms of size, shape, distribution, and connectivity influence homogenization in different countries?
3. How does homogenization, if detected, affect the surface urban heat island intensity?

Past research at this scale has been limited by data availability and computation power. Advances in remote sensing, parallel and cloud computing, and tools such as Google Earth Engine—which leverage these technological advances—allow research to be conducted at an unprecedented spatial scale with greater temporal and finer spatial resolution (Gorelick et al. 2017). The petabytes of data stored in the Earth Engine data catalog also streamlines the process of integrating datasets from multiple satellite and aerial sensors. Together, these innovations allow us to address our three questions by 1) classifying urbanization in the fifty largest cities of China, India, and the US, 2) examining how the composition and configuration of urban areas have changed over

time (1995-2015), and 3) quantifying the temporal relationship between urban form and surface urban heat island intensity.

4.3 Methodology

4.3.1 Study Areas

4.3.1.1 China

In the 1950s about 12% of China's population lived in urban areas, but by 2015, 56% of the country's population of approximately 1.4 billion people were urban residents (United Nations 2018a). During this rapid urbanization, the government of China invested considerably in urban infrastructure—about $116 per capita—and had an urbanization rate of 41% (Dobbs and Sankhe 2010). The urban population density of China is approximately 150 people per square kilometer (United Nations 2018a).

4.3.1.2. India

17% of India's population lived in urban areas in 1950; by 2015 33% of India's population of 1.3 billion people lived in urban areas (United Nations 2018a). India has very high urban population densities—approaching 441 people per square kilometer in 2015—but only spends about $17 per capita on capital investments in urban infrastructure with very little government oversight to growth (Dobbs and Sankhe 2010; United Nations 2018a). Between 1950 and 2005, the country had a 29% growth rate (Dobbs and Sankhe 2010; United Nations 2018a).

4.3.1.3 United States

Initial urban growth occurred in the US between 1790 and 1890, with increasing urbanization ever since (Census Bureau 2012). In 1950, 64% of the population lived in urban areas; by 2015, 82% of the country's population of approximately 321 million people lived in urban areas (Census Bureau 2016; United Nations 2018a). Controlled locally, urbanization in the US is often sprawling with discontinuous and spatially

expansive low-density development (Carruthers 2002); the population density in urban areas is a low 35.1 people per square kilometer (United Nations 2018a).

4.3.2 City Selection

The fifty most populous cities in each country in 2015 according to the GPWv4: Gridded Population of the World Version 4.1, UN-Adjusted Population Count (CIESIN and Columbia University 2018) were selected for analysis (Figure 1).

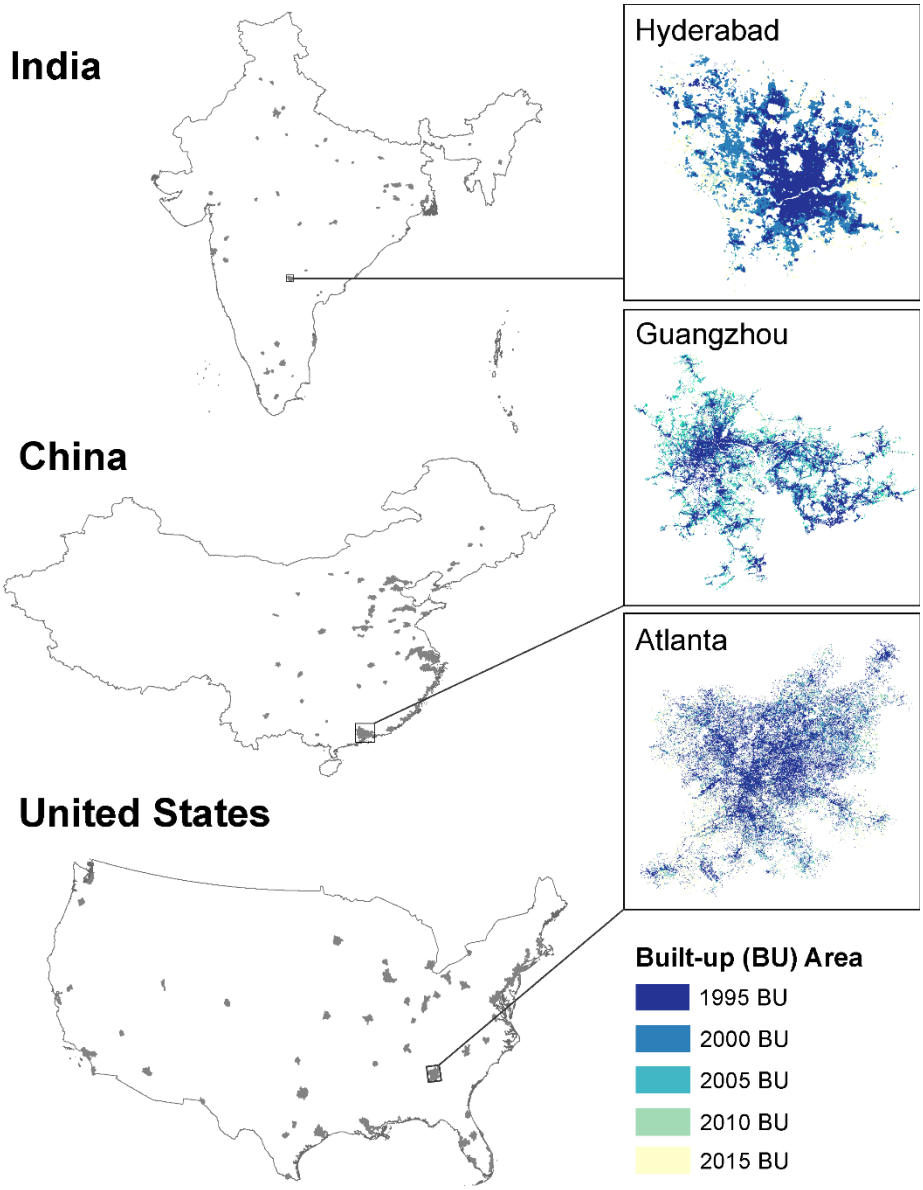

Figure 1. The fifty most populous cities in China, India, and the US (in grey). The insets are examples of urban growth from 1995-2015 in Guangzhou, China; Hyderabad, India; and Atlanta, USA.

We selected the same number of cities from each country instead of using a population threshold in order to prevent a wide variation in the number of cities analyzed per country. As noted, the US, India, and China have dramatically different per city populations and proportions of the population living in urban areas. We focused on large cities because their size suggests increased integration into the global economy with various shared interests affecting growth.

4.3.3 Data

A machine learning classification algorithm developed by Goldblatt et al. (2018) utilizing Landsat and nighttime light imagery was employed. The years of satellite launches and decommissions determined which satellite could be used for which years (Table 1).

Table 1. Landsat and nighttime light satellites available for use for each year of analysis

Year	Landsat Number	Nighttime Lights
1995	Landsat 5	DMSP-OLS
2000	Landsat 7	DMSP-OLS
2005	Landsat 7	DMSP-OLS
2010	Landsat 7	DMSP-OLS
2015	Landsat 8	VIIRS

To determine whether the different satellites could be substituted in our algorithm, Landsat 7 and Landsat 8 were tested and compared, as were DMSP-OLS and VIIRS for 2013, when all these sensors overlap. We found that the balanced accuracy of the Landsat 7 and 8 classifications are within one percentage point of each other for India and the US. Employing VIIRS (instead of DMSP-OLS) resulted in the same balanced accuracy in the US and improved the balanced accuracy in India by 4% (Appendix D, Table 1). China was not included in Goldblatt et al. (2018), so new thresholds were determined using the original methods.

4.3.3.1 Generating Training Data

A data-driven method was used to generate and label training data because of the large spatial and temporal coverage of our classification. To start, the landscape was subdivided into hexagons of three different sizes (Fig. 2). Using hexagons, which tile well over a round surface, reduced processing time and allowed the training data and classification to be calibrated to the landscape of that region.

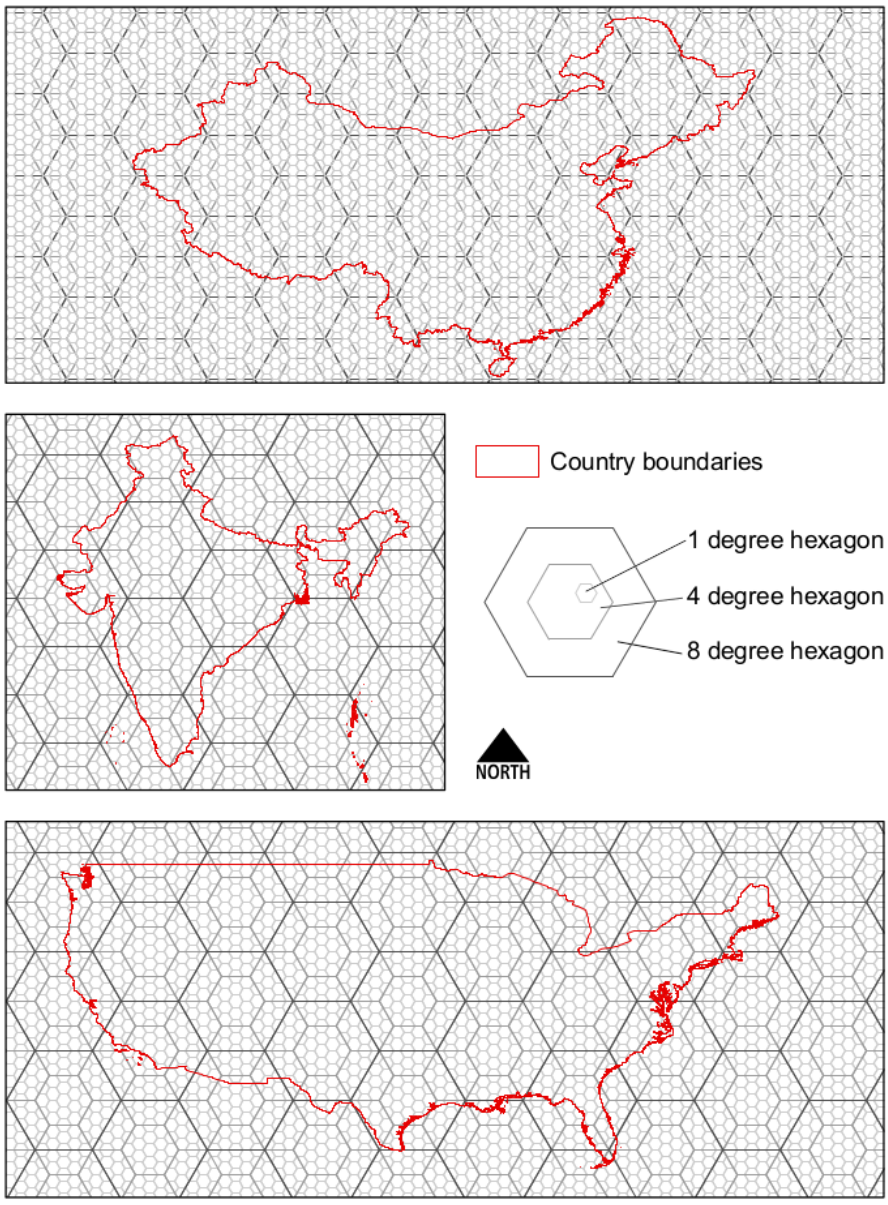

Figure 2. Hexagon sizes used in analysis (1, 4, and 8 decimal degrees) overlaid on unprojected country boundaries for China, India, and the US.

Within each hexagon, several thresholds were used to determine what area of the hexagon were likely built-up or non built-up. First, we calculated high and low nighttime light thresholds. All areas above the high threshold were likely built-up and all areas below the threshold were likely non built-up. From the likely built-up region, highly vegetated areas (using a NDVI threshold) as well as bodies of water (using a NDWI threshold) were masked out. NDVI, NDWI, and high and low nighttime light thresholds by country and sensor are presented in Appendix D, Table 2.

An equal number of points were scattered in the "likely built-up" and the "likely non built-up" regions delineated by the thresholds. Pixels in the range between the two were not sampled from. This method, applied to each hexagon, ensured that training samples were selected in a way that captured the variation between hexagons regardless of the level of nighttime lights in that hexagon. In total 120,000 points per country were randomly scattered.

4.3.4 Classification

These points and their corresponding labels of built-up (BU) or non built-up (NBU) were input into a Random Forest classifier with twenty trees. Twenty trees were used because the improvement in accuracy has been shown to level out between ten and one hundred trees (Goldblatt et al. 2016). The classification algorithm was applied every five years from 1995 to 2015. Imagery from years immediately before and after a given year were used to fill in any data gaps caused by clouds or Landsat 7's broken scanline corrector.

The classification was run within the set of interlocking hexagons (Fig. 2) and then all hexagons of corresponding size and country were mosaicked. For each country, two different sized hexagons were used to create the final classification composite. The most accurate hexagon size for each country made up the majority of the composite with

a different hexagon size filling in missing hexagons (i.e., hexagons that were excluded due to insufficient nighttime light data). In the US, 4-degree hexagons were used for the majority of the country with 1-degree hexagons filling in below and on the coasts. In India, 1-degree hexagons were used for the majority of the country with 8-degree hexagons filling in below and on the coasts. In China, 1-degree hexagons were used for the majority of the country with 4-degree hexagons filling in below and on the coasts.

The classification algorithm outputs a posterior probability between 0 and 1 for each pixel; the posterior probability threshold for each hexagon was selected using the Otsu method, which has been previously employed to threshold images with non-normal distributions of pixel values (Ng 2006). The Otsu algorithm utilizes nonparametric and unsupervised methods for automatic threshold selection (Otsu 1979). Here it was used to determine the threshold at which the variance between the BU and NBU class is maximized, resulting in a binary classification (Goldblatt et al. 2018). For the final post-processing, water (Carol et al. 2017) and gas flares (Elvidge et al. 2009) were masked out. Additionally, a 3x3 pixel square-kernel moving window and a year-over-year consistency check was applied to the finalized time series. Pixels which experience "impossible" oscillations between BU and NBU were recoded to their most likely class. An "impossible" oscillation is any pixel which deurbanizes for only one time-period after it urbanizes as well as the inverse (Schneider and Mertes 2014).

4.3.5 Accuracy Assessment

Accuracy assessments were undertaken using the original 61,953 validation polygons collected for Goldblatt et al. (2018). An additional 150,000 validation points were added for the years 1995, 2000, 2005, 2010, and 2015, with 10,000 points for each country and each year. The additional validation points were scattered via stratified random sampling as in Goldblatt et al. (2018). Hand labels of BU or NBU were

determined based on Landsat imagery (because of the lack of high-resolution imagery for the early years of the analysis) by two undergraduate researchers with a graduate researcher tie-breaking any label for which there was disagreement. Half of the total set of labeled points were used for threshold testing, and the full set of validation points was used to determine the final accuracy of each classification after post-processing.

Six accuracy metrics—overall accuracy, precision, true positive rate (TPR), true negative rate (TNR), balanced accuracy, and the F-measure—were calculated. We refer to the BU class as positive and the NBU class as negative. Thus, the number of correctly classified BU pixels was true positive (TP), the number of correctly classified NBU pixels was true negative (TN), the number of NBU pixels incorrectly classified as BU was false positive (FP), and the number of BU pixels incorrectly classified as NBU was false negative (FN).

$$Overall\ accuracy = \frac{TP + TN}{TP + TN + FP + FN}$$

$$Precision\ (a.k.a. user's\ accuracy) = \frac{TP}{TP + FP}$$

$$TPR\ (a.k.a. sensivity, recall, or\ producer's\ accuracy) = \frac{TP}{TP + FN}$$

$$TNR\ (a.k.a. specificity) = \frac{TN}{TN + FP}$$

$$Balanced\ accuracy = \frac{TPR + TNR}{2}$$

$$F\text{-}measure = 2 \times \frac{precision\ \times recall}{precision + recall}$$

4.3.6 Calculation of Landscape Metrics

Due to variation in the way that China, India, and the US define metropolitan boundaries, the City Clustering Algorithm was used to determine the extent of each metropolitan area (Rozenfeld et al. 2008). All pixels within a 5 km circular kernel were determined to be part of the same metropolitan area until no connected urban pixels remained (Oliveira, Andrade, and Makse 2014). Five landscape metrics were calculated

to quantify the size, shape, distribution, and connectivity of built-up land in each of the 150 metropolitan boundaries defined by the City Clustering Algorithm (Table 2). Landscape metrics are algorithms that quantify the spatial structure of land units, which we defined as groupings of pixels identified as built-up (Frazier 2019).

Table 2. Definition and equations for the landscape metrics used to quantify composition and configuration. Parenthesis below metric description is the name of the metric.

	Metric	Definition	Equation
SIZE composition	Area	Sum of the area of all pixels within the urban extent classified as built-up. Calculated in km².	$\sum_{j=i}^{n} a_{ij} \times 0.0009$
SHAPE configuration	Shape Complexity (Edge Density)	Measure of shape complexity. Calculated by taking the ratio of the length of edge to the total area.	$\frac{\sum_{k=1}^{m} e_{ik}}{A}$ (10000)
	Shape Compactness (Reock Score)	Measure of shape compactness. Calculated by finding the ration of class area to its minimum bounding circle.	$\frac{A}{C}$
CONNECTIVITY configuration	Connectedness (Patch Cohesion Index)	Measure of connectedness defined by the area and perimeter of groups of connected built-up pixels.	$\left[1 - \frac{\sum_{j=1}^{n} p_{ij}}{\sum_{j=1}^{n} p_{ij}\sqrt{a_{ij}}}\right] \times \left[1 - \frac{1}{\sqrt{Z}}\right]^{-1} \times 100$
DISTRIBUTION configuration	Adjacency (Percentage of Like Adjacencies)	Calculates the number of built-up pixels that are adjacent to built-up pixels divided by the total number of pixel adjacencies.	$\left(\frac{g_{ii}}{\sum_{k=1}^{m} g_{ik}}\right)(100)$

WHERE:
$a_{ij} = area\ in\ terms\ of\ number\ of\ cells,$
$A = \ total\ class/landscape\ area\ (m^2),$
$e_{ik} = total\ length\ (m)\ of\ edge\ involving\ class\ i\ and\ k,$
$p_{ij} = perimeter\ of\ patch\ ij\ in\ terms\ of\ number\ of\ cell\ surfaces,$
$Z = total\ number\ of\ cells\ in\ the\ landscape,$
$g_{ii} = number\ of\ like\ adjacencies\ between\ pixels\ of\ class\ i,$
$g_{ik} = number\ of\ like\ adjacencies\ between\ pixels\ of\ classes\ i\ \&\ k,$
$C = area\ of\ class'\ minimum\ bounding\ circle$

Edge Density, Percentage of Like Adjacencies, and the Patch Cohesion Index were calculated using FRAGSTATS version 4 (McGarigal, Cushman, and Ene 2012), and the Reock score (Reock 1961) was calculated using the compactr R function (Migurski 2018). These five metrics were chosen because of their use in previous research on urban areas (Alberti et al. 2007; Connors, Galletti, and Chow 2013; Fan et al. 2015; Kong et al. 2010).

4.3.7 Surface Urban Heat Island Intensity

To measure differences in land surface temperature (LST) between the cities and their outlying rural areas, a methodology similar to that employed by Debbage and Shepherd (2015) and Peng et al. (2012) was utilized. A buffer was set around the metropolitan boundary of a city. The size of the buffer was determined in accordance with the average city size per country: a 50km buffer is used in the US, 25km buffer in China, and a 1km buffer in India. To correct for the intervening effects of nearby water and urban areas—surface water and neighboring urban areas were subtracted from the buffer region. Surface water was defined using the MOD44W.006 Land Water Mask derived from MODIS and SRTM (Carol et al. 2017), and urban areas were defined using our classification. Additionally, to correct for the effect elevation has on temperature, only pixels that were within 50 meters of the average elevation of the urban area (Farr et al. 2007) were included in the rural buffer region (Debbage and Shepherd 2015).

Within the resulting urban and rural boundaries, the average daytime and nighttime summer LST was calculated. LST values were derived from the average of MOD11A2.006 Terra Land Surface Temperature and Emissivity 8-Day Global 1km images (Wan, Hook, and Hulley 2015) of three summer months (exact months vary by climate zone: June-August in China and the US and March-May in India) disregarding all pixels for which the QC band has a LST error > 2K as in Zhou et al. (2017).
The urban and rural values were then differenced—

$\Delta T = T_U - T_R$, where: T_U = urban temperature and T_R = rural temperature —to determine the magnitude of the surface urban heat island. This calculation was conducted for all 150 cities in our analysis for the years when MODIS is available (2000, 2005, 2010, 2015).

4.3.8 Statistical Analyses

Changes in the magnitude and the variation of urban form values over multiple years (i.e., temporal trends in homogenization or heterogenization) were first examined by via box and whisker plots. Second, a Kruskal-Wallis test was used to determine if the changes in the distribution were statistically significant. The Kruskal-Wallis test was appropriate because the distribution of the urban form values did not satisfy regression assumptions.

Repeated measures correlations were employed to determine if there was a statistically significant relationship between the change in the composition and configuration of a city and its SUHI intensity over time. Repeated measures correlations were preferred over a simple regression because the year-over-year urban form and SUHI values were not independent observations (Bakdash and Marusich 2017). We calculated the association of one area/pattern metrics with the SUHI intensity values for a group of cities using the Rmcorr R package (Marusich and Bakdash 2018). The regression assumptions of repeated measures correlations (linearity, equal variance, and normally distributed errors) were checked by using Q-Q plots and plotting the residuals.

SUHI intensity as well as the role of composition and configuration on SUHI processes have been found to vary based on the climatological conditions of the city (Imhoff et al. 2010; Zhou, Wang, and Cadenasso 2017), so we tested separating cities based on biome data from Dinerstein et al. (2017) which resulted in ten biome

groupings. We did not find biome to substantially effect our results; results separated by biome are available in Appendix D.

4.4 Results

4.4.1 Accuracy Assessment

Fifteen urban classifications were created—one for each country and for each year. Table 3 presents the performance measures of the fifteen classifications by country and year.

Table 3. Accuracy assessment of China, India, and US urban classification for the years 1995, 2000, 2005, 2010, and 2015.

	India				
	1995	**2000**	**2005**	**2010**	**2015**
Overall Accuracy	70.88%	75.97%	76.83%	76.91%	80.04%
Precision	89.64%	91.49%	93.06%	93.44%	89.76%
TPR	38.44%	52.88%	55.76%	56.78%	67.19%
TNR	96.49%	95.78%	96.18%	96.18%	92.54%
Balanced Accuracy	67.47%	74.33%	75.97%	76.48%	79.86%
F-measure	53.81%	67.02%	69.74%	70.63%	76.85%
	China				
	1995	**2000**	**2005**	**2010**	**2015**
Overall Accuracy	89.97%	89.83%	89.52%	91.21%	90.93%
Precision	80.90%	82.42%	86.76%	91.42%	97.14%
TPR	78.74%	81.70%	81.78%	86.15%	82.09%
TNR	93.75%	93.07%	93.53%	94.59%	98.05%
Balanced Accuracy	86.25%	87.38%	87.65%	90.37%	90.07%
F-measure	79.81%	82.06%	84.20%	88.71%	88.98%
	United States				
	1995	**2000**	**2005**	**2010**	**2015**
Overall Accuracy	80.46%	81.85%	83.28%	84.56%	84.63%
Precision	85.88%	87.31%	89.41%	90.07%	87.70%

TPR	58.11%	62.59%	66.30%	70.16%	72.89%
TNR	94.15%	94.18%	94.71%	94.60%	92.84%
Balanced Accuracy	76.13%	78.39%	80.51%	82.38%	82.87%
F-measure	69.32%	72.91%	76.14%	78.88%	79.61%

Despite disproportionately representing urban land in the stratified random sample, our validation dataset contained greater NBU points, so we focused primarily on the balanced accuracy, which corrects for this imbalance.

The lowest balanced accuracy for all three countries was 1995, with improvements in accuracy for subsequent years. We attribute lower accuracy in the early years to the fewer number of bands and the lower spatial resolution for some bands on Landsat 5 as well as greater difficulty in obtaining accurately labeled validation data (i.e., high resolution imagery is not widely available for this period). Of the three countries, China had the highest balanced accuracy, the US the second, and India the lowest. The wide variety of potential spectral signatures in urban areas in India along with the higher prevalence of informal developments made India more difficult to classify using transfer learning from nighttime lights. Overall, we found that our classification method was more or as accurate than other global classifications. Appendix D, Table 4 provides the balanced accuracy of MODIS MCD12Q2.006 Land Cover Dynamics Yearly Global 500m dataset (Friedl and Sulla-Menashe 2019) and GlobCover: Global Land Cover Map (European Space Agency and Université Catholique de Louvain 2010) using our validation set.

4.4.2 Research Question 1: Homogenization

We first examined homogenization descriptively with the distribution of urban composition and configuration values 1995 to 2015 (Fig. 3). A Kruskal-Wallis test was used to determine if the change over time had at least one statistically significant

difference between the median values of each year (Fig. 3). All were statistically significant, but larger chi-squared values correspond to greater change.

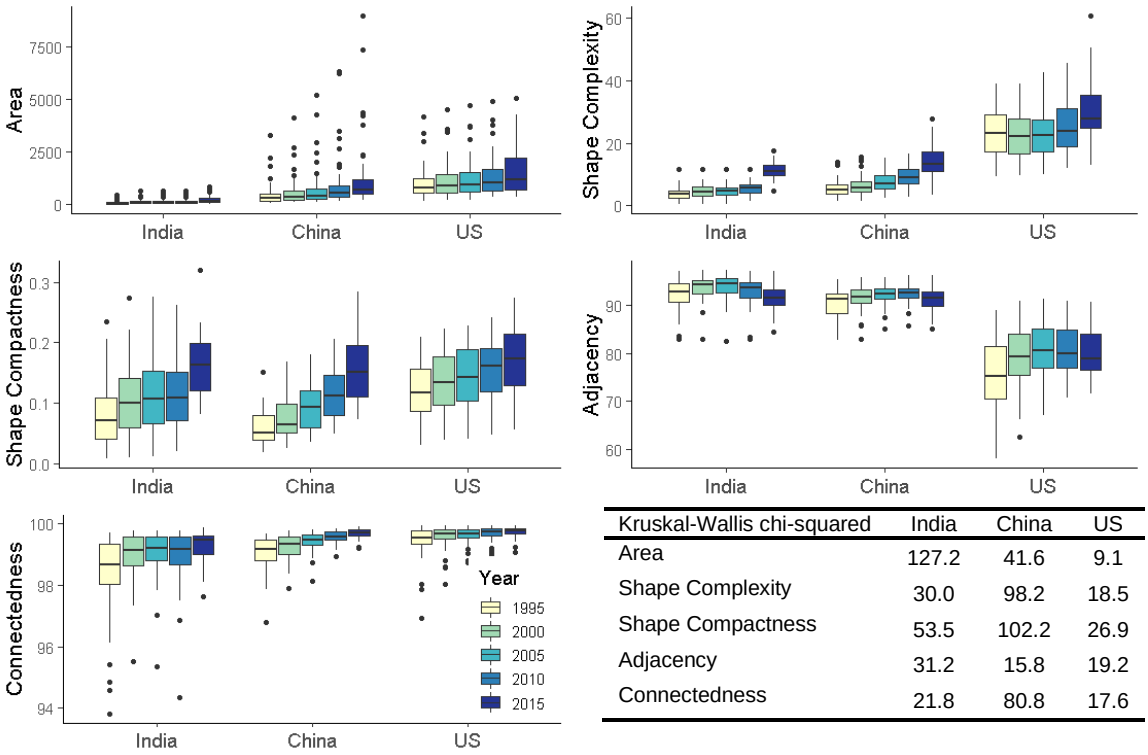

Kruskal-Wallis chi-squared	India	China	US
Area	127.2	41.6	9.1
Shape Complexity	30.0	98.2	18.5
Shape Compactness	53.5	102.2	26.9
Adjacency	31.2	15.8	19.2
Connectedness	21.8	80.8	17.6

Figure 3. Distribution of area and pattern metrics for the 50 largest cities in China, India, and the US for 1995-2015. Area, shape compactness, connectivity, and shape complexity increase each year. Adjacency is the exception—it peaks around 2005 or 2010 (depending on the country) and then declines in 2015. The table presents the Kruskal-Wallis chi-squared test results. All values are statistically significant ($p < 0.05$).

Area, shape complexity, and connectedness increased and shape compactness decreased (0 = most compact) for the large, populous cities in each country. Adjacency peaked in 2010 for China and 2005 for India and the US. Connectedness—because of the similar trend and decreasing variance—was the only metric that showed potential homogenization across all 50 cities in each country. The saturation of very high connectedness values may be an argument against homogenization, but adjacency saw a similar saturation in the peaks of 2005 and 2010 but did not continue to homogenize in the same way that connectedness continued to.

The case for homogenization is stronger for the ten largest cities in each country (Fig. 4).

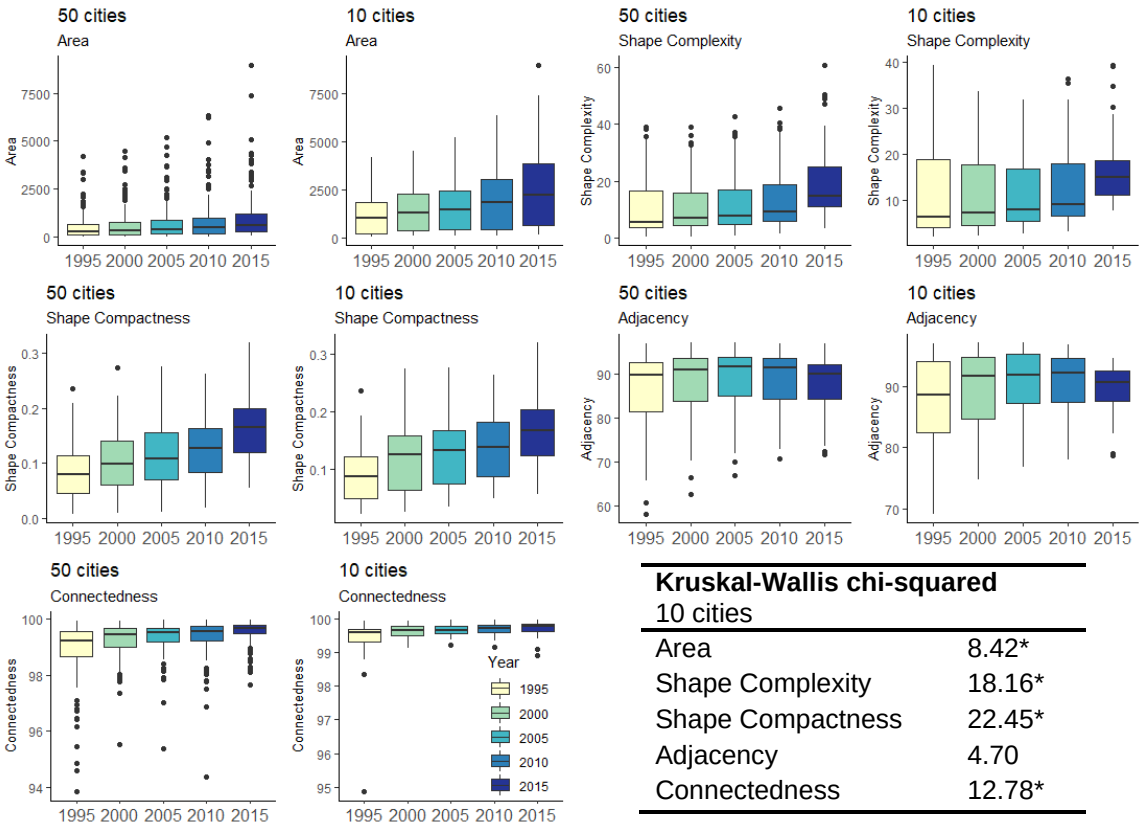

Kruskal-Wallis chi-squared 10 cities	
Area	8.42*
Shape Complexity	18.16*
Shape Compactness	22.45*
Adjacency	4.70
Connectedness	12.78*

Figure 4. Distribution of composition and configuration metrics for the 50 (left) and 10 (right) most populous cities in China, India, and the US for 1995-2015. For the 10 most populous cities in each country (30 total), area, shape complexity, shape compactness and connectivity have a statistically significant differences between years ($p < 0.05$). Adjacency peaks in 2010 and is not statistically significant. Except for area, the variance of the metrics values decreases, pointing to homogenization in the very largest cities of each country. All statistically significant values in the Kruskal-Wallis table are marked *.

These larger cities were more likely to be shaped by global forces, such as international trade, and the analysis showed a trend toward homogenization for the two measures of shape (complexity and compactness) in addition to connectivity.

4.4.3 Research Question 2: Rate of Change

Many of the composition and configuration metrics followed similar trends, but the pace of change was distinct for each country. The average percent change was largest for India and smallest for the US (Table 4).

Table 4. Average percent change of urban form by country from 1995-2015. Left column presents the percent change for the 50 most populous cities, right column is just the 10 most populous.

Average Percent Change (1995-2015)	India		China		United States	
No. of cities:	**50**	**10**	**50**	**10**	**50**	**10**
Area	330.6%	165.0%	210.5%	196.8%	61.1%	43.7%
Shape Complexity	333.8%	212.4%	188.2%	162.1%	31.2%	6.67%
Shape Compactness	201.7%	139.7%	192.9%	199.3%	56.2%	37.7%
Adjacency	-0.57%	-1.1%	1.05%	1.84%	6.25%	7.61%
Connectedness	1.0%	0.52%	0.63%	0.57%	0.30%	0.10%

The average rate of change for the 10 most populous cities in each country was lower than the average for all 50 (Table 4), which suggests that the majority of urban form change was not occurring in the 10 most populous cities. Of the three countries, India had the largest gap in the rate of change between 50 cities and 10 cities, indicating that mid-sized cities (the remaining 40 of the 50 most populous) were changing the fastest in India.

These rates of change (Table 4) as well as the distribution of metric values (Fig. 3) suggest that India, China, and the US may represent three snapshots along a homogenization trajectory. Descriptively for all 150 cities, India in 2015 had an urban form similar to China in 1995 and China in 2015 showed similarities to the urban form of the US in 1995 (Fig. 3). These trends were particularly salient for area, shape complexity and shape compactness which are related to urban expansion and sprawl.

4.4.4 Research Question 3: Homogenization and Surface Urban Heat Island

The homogenization of the configuration of major cities in China, India, and the US has implication for the SUHI experienced by the millions of residents of these

metropolitan areas. Figure 5 visualizes the distribution of daytime and nighttime SUHI intensity for the 50 largest cities in each country from 2000 – 2015.

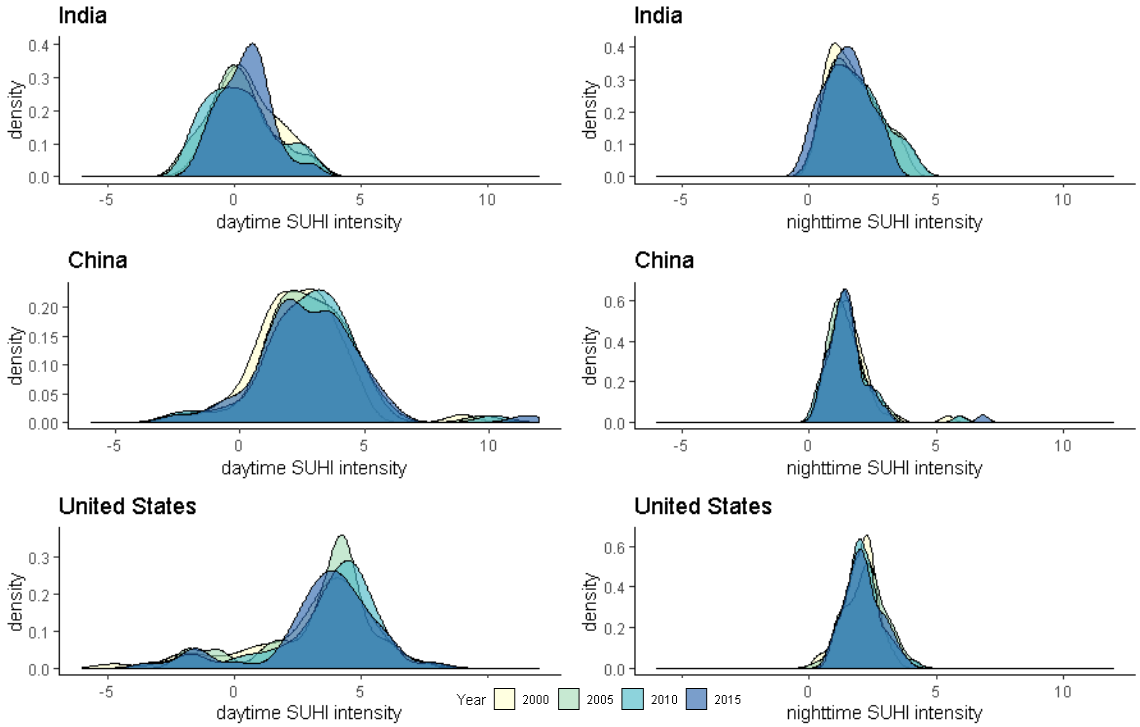

Figure 5. Distribution of yearly daytime and nighttime surface urban heat island (SUHI) intensity by country. China and the US had a greater range of SUHI intensities and more outliers.

Daytime SUHI intensity ranged from less than -5°C to greater than 10°C. Cities in China and the US experienced nearly the full range, while cities in India had a narrower range. Nighttime SUHI intensity were largely between 0-5°C, with ~2°C being the most common nighttime SUHI intensity. Temporal trends between the countries were fairly uneven. Generally, 2015 had a narrower spread of values but daytime SUHI in the US was an exception. See Appendix D for a discussion on how SUHI intensity differed by biome.

The change in SUHI intensity over time had statistically significant relationships with changes in the composition and configuration of the built-up land in the 150 large, populous cities in India, China, and the United States (Figure 6).

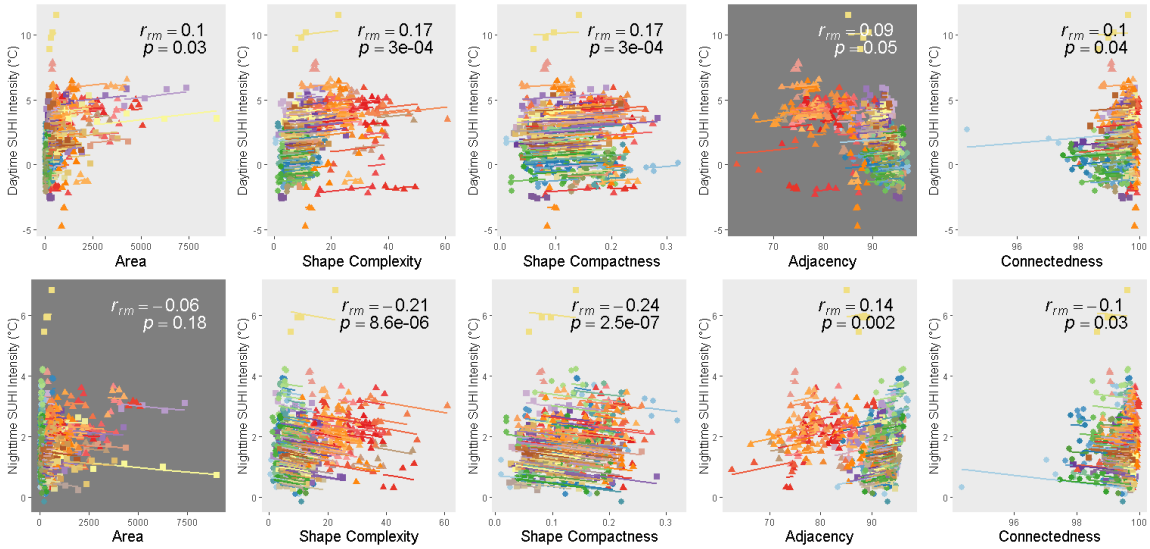

Figure 6. Repeated measures correlation for the 150 cities between area, shape complexity, shape compactness, adjacency, connectedness, daytime (top row), and nighttime (bottom row) surface urban heat island intensity. Each color corresponds to a different city with the points marking the yearly relationship (one point is one year) between a given pattern metric and surface urban heat island intensity. Circular points correspond to Indian cities, triangular points correspond to US cities, and square points correspond to Chinese cities. The lines are the common regression slopes for each of the 150 cities over time. Light grey plots are statistically significant (p<0.05) and dark grey plots are not.

Daytime SUHI intensity had statistically significant relationships with area, shape complexity, shape compactness, and connectedness. As area, shape complexity, and connectedness increased and as shape compactness decreased over time, the daytime SUHI intensity increased. Nighttime SUHI intensity has statistically significant relationships with shape complexity, shape compactness, adjacency, and connectedness. As shape complexity increased, connectedness increased, and shape compactness decreased, nighttime SUHI decreased; but as adjacency increased over time, so did nighttime SUHI. Shape complexity, shape compactness, and connectedness were significant for both daytime and nighttime SUHI intensity, but they had opposite relationships. See Appendix D for a discussion on the similarities and differences between the statistically significant repeated measures trends and the individual city trends.

Shape compactness and shape complexity had the highest R_{rm} coefficients, suggesting that changes to shape complexity and compactness would affect SUHI more than the other composition and configuration change. Shape complexity and compactness are related to sprawl: shape compactness is a function of the directions of development from the city center and infill (or the lack thereof), while shape complexity measures the jaggedness of a city's boundaries (Bhatta, Saraswati, and Bandyopadhyay 2010). Additionally, nighttime SUHI had higher R_{rm} coefficients for shape compactness and complexity than daytime SUHI, suggesting that nighttime SUHI intensity may be more substantially altered by changes in urban form. This is corroborated by the SUHI, shape compactness, and shape complexity trajectories for the subset of the ten largest cities in each country (Fig. 7).

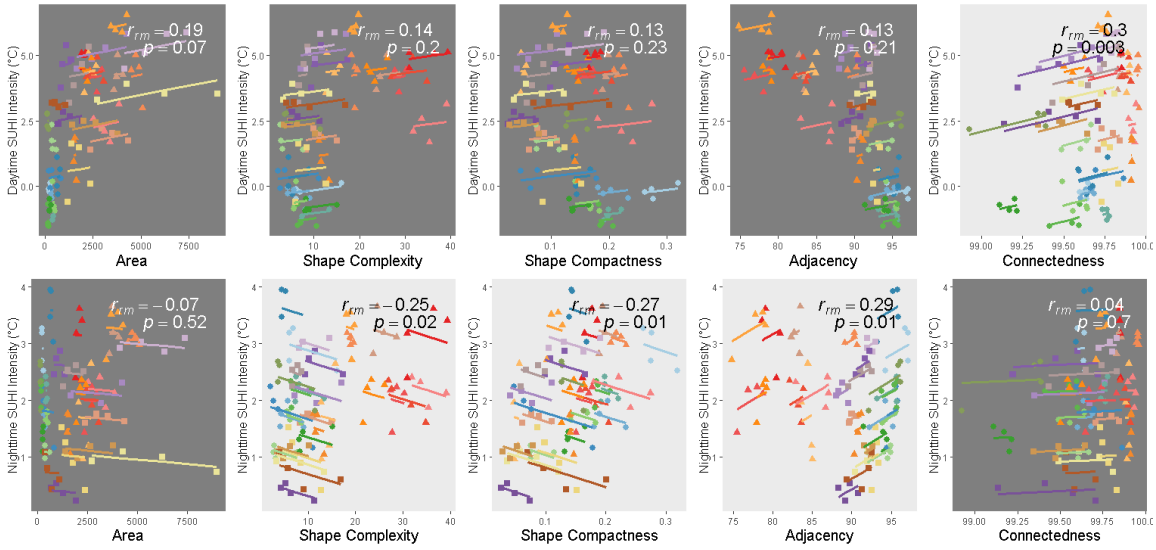

Figure 7. Repeated measures correlation for the 30 most populous cities between area, shape complexity, shape compactness, adjacency, connectedness, daytime (top row), and nighttime (bottom row) surface urban heat island intensity. Each color corresponds to a different city with the points marking the yearly relationship between a given pattern metric and surface urban heat island intensity. The lines are the common regression slopes for each of the 30 cities over time. Light grey plots are statistically significant (p<0.05) and dark grey plots are not. Circular points correspond to Indian cities, triangular points correspond to US cities, and square points correspond to Chinese cities.

The ten largest cities in each country had fewer statistically significant relationships with composition and configuration because their composition and configuration were not changing as rapidly as smaller cities (Table 4). The relationships that were statistically significant have the same direction of trend as when all 50 cities in each country are considered (Fig. 6). Showing similar arrangement, but more visible in this subset of cities, is the SUHI and urban form difference between the US, China, and India.

The 10 largest cities in each country clearly illustrate the differences and similarities in how the homogenization of urban form affected the SUHI in each country. The US often had greater daytime SUHI intensity and corresponding metric values (i.e., greater area and shape complexity), with China overlapping or a couple of years behind. India consistently had the lowest daytime SUHI but with later years beginning to overlap with the end range of US and China. Conversely, nighttime SUHI had a greater mix of countries at high and low intensity, especially in the middle range between 1-3°C.

4.5 Discussion

4.5.1 Homogenization

Often hypothesized, but rarely tested, we have found that the built-up footprint of global cities around the world are homogenizing in some respects. The 50 largest cities in China, India, and the US showed a homogenization of urban form in terms of connectivity (Fig. 3) and the 10 largest cities in each country show a homogenization in terms of connectivity and shape (Fig.4). This homogenization is congruent with that identified in previous research on cities in China (Seto and Fragkias 2005) and globally (Jenerette and Potere 2010). Additionally, it corresponds with examinations focused on homogenization of suburban landscapes, in particular residential landscapes (Groffman et al. 2014; Polsky et al. 2014).

4.5.2 Homogenization and Surface Urban Heat Island Intensity

Considerable previous research has examined the relationship between urban form and SUHI intensity (Debbage and Shepherd 2015; J. Li et al. 2011; Xiaoxiao Li et al. 2016; Pierer and Creutzig 2019; Zhang, Middel, and Turner 2019; B. Zhou, Rybski, and Kropp 2017; Galletti, Li, and Connors 2019). In order to examine the specific effect of homogenization on SUHI, our analysis considered the relationship between urban form and SUHI intensity as the cities grew in size and became more similar in terms of configuration. We found that two measures of shape—complexity and compactness—were changing the fastest (Table 4), had higher R_{rm} coefficients (Fig. 6), and were homogenizing in the 10 largest cities (Fig. 4). While previous research is divided on whether composition (size) or configuration (shape, connectivity, adjacency) has a larger role in SUHI intensity, this study and others find that configuration, in particular shape, is significant and may have primacy (Li et al. 2016; Stuhlmacher et al. 2020).

The intensity of the daytime and nighttime SUHI effect had opposing relationships with urban form (Fig. 6, 7). The diurnal differences in urban heat islands are well known (Arnfield 2003; Kalnay and Cai 2003; Oke et al. 2017) and previous research on urban form, daytime, and nighttime SUHI intensity has suggested that daytime and nighttime SUHI heat island operate via different mechanisms (Peng et al. 2012; Zhang, Middel, and Turner 2019). Adding to this literature, our paper is among the first to consider SUHI and urban form change over multiple years. We find that daytime SUHI intensity had greater variation in yearly values and year-over-year values than nighttime SUHI intensity (Fig. 5) but that nighttime SUHI had stronger relationships with urban form over time (Fig. 6 & 7).

4.5.3 Implications for Cities

The homogenization of urban form suggests that global cities will face similar challenges induced by similarities in the configuration of their urban landscape. Urban form has consequences for a variety of processes in cities including the rates of plant and animal phenology change (Alberti et al. 2017), urban hydrological networks (Hurkmans et al. 2009; McPhillips et al. 2019), energy, carbon, and nutrient flows (Chen and Chen 2015; Lin et al. 2014; Seto, Güneralp, and Hutyra 2012), habitat availability (Hahs et al. 2009) and, as discussed here, SUHI intensity. The consequences of homogenizing urban form on these processes can be both positive and negative. To mitigate negative consequences, urban planning practitioners can make interventions that modify urban form. Our findings have two implications for urban planning and other city practitioners.

First, we consistently found that urban form related to sprawl—shape complexity and compactness—changed the fastest and were most relevant in terms of both homogenization and SUHI intensity (Table 4, Figs. 4, 6). City sprawl is relevant in the US (Bounoua et al. 2018) which already has very high levels as well as in China and India (Deng et al. 2019; Rahman et al. 2011) where sprawl is increasing quickly (Fig. 3, Table 4). In particular, we find urban expansion and increased sprawl to be fastest in mid-sized cities (Table 4) which is consistent with the higher rates of growth of small-medium urban areas noted in a recent global synthesis (Güneralp et al. 2020).

In addition to contributing to SUHI, sprawl has a variety of other socio-environmental consequences that warrant attention (Ewing et al. 2016; Nechyba and Walsh 2004). Reducing sprawl (i.e., decreasing shape complexity and increasing shape compactness) corresponds to lower daytime SUHI intensity but higher nighttime SUHI intensity (Figs. 6, 7). When making decisions that change urban form, urban planners

will have to make trade-offs or optimizations between daytime and nighttime SUHI (as well as other socio-ecological consequences).

Second, a descriptive interpretation of our results is that the urban form of India, China, and the US represent sequential snapshots on a trajectory towards potential homogenization. Congruent with each country's current development trajectory (Seto et al. 2011), India in 2015 looks similar to China in 1995 and China in 2015 looks similar to the US in 1995 (Fig. 3). We find these snapshots mirrored in the percent change each country experiences: India has the fastest rate of change, China the second, and the US the slowest (Table 4). As well as in the countries' trajectories in relation to urban form and SUHI (Fig. 7). Following each other on a trajectory towards homogenization means there is potential for learning from the country or city that is just ahead or farther ahead on the trajectory (Boone et al. 2012). Cities contending with similar globalized forces stand to benefit most. In response, creating and strengthening networks among the world's largest cities to share best-practices may improve urban sustainability and resilience worldwide (Childers et al. 2014).

4.6 Conclusion

The urban form of the most populous cities in China, India, and the US homogenized in terms of shape and connectivity between 1995 and 2015. The rate at which the urban form changed was highest in India and lowest in the US. While this homogenization has implications for numerous socio-environmental processes, those involving the intensity of the SUHI effect indicated that shape complexity and shape compactness (measures of sprawl) were most important. Day and night SUHI intensities exhibited the opposite relationship with sprawl, indicating there are tradeoffs or optimizations that must be made in the mitigation process.

As a result of urban form homogenization and global environmental change, cities around the world are facing similar challenges. Attention to the spatial arrangement of urban areas can help illuminate the linkages between urban form and environmental outcomes. While research of this kind has begun to increase, more effort is required from various communities of researchers to address the fundamental processes of and the complex challenges posed by our urban landscapes.

4.7 Acknowledgements

This research was carried out in the Environmental Remote Sensing and Geoinformatics Lab at Arizona State University (ASU). We thank Asher, Sam Meltzer, Jessica Leffel, Allison Kubaik, Julia Marturano, and Richard Teasdale for their assistance in creating the validation dataset. Thank you also to Vishesh Gupta who ran early versions of the India classification.

MS and MG were supported by the National Science Foundation Sustainability Research Network (SRN) Cooperative Agreement 1444758, the Urban Water Innovation Network (UWIN).

CHAPTER 5

LANDSCAPE TO PATCH: CONCLUDING THOUGHTS

Geography has a long tradition of studying human-environment relationships, stretching from Alexander von Humboldt's insistence on integrated science through the *landschaft* work in Germany, landscape morphology, environmental hazards in the United States, and into contemporary interests in cultural and political ecology and land system science (LSS) (Turner 2002). LSS constitutes a science-based vision of human-environment relationships, growing from cultural ecology (e.g., Moran 2016) and stimulated by international research agendas on global environmental change and sustainability (Turner, Lambin, and Reenberg 2007). It focuses on the interactive human-environmental dynamics affecting landscapes or land systems, with various implications examined. Importantly, LSS integrates two historically distinctive dimensions of the geographical sciences, the spatial-temporal dimensions focused on the spatial attributes of phenomena and human-environmental ones (Turner, Lambin, and Reenberg 2007).

This dissertation is embedded in LSS, addressing questions about human-environmental dynamics and employing spatial analysis—especially remote sensing—to explore questions about land system architecture (LSA) (Turner et al. 2013). As such this dissertation melds the interests of each geographical dimension through three case studies operating at three distinctive spatial scales. Each case study examined how broad socio-economic or political-institutional drivers affected the architecture or design of the land system, with consequences for the environmental outcomes of that system. Results from each of the case studies are reviewed below.

5.1 Summaries of Chapters

5.1.1 Chapter Two

In the second chapter, LSA and environmental consequences of two development project in the Phoenix metropolitan area were examined. We found that divergent design intentions affected the resultant LSA at the Rio Salado and New River riparian sites. Two LSA changes, in particular, resulted in divergent environmental outcomes for the redevelopment of the Rio Salado site. The first is related to configuration. The distribution of the built-up, vegetation, and desert classes had statistically significant relationships with all examined environmental variables (i.e., land surface temperature, vegetation, and bird community). The second is related to composition, in particular the addition of Tempe Town Lake. The 4% increase in water allowed the site to support more waterbird and warbler species than the conventional development around the New River wash.

The results of this work provide insights about identifying and monitoring the success of urban riparian redevelopment goals. Many riparian redevelopments are focused on water, and while the composition of water did have a sizeable effect on the environmental outcomes at the Rio Salado, the configuration of the landscape had a greater number of statistically significant relationships. Building from the broadened perspective of the landscape, the incorporation of both social and environmental dimensions—as well as the corresponding stakeholders—is essential to identify and monitor relevant socio-environmental outcomes.

5.1.2 Chapter Three

The third chapter used patch as the unit of analysis to examine if the LSA of Cuba changed as a result of the institutional shifts brought about by the 1991 collapse of the Soviet Union and how this change related to certain environmental outcomes. We found

statistically significant LSA change that linked to policies enacted in response to the Soviet Union's collapse and subsequent economic crisis. Depending on the element of LSA or the environmental outcome variable (i.e., brightness, greenness, wetness) examined, statistically significant change occurred five years to a several decades after the collapse of the Soviet support.

We found that when specific polices were implemented, and how, played a large role in the timing and type of change for croplands and the lack of change in forest lands. Croplands were the most affected class; they transitioned from large, standard sized plots associated with Soviet subsidized industrial agriculture to irregularly shaped, small plots, farmed with low-input methods by cooperative community groups. The policies of this period showed a clear trajectory of support for this transition with modifications to land tenure, establishing a free market for agricultural goods, and expanding other legal protections for farmers. Forest lands had the lowest magnitude of change, owing in part, to the environmental policies enacted starting in 1991 establishing a national system of protected areas and protecting forest lands in particular.

5.1.3 Chapter Four

The fourth chapter was focused on just one class: built-up lands in the fifty most populous cities in China, India, and the United States. It aimed to determine if the urban form (LSA) of cities was homogenizing and the significance of homogenization for the surface urban heat island (SUHI) effect. We found that all 150 cities are following a similar trend (becoming larger, similar in shape, and connected) but homogenization was most evident in the three country's thirty largest cities. This urban form change was associated with a change in SUHI intensity particularly for form changes related to sprawl (shape complexity and shape compactness). Shape complexity and compactness, however, had opposite relationships with daytime and nighttime SUHI.

These findings have implications for designing urban landscapes. Sprawl has a complicated relationship with SUHI, so should be managed in relation to the desired reduction of SUHI as well as other negative impacts of sprawl, such as economic inefficiencies, ecological problems, and social inequitable conditions (Ewing et al. 2016; Nechyba and Walsh 2004). Reducing sprawl corresponds to decreasing shape complexity and increasing shape compactness but daytime and nighttime SUHI have opposite relationships—decreased shape complexity corresponds to lower daytime SUHI but higher nighttime SUHI and increasing shape compactness corresponds to lower daytime SUHI but higher nighttime SUHI. Thus, reducing sprawl involves making trade-offs or optimizations between reducing SUHI during daytime or nighttime (Zhang, Murray, and Turner 2017). Balancing these trade-offs should be specific to the priorities of a given city, which for SUHI, are likely associated with a city's climatic conditions. Phoenix, for example, may choose to prioritize reducing nighttime SUHI because it contributes to higher heat-related mortality when homeless people (or other people without access to adequate air conditioning or cooling shelters) are unable to cool their core body temperature overnight (Laaidi et al. 2012).

5.2 Landscape Metrics

A core component of this dissertation are the metrics used to quantify landscape composition and configuration. For each dissertation chapter, a larger set of metrics was calculated and then subset based on relevance to the case study's research questions and data. Table 1 presents the final set of landscape metrics that were used in each case study.

Table 1. Names, definitions, and equations of the landscape metrics used for each chapter of the dissertation. Aspects of composition and configuration are in the left column with corresponding metrics in columns to the right.

	CHAPTER 2	CHAPTER 3	CHAPTER 4
SIZE (composition)	Percentage of Landscape Proportional abundance of each class type in the landscape. Calculated: $\frac{\sum_{j=i}^{n} a_{ij} \times 900}{Z}$	Patch Area Sum of all pixels in a given patch. Calculated in hectares: $a_{ij} \times 250$	Class Area Sum of the area of all pixels within the urban extent classified as built-up. Calculated in km²: $\sum_{j=i}^{n} a_{ij} \times 0.0009$
SHAPE (configuration)	Median Shape Index Median value of each patch in a given class' shape complexity as defined by: $\left(\frac{p_{ij}}{\min p_{ij}}\right)_{50\%}$	Fractal Dimension Index Measure of shape complexity computed with a patch's area and perimeter: $\frac{2 \times \ln(0.25(p_{ij} \times 500))}{\ln(a_{ij} \times 250{,}000)}$	Edge Density Measure of edge complexity by computing the ratio of the length of edge to the total area: $\frac{\sum_{k=1}^{m} e_{ik}}{A}$ (10000) Reock Score Ratio of class area to its minimum bounding circle: $\frac{A}{C}$
CONNECTIVITY (configuration)	Median Euclidean Nearest-Neighbor Index Median value of the distance each patch to the nearest patch of the same class. Equation is represented as: $h_{ij_{50\%}}$	Contiguity Index Assess spatial connectedness of pixels in the same patch: $\frac{\left[\frac{\sum_{r=1}^{z} c_{ijr}}{a_{ij}}\right] - 1}{v - 1}$	Patch Cohesion Index Measure of connectedness defined by the area and perimeter of groups of connected built-up pixels: $\left[1 - \frac{\sum_{j=1}^{n} p_{ij}}{\sum_{j=1}^{n} p_{ij}\sqrt{a_{ij}}}\right] \times \left[1 - \frac{1}{\sqrt{Z}}\right]^{-1} \times 100$

DISTRIBUTION (configuration)	Interspersion and Juxtaposition Index Ratio of observed interspersion over maximum possible interspersion: $\frac{-\sum_{k=1}^{m}\left[\left(\frac{e_{ik}}{\sum_{k=1}^{m} e_{ik}}\right)\ln\left(\frac{e_{ik}}{\sum_{k=1}^{m} e_{ik}}\right)\right]}{\ln(m-1)} \times 100$	Euclidean Nearest Neighbor Index Distance of each patch to the nearest patch of the same class. Equation represented as: h_{ij}	Percentage of Like Adjacencies Calculates the number of built-up pixels that are adjacent to built-up pixels divided by the total number of pixel adjacencies: $\left(\frac{g_{ii}}{\sum_{k=1}^{m} g_{ik}}\right)(100)$

WHERE:
$a_{ij} = area\ in\ terms\ of\ number\ of\ cells,$
$A =\ total\ class/landscape\ area\ (m^2),$
$e_{ik} = total\ length\ (m)\ of\ edge\ involving\ class\ i\ and\ k,$
$p_{ij} = perimeter\ of\ patch\ ij\ in\ terms\ of\ number\ of\ cell\ surfaces,$
$Z = total\ number\ of\ cells\ in\ the\ landscape,$
$g_{ii} = number\ of\ like\ adjacencies\ between\ pixels\ of\ class\ i,$
$g_{ik} = number\ of\ like\ adjacencies\ between\ pixels\ of\ classes\ i\ \&\ k,$
$c_{ijr} = contiguity\ value\ for\ pixel\ r\ in\ patch\ ij,$
$v = size\ of\ filter\ matrix,$
$h_{ij} = distance\ to\ the\ nearest\ neighboring\ patch\ of\ the\ same\ class\ i\ (m),$
$m = number\ of\ classes\ present\ in\ the\ landscape,$
$C = area\ of\ class'\ minimum\ bounding\ circle$

These metrics draw from patch-based and spatial science methods and were calculated using the FRAGSTATS GUI as well as compactR, and landscapemetric R packages (McGarigal, Cushman, and Ene 2012; Hesselbarth et al. 2019; Migurski 2018).

5.2.1 Size

Size is a measure of composition and is the relative extent of an area of a particular land cover. In the case studies, size was measured either in total area or the proportion of total area. For the analysis of the Rio Salado and New River developments, using the Percentage of Landscapes to represent size was appropriate because the metric inherently considers the whole landscape. This focus on the landscape was mirrored in the statistical tests used in the analysis, such as the repeated measures correlation. Chapters 3 and 4 used patch and class area, respectively. Chapter 3 employs patch area in order have enough data to conduct statistically robust tests on change over time. For

testing for urban homogenization in Chapter 4, class area provided a relevant value that was also easily comparable across cities.

5.2.2 Shape

Shape is a measure of configuration and is defined by the form of an area of a particular land cover (i.e., elliptical, rectilinear), including the complexity of the boundaries (Connors, Galletti, and Chow 2013). Most of the measures of shape used in the case studies were measures of shape complexity that compared the perimeter of the patch/class to a simplified perimeter or total area (Median Shape Index, Fractal Dimension Index, and Edge Density). In Chapter 4, an additional measure of shape that examined the compactness of the class, the Reock Score (Reock 1961), was also used. Together these metrics captured distinct shape change that, in the case of this research, correspond to increasing urban sprawl: Edge Density showed an increase in shape complexity and Reock Score showed a decrease in shape compactness. This suggests that for some contexts, using two metrics to capture these two aspects of shape is important (this is elaborated upon below in section 5.3.3).

5.2.3 Connectivity

Connectivity is a measure of configuration and is the linking, or lack thereof, between land covers of the same class (Schumaker 1996). The metrics used for connectivity vary by case study. For the Rio Salado and New River sites (Chapter 2), class-level connectivity was measured by the median distance between patches of the same class (Euclidean Nearest Neighbor Index). This was an appropriate measure because of the relatively small spatial extent of the study areas and the focus on bird biota which fly between habitat patches. The Cuba case study (Chapter 3) necessitated patch level metrics so the Contiguity Index, a measure of within patch connectivity, was most appropriate. Lastly, the urban case study (Chapter 4) examined class level

connectivity (i.e., all built-up land in a given urban area) so the Patch Cohesion Index, a class level measure that looked at the connectedness of built-up patches, was applicable.

5.2.4 Distribution

Distribution is a measure of configuration and is the spatial arrangement of land-cover types, such as random, aggregated, or uniform, as well as their density (Gustafson 1998). The metrics used to measure distribution varied by study area and research contexts. The Rio Salado and New River analysis used the Interspersion and Juxtaposition Index which considered observed interspersion in relation to maximum possible interspersion. This was appropriate for the landscape approach of Chapter 2 because the resulting metric values could be easily compared between classes. The Cuba case study (Chapter 3) employed the distance between patches of the same class (Euclidean Nearest Neighbor Index) as a measure of distribution. Distribution is inherently a measure that relates more than one patch to each other, and when calculating patch level metrics this was the only metric that takes other patches into account. Last, the urban case study (Chapter 4) employed Percentage of Like Adjacencies which calculates, for built-up pixels, the proportion of adjacent pixels that are also built-up. It captures the distribution of built-up land in the metropolitan area in a way that has previously been linked to socio-environmental urban processes (Alberti et al. 2007).

5.3 Cross-Case Study Conclusions

In the early stages of LSA research, a variety of metrics from a range of fields should be tested for their applicability. Based on the three case studies in this dissertation, several conclusions are relevant to the continued use and testing of metrics for LSA research. First, LSA research should take a flexible, but context-specific approach in the selection of metrics. A potential workflow to aid in the metric selection process is outlined in section 5.3.1. Second, all three case studies found configuration to

have more statistically significant relationships with environmental variables than composition did. This is elaborated on in section 5.3.2, but may be a function of incorporating new metrics into LSA research. In particular, some of the case studies point to the importance of using two different metrics to capture the interrelated aspects of shape—one for shape compactness and one for shape complexity. This is explored in section 5.3.3.

5.3.1 Selecting Context Appropriate Metrics

Across the three case studies, there was very little overlap in the final subset of metrics that were used. This suggests that there is not a single set of metrics that should be used for all LSA research. Instead, determining which metrics are suitable for a given LSA research question is highly context dependent, with the spatial scale and socio-ecological variables of interest having the greatest impact on selecting metrics.

Based on the selection processed used in the three case studies, several steps related to identifying appropriate metrics are recommended. First, determine what level of metrics the research question requires: patch, class, or landscape. In this dissertation the choice was a function of the land-use and land-cover data and the number of observations that the selected statistical tests needed. Each case study in this dissertation used only one metric level (class for Chapters 2 and 4, patch for Chapter 3) but other analyses may require multiple levels.

Second, categorize metrics according to the components of landscape composition and configuration that need to be measured. This will likely be the four components of LSA—size, shape, connectivity, and distribution—but may not be in every case. In doing so, remove metrics that are mathematically redundant. For example, at the patch level, Related Circumscribing Circle (CIRCLE) from FRAGSTATS (McGarigal,

Cushman, and Ene 2012) and the Reock Score from spatial sciences (Reock 1961) are redundant.

Third, consider the socio-environmental processes that are relevant to your research question. This can be done by reviewing metrics used successfully in previous research but should also involve considering the way in which landscape structure is hypothesized to be relevant. For example, graph theory metrics ended up not being used in any of the case studies, despite testing them on multiple cases, because these metrics are most useful for representing ecological flow probability or a species' ability to move between habitats (Baranyi et al. 2011). This dissertation's reliance on satellite imagery for the majority of environmental variables made graph theory metrics less applicable.

Finally, because many metrics come from applications other than LSA, adopt a flexible approach in determining which metrics are suitable. Chapter 2 and 3 used Euclidean Nearest Neighbor distance as measures of connectivity and distribution respectively. Using one metric for two different aspects of LSA is not problematic because the appropriateness and interpretation of metrics varies dramatically by research contexts and spatial scale. In addition to the justifications noted above (sections 5.2.3 & 5.2.4), one of the most important differences between the two cases is that the metrics for Chapter 2 were calculated at the class level, while the metrics for Chapter 3 were calculated at the patch level. Flexibility in incorporating new metrics is essential in the early phases of LSA research. Incorporation of new metrics is potentially one of the reasons some LSA research has found configuration to be as or more important than composition.

5.3.2 Composition and Configuration

In each of the case studies, measures of configuration had greater statistical significance than measures of composition. This is contrary to previous findings on the

primacy of configuration (Li et al. 2017; Li et al. 2012; Zhou, Wang, and Cadenasso 2017; Zhou, Huang, and Cadenasso 2011) but joins a small and growing amount of research which has found configuration to be as or more important (Li et al. 2016; Zhang, Murray, and Turner 2017). As noted above, the metric used to measure configuration appears to be central to these findings.

Most LSA research has employed patch-based methods (i.e., FRAGSTATS), but research that has found configuration to be more important has often employed other means of calculating configuration. For example, Li *et al.* (2016) uses the normalized moment of inertia drawn from spatial science as opposed to patch-based methods. Thus, there is continued need to test the appropriateness of non patch-based metrics for use in LSA research with particular attention to what aspect of composition a given metric is capturing. This is because the divergent results around configuration may also link to the multiple ways of measuring shape (i.e., complexity vs. compactness).

5.3.3 Shape Complexity vs. Compactness

Shape is considered one of three aspects of composition (along with distribution and connectivity). Chapter 4 found that two aspects of shape—shape complexity and shape compactness—while related, cannot both be captured with the same metric. For example, two patches could have the same area and minimum bounding circle, but have very different complexities. In the urban case study (Chapter 4) two measures of shape were used, producing unique results and trends (Fig. 1).

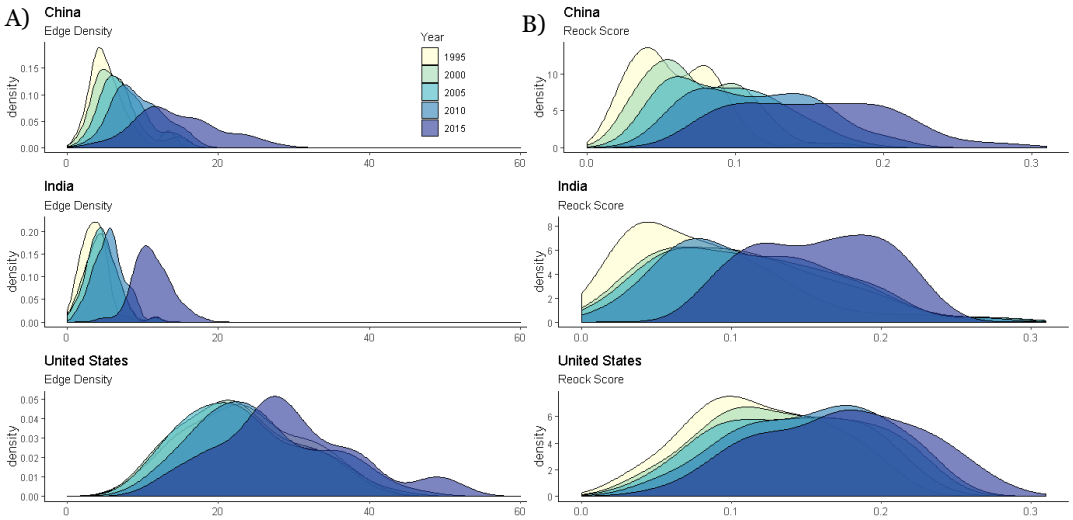

Figure 1. Density plots for the distribution of A) edge density (a measure of shape complexity) and B) reock score (a measure of shape compactness) for the 50 cities of China, India, and the United States. The US from 1995-2005 is a good example of the two metrics exhibiting different rates of change.

Additionally, the metrics produced unique values measuring different aspects of urbanization. Increasing Edge Density signals that city's boundaries were becoming more complex and the increasing Reock scores means there was a decrease in the cities' compactness. Together the metrics suggested an increase in urban sprawl over time.

Patch level metrics used in the Cuba case study (Chapter 3) also showed differences between shape complexity and compactness. Fractal Dimension Index was used in the analysis and is a measure of shape complexity. Related Circumscribing Circle was calculated for this concluding chapter as an example of a shape compactness. Figure 2 depicts these differences for the built-up class.

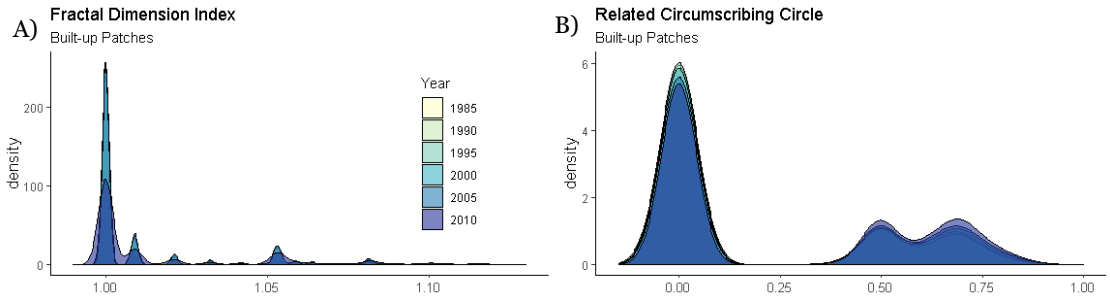

Figure 2. Density plots for built-up patch values of A) fractal dimension index (a measure of shape complexity) and B) related circumscribing circle (a measure of shape compactness).

Both fractal dimension index and related circumscribing circle had peaks at the right end of the graph—the least complex (fractal dimension index = 1) and most compact (related circumscribing circle = 0)—for all patches that are made up of one pixel or are perfectly square. Beyond this similarity, however, the two metrics had unique trends and signify different types of LSA change. For example, the related circumscribing circle had a slower rate of change between 1985 and 2010 which suggests that patches were changing in complexity faster than they were changing in compactness.

5.4 Contributions of Research

This dissertation expanded the applications in which LSA approaches have been applied, produced case study specific results with implications relevant to the design of landscapes, and provided some insight on the selection and use of metrics in LSA research.

5.4.1 Expanded Application of LSA Approach

LSA's consideration of composition, configuration, and their socio-environmental consequences is widely relevant, but to date, LSA research has largely been focused on city-scale examinations of urban heat and its associated impacts (Li et al. 2017; Turner 2016; Zhang, Murray, and Turner 2017; Connors, Galletti, and Chow 2013). While this dissertation engaged with urban heat in Chapters 2 and 4, urban heat was often part of a

broader set of environmental outcomes such as bird biota (Ch. 2) or tasseled cap variables (Ch. 3). Additionally, Chapters 3 and 4 expanded beyond the examination of a single city to evaluate the LSA of a country (Ch. 3) or cities across multiple countries (Ch. 4). Expanding the scope of LSA furthers its contributions to the landscape composition and configuration research occurring in cognate fields—such as landscape ecology, landscape architecture, urban climatology and geodesign—and begins to incorporate LSS in conversations around landscape design.

5.4.2 Landscape Design

The composition and configuration of the Earth's surfaces are dominant factors in the environmental benefits and burdens a land system—rural to urban—can provide. Human uses affect these services through the "design" of the built environment (Osborne and Kovacic 1993). An important implication of LSA research is the ability to design landscape mosaics that optimize social and ecological trade-offs to improve resilience (Nassauer and Opdam 2008; B. L. Turner et al. 2013). Furthering landscape design, each case study provided context-specific findings relevant to the design of landscapes.

Additionally, the case studies together provide insights on selecting metrics for use in LSA research. Improved application of landscape metrics will further land assessment research by providing a meaningful quantitative measure for understanding land-cover changes and socio-environmental trade-offs that must be made when modifying landscapes (Dramstad 2009; Kupfer 2012). As a result, researchers will be able to provide decision makers with improved understanding of outcomes on which to construct options that enhance sustainability and resilience.

5.4.3 Metric Evaluation

The metric evaluation conducted as part of this dissertation marks the beginning of a discussion on which metrics are suitable for use in LSA. A flexible, context-specific

approach is recommended for selecting metrics with particular attention to how shape is measured. I suggest using two metrics to measure shape, one which captures shape complexity and one which captures shape compactness. Continued attention on configuration metrics can help tease apart the role that composition and configuration play separately and together. These results will have implications beyond the sub-field of LSA. Urban climate research, urban ecology, landscape ecology, landscape architecture, and geodesign scholars also use landscape pattern metrics and thus will benefit from greater clarity on meaningfully and accurately applying metrics.

5.5 Challenges and Directions for Future Research

First, based on findings in my dissertation and the inconsistencies that have emerged in other research (Leitao et al. 2006; Luck and Wu 2002; Seto and Fragkias 2005), future work is need on landscape metrics that are suitable for studying urban systems. In particular, I see potential in applying landscape metrics that use fuzzy or non-binary classifications (to capture different levels of urbanization) or 3D metrics (Kedron, Zhao, and Frazier 2019; McGarigal, Tagil, and Cushman 2009; McIntyre and Barrett 1992). The landscape metrics used in the urban case study (Chapter 4) captured city-level changes in composition and configuration which was a fit our dataset and research questions comparing 2D LSA change across cities. In future research on city LSA change, however, non-categorical metrics or 3D metrics could provide a much more nuanced perspective. For example, using 3D metrics would have shown greater contrast between the Rio Salado's density of high-rise developments and the low density residential and retail development that occurred at the New River site.

Second, I am interested in understanding the impact policy has on land, especially urban land. Much policy research is focused on the impacts for people or firms, with minimal emphasis on the land system or environmental impacts. Employing

longitudinal data from satellite imagery, there is potential to examine land and environmental impacts at a variety of scales and to link the impacts of one scale to another. The scale at which policy influences urban land systems can be large and systematic (such as an urban growth boundary) or relatively fine-grained (such as a zoning policy) with interactions between the scales.

Third, in future research I aim to integrate design—the intentional modifications to the composition and configuration of a landscape—into LSS research. With the growing emphasis on transdisciplinary and convergent research, design can be fertile ground for integrating practitioners and other stakeholders into LSS research. LSA, with its focus on composition and configuration, is well poised to contribute to this integration.

The lack of interpretability of some landscape metrics is a current challenge for transdisciplinary land system architecture research. In future work, a greater focus needs to be put on making sure that the metrics used to quantify landscape pattern are not only context appropriate, but also easily interpretable by decision makers. As an example, if urban planners and land managers do not understand how to raise or lower a landscape's Fractal Dimension Index, the possibility of operationalizing any findings about the metric will be significantly reduced.

In conclusion, there is a need for continued exploration of landscape metrics that are suitable for LSA and interpretable by stakeholders, especially in urban areas. I plan to continue this work and apply landscape metrics to questions of urban design, environmental outcomes, and policy impacts. Together, my aim is that this research speaks to the broader question: How can (urban) landscapes be managed in order to balance social and ecological well-being?

REFERENCES

Ahern, Jack. 2013. “Urban Landscape Sustainability and Resilience: The Promise and Challenges of Integrating Ecology with Urban Planning and Design.” *Landscape Ecology* 28 (6): 1203–12. https://doi.org/10.1007/s10980-012-9799-z.

Alarcón de Quesada, Ricardo. 1995. *Ley No. 76: Ley de Minas*.

———. 1997. *Ley No. 81: De medio ambiente*.

———. 1998. *Ley No. 85: Ley Forestal*.

Alberti, Marina. 2005. “The Effects of Urban Patterns on Ecosystem Function.” *International Regional Science Review* 28 (2): 168–92. https://doi.org/10.1177/0160017605275160.

Alberti, Marina, Derek Booth, Kristina Hill, Bekkah Coburn, Christina Avolio, Stefan Coe, and Daniele Spirandelli. 2007. “The Impact of Urban Patterns on Aquatic Ecosystems: An Empirical Analysis in Puget Lowland Sub-Basins.” *Landscape and Urban Planning* 80 (4): 345–61. https://doi.org/10.1016/j.landurbplan.2006.08.001.

Alberti, Marina, Cristian Correa, John M. Marzluff, Andrew P. Hendry, Eric P. Palkovacs, Kiyoko M. Gotanda, Victoria M. Hunt, Travis M. Apgar, and Yuyu Zhou. 2017. “Global Urban Signatures of Phenotypic Change in Animal and Plant Populations.” *Proceedings of the National Academy of Sciences* 114 (34): 8951–56. https://doi.org/10.1073/pnas.1606034114.

Allen, Daniel C., Heather L. Bateman, Paige S. Warren, Fabio Suzart de Albuquerque, Sky Arnett-Romero, and Bridget Harding. 2019. “Long-term Effects of Land-use Change on Bird Communities Depend on Spatial Scale and Land-use Type.” *Ecosphere* 10 (11). https://doi.org/10.1002/ecs2.2952.

Altieri, Miguel A., and Fernando R. Funes-Monzote. 2012. “The Paradox of Cuban Agriculture.” *Monthly Review* 63 (8): 23–33.

Alvarez, Jose. 2004. *Cuba’s Agricultural Sector*. Gainesville, Fla.: University Press of Florida.

Andrade, Riley, Heather L. Bateman, Janet Franklin, and Daniel Allen. 2018. “Waterbird Community Composition, Abundance, and Diversity along an Urban Gradient.” *Landscape and Urban Planning* 170 (February): 103–11. https://doi.org/10.1016/j.landurbplan.2017.11.003.

Aragon, Nazli Z. Uludere, Michelle Stuhlmacher, Jordan P. Smith, Nicholas Clinton, and Matei Georgescu. 2019. “Urban Agriculture’s Bounty: Contributions to Phoenix’s

Sustainability Goals." *Environmental Research Letters*, September. https://doi.org/10.1088/1748-9326/ab428f.

Arnfield, A. John. 2003. "Two Decades of Urban Climate Research: A Review of Turbulence, Exchanges of Energy and Water, and the Urban Heat Island." *International Journal of Climatology* 23 (1): 1–26. https://doi.org/10.1002/joc.859.

Aspinall, Richard, and Michele Staiano. 2019. "Ecosystem Services as the Products of Land System Dynamics: Lessons from a Longitudinal Study of Coupled Human–Environment Systems." *Landscape Ecology* 34 (7): 1503–24. https://doi.org/10.1007/s10980-018-0752-7.

Bakdash, Jonathan Z., and Laura R. Marusich. 2017. "Repeated Measures Correlation." *Frontiers in Psychology* 8 (April). https://doi.org/10.3389/fpsyg.2017.00456.

Banville, Mélanie J., Heather L. Bateman, Stevan R. Earl, and Paige S. Warren. 2017. "Decadal Declines in Bird Abundance and Diversity in Urban Riparian Zones." *Landscape and Urban Planning* 159 (March): 48–61. https://doi.org/10.1016/j.landurbplan.2016.09.026.

Baranyi, Gabriella, Santiago Saura, János Podani, and Ferenc Jordán. 2011. "Contribution of Habitat Patches to Network Connectivity: Redundancy and Uniqueness of Topological Indices." *Ecological Indicators* 11 (5): 1301–10. https://doi.org/10.1016/j.ecolind.2011.02.003.

Barrett, Scott, and Kathryn Graddy. 2000. "Freedom, Growth, and the Environment." *Environment and Development Economics* null (04): 433–456. https://doi.org/null.

Batchelder, Robert B. 1952. "The Evolution of Cuban Land Tenure and Its Relation to Certain Agro-Economic Problems." *Southwestern Social Science Quarterly* 33 (January): 239–246.

Bateman, H. L., J. C. Stromberg, M. J. Banville, E. Makings, B. D. Scott, A. Suchy, and D. Wolkis. 2015. "Novel Water Sources Restore Plant and Animal Communities along an Urban River." *Ecohydrology* 8 (5): 792–811. https://doi.org/10.1002/eco.1560.

Bateman, Heather L., Daniel L. Childers, Madhusudan Katti, Eyal Shochat, and Paige S. Warren. 2017. "Point-Count Bird Censusing: Long-Term Monitoring of Bird Abundance and Diversity in Central Arizona-Phoenix, Ongoing since 2000." *Environmental Data Initiative*, November. https://doi.org/10.6073/pasta/201add557165740926aab6e056db6988.

Bennett, Elena M., Garry D. Peterson, and Line J. Gordon. 2009. "Understanding Relationships among Multiple Ecosystem Services." *Ecology Letters* 12 (12): 1394–1404. https://doi.org/10.1111/j.1461-0248.2009.01387.x.

Bergen, K.M., T. Zhao, V. Kharuk, Y. Blam, D.G. Brown, L.K. Peterson, and N. Miller. 2008. "Changing Regimes." *Photogrammetric Engineering & Remote Sensing* 74 (6): 787–98. https://doi.org/10.14358/PERS.74.6.787.

Bettencourt, Luís M. A., José Lobo, Dirk Helbing, Christian Kühnert, and Geoffrey B. West. 2007. "Growth, Innovation, Scaling, and the Pace of Life in Cities." *Proceedings of the National Academy of Sciences* 104 (17): 7301–6. https://doi.org/10.1073/pnas.0610172104.

Bhatta, B., S. Saraswati, and D. Bandyopadhyay. 2010. "Urban Sprawl Measurement from Remote Sensing Data." *Applied Geography*, Climate Change and Applied Geography – Place, Policy, and Practice, 30 (4): 731–40. https://doi.org/10.1016/j.apgeog.2010.02.002.

Biegon, Rubrick. 2020. "The Normalization of U.S. Policy Toward Cuba? Rapprochement and Regional Hegemony." *Latin American Politics and Society* 62 (1): 46–72. https://doi.org/10.1017/lap.2019.45.

Bono, Federica, and John C. Finn. 2017. "Food Diaries to Measure Food Access: A Case Study from Rural Cuba." *The Professional Geographer* 69 (1): 59–69. https://doi.org/10.1080/00330124.2016.1157499.

Boone, Christopher G., Elizabeth Cook, Sharon J. Hall, Marcia L. Nation, Nancy B. Grimm, Carol B. Raish, Deborah M. Finch, and Abigail M. York. 2012. "A Comparative Gradient Approach as a Tool for Understanding and Managing Urban Ecosystems." *Urban Ecosystems* 15 (4): 795–807. https://doi.org/10.1007/s11252-012-0240-9.

Bounoua, Lahouari, Joseph Nigro, Ping Zhang, Kurtis Thome, and Asia Lachir. 2018. "Mapping Urbanization in the United States from 2001 to 2011." *Applied Geography* 90 (January): 123–33. https://doi.org/10.1016/j.apgeog.2017.12.002.

Brinck, Katharina, Rico Fischer, Jürgen Groeneveld, Sebastian Lehmann, Mateus Dantas De Paula, Sandro Pütz, Joseph O. Sexton, Danxia Song, and Andreas Huth. 2017. "High Resolution Analysis of Tropical Forest Fragmentation and Its Impact on the Global Carbon Cycle." *Nature Communications* 8 (1): 1–6. https://doi.org/10.1038/ncomms14855.

Cadenasso, M. L., S. T. A. Pickett, Brian McGrath, and Victoria Marshall. 2013. "Ecological Heterogeneity in Urban Ecosystems: Reconceptualized Land Cover

Models as a Bridge to Urban Design." In *Resilience in Ecology and Urban Design*, 107–129. Springer.

Cadenasso, Mary L., and Steward T. A. Pickett. 2013. "Three Tides: The Development and State of the Art of Urban Ecological Science." In *Resilience in Ecology and Urban Design : Linking Theory and Practice for Sustainable Cities*, edited by Steward T. A. Pickett, Mary L. Cadenasso, and Brian McGrath, 3:29–46. Future City. Dordrecht: Springer.

Carol, M.L., C.M. DiMiceli, M.R. Wooten, A.B. Hubbard, R.A. Sohlberg, and J. R. G. Townshend. 2017. "MOD44W MODIS/Terra Land Water Mask Derived from MODIS and SRTM L3 Global 250m SIN Grid V006." *NASA EOSDIS Land Processes DAAC*. https://doi.org/10.5067/MODIS/MOD44W.006.

Carruthers, John I. 2002. "The Impacts of State Growth Management Programmes: A Comparative Analysis." *Urban Studies* 39 (11): 1959–82. https://doi.org/10.1080/0042098022000011317.

Castro, Fidel, and Ignacio Ramonet. 2008. *Fidel Castro My Life : A Spoken Autobiography*. 1st ed. New York: Scribner.

Castro Ruz, Fidel. 1980. *Decreto No. 66: Reglamento de Mercado Libre Campesino*.

———. 1983. *Decreto Ley No. 63: Sobre la Herencia de la Tierra Propiedad de los Agricultores Pequeños*.

———. 1991. *Decreto Ley No. 125: Regimen de posesion, propiedad y herencia de la tierra y bienes agropecuarios*.

———. 1993a. *Decreto Ley No. 136: Del patrimonio forestal y la fauna silvestre*.

———. 1993b. *Decreto Ley No. 138: De las aguas terrestres*.

———. 1994. *Decreto Ley No. 153: De las regulaciones de la sanidad vegetal*.

———. 1999b. *Decreto Ley No. 201: Del sistema nacional de areas protegidas*.

———. 2008. *Decreto Ley No. 259: Sobre la entrega de tierras ociosas en usufructo*.

Castro Ruz, Fidel, Jorge Aspiolea Ruiz, and Carlos Lage Dávila. 1995. *Decreto No. 199: De contravenciones de las reglaciones para la protección y uso racional de los recursos hidráulicos*.

Castro Ruz, Fidel, María del Carmen Peréz Hernández, Ulises Rosales del Toro, and Carlos Lage Dávila. 2008. *Decreto No. 282: Reglamento para la implementacion de la entrega de tierras ociosas en usufructo*.

Castro Ruz, Fidel, Alfredo Jordán Morales, and Carlos Lage Dávila. 1999. *Decreto No. 268: Contravenciones de las regulaciones forestales*.

Castro Ruz, Fidel, Marcos Portal León, and Carlos Lage Dávila. 1997. *Decreto No. 222: Reglamento de la ley de minas*.

Castro Ruz, Fidel, and Manuel Villa Sosa. 1982. *Decreto No. 106: Reglamente del Mercado Libre Campesino*.

Castro Ruz, Raúl. 2012. *Decreto Ley No. 300: Sobre la entrega de tierras estatales ociosas en usufructo*.

Census Bureau, United States. 2012. "Increasing Urbanization: Population Distribution by City Size, 1790 to 1890." Data Visualization. https://www.census.gov/dataviz/visualizations/005/.

———. 2016. "New Census Data Show Differences Between Urban and Rural Populations." Press Release CB16-210. American Community Survey 2011-2015: U.S. Census Bureau. https://www.census.gov/newsroom/press-releases/2016/cb16-210.html.

Chazal, Jacqueline de, and Mark D. A. Rounsevell. 2009. "Land-Use and Climate Change within Assessments of Biodiversity Change: A Review." *Global Environmental Change*, Traditional Peoples and Climate Change, 19 (2): 306–15. https://doi.org/10.1016/j.gloenvcha.2008.09.007.

Chen, Shaoqing, and Bin Chen. 2015. "Urban Energy Consumption: Different Insights from Energy Flow Analysis, Input–Output Analysis and Ecological Network Analysis." *Applied Energy* 138 (January): 99–107. https://doi.org/10.1016/j.apenergy.2014.10.055.

Chhetri, Netra, Michelle Stuhlmacher, and Asif Ishtiaque. 2019. "Nested Pathways to Adaptation." *Environmental Research Communications* 1 (1): 015001. https://doi.org/10.1088/2515-7620/aaf9f9.

Childers, Daniel L., Mary L. Cadenasso, J. Morgan Grove, Victoria Marshall, Brian McGrath, and Steward T. A. Pickett. 2015. "An Ecology for Cities: A Transformational Nexus of Design and Ecology to Advance Climate Change Resilience and Urban Sustainability." *Sustainability* 7 (4): 3774–91. https://doi.org/10.3390/su7043774.

Childers, Daniel L., Steward TA Pickett, J. Morgan Grove, Laura Ogden, and Alison Whitmer. 2014. “Advancing Urban Sustainability Theory and Action: Challenges and Opportunities.” *Landscape and Urban Planning* 125: 320–328.

Choy, Armando, Gustavo Chui, Moisés Sío Wong, and Mary-Alice Waters. 2005. *Our History Is Still Being Written :The Story of Three Chinese-Cuban Generals in the Cuban Revolution*. 1st ed. New York: Pathfinder. http://www.loc.gov/catdir/toc/fy0609/2005909294.html.

CIESIN, and Columbia University. 2018. “Gridded Population of the World, Version 4 (GPWv4): Population Count Adjusted to Match 2015 Revision of UN WPP Country Totals, Revision 11.” Center for International Earth Science Information Network. Palisades, NY: NASA Socioeconomic Data and Applications Center (SEDAC). https://doi.org/10.7927/H4PN93PB.

City of Peoria. 2014. “Community Services Mater Plan: Implementation Strategies for Parks, Recreation, Open Space, Trails, Sports Facilities, Public Art and Libraries.” City of Peoria, Arizona: Approved by Mayor and City Council. https://www.peoriaaz.gov/home/showdocument?id=5138.

City of Tempe. 1982. “Rio Salado Plan.” Tempe, Arizona, USA: City of Tempe.

Clarke, K. Robert. 1993. “Non-Parametric Multivariate Analyses of Changes in Community Structure.” *Australian Journal of Ecology* 18 (1): 117–143.

Clinton, Nicholas, and Peng Gong. 2013. “MODIS Detected Surface Urban Heat Islands and Sinks: Global Locations and Controls.” *Remote Sensing of Environment* 134 (July): 294–304. https://doi.org/10.1016/j.rse.2013.03.008.

Clinton, Nicholas, Michelle Stuhlmacher, Albie Miles, Nazli Uludere Aragon, Melissa Wagner, Matei Georgescu, Chris Herwig, and Peng Gong. 2018. “A Global Geospatial Ecosystem Services Estimate of Urban Agriculture.” *Earth’s Future* 6 (1): 40–60. https://doi.org/10.1002/2017EF000536.

Cohn, Jeffrey P. 2010. “Opening Doors to Research in Cuba: Although Hurdles Remain, the Recent Thaw in US–Cuba Relations Has Improved Prospects for Biological Research and Conservation in Cuba.” *Bioscience* 60 (2): 96.

Collinge, Sharon K. 1996. “Ecological Consequences of Habitat Fragmentation: Implications for Landscape Architecture and Planning.” *Landscape and Urban Planning* 36 (1): 59–77. https://doi.org/10.1016/S0169-2046(96)00341-6.

Congleton, Roger D. 1992. “Political Institutions and Pollution Control.” *The Review of Economics and Statistics* 74 (3): 412–21. https://doi.org/10.2307/2109485.

Connors, John Patrick, Christopher S. Galletti, and Winston T. L. Chow. 2013. "Landscape Configuration and Urban Heat Island Effects: Assessing the Relationship between Landscape Characteristics and Land Surface Temperature in Phoenix, Arizona." *Landscape Ecology* 28 (2): 271–83. https://doi.org/10.1007/s10980-012-9833-1.

Coseo, Paul, and Larissa Larsen. 2015. "Cooling the Heat Island in Compact Urban Environments: The Effectiveness of Chicago's Green Alley Program." *Procedia Engineering*, Defining the future of sustainability and resilience in design, engineering and construction, 118 (January): 691–710. https://doi.org/10.1016/j.proeng.2015.08.504.

Crawford, Sue E. S., and Elinor Ostrom. 1995. "A Grammar of Institutions." *The American Political Science Review* 89 (3): 582–600. https://doi.org/10.2307/2082975.

Crist, Eric P., and Richard C. Cicone. 1984. "A Physically-Based Transformation of Thematic Mapper Data—The TM Tasseled Cap." *IEEE Transactions on Geoscience and Remote Sensing* GE-22 (3): 256–63. https://doi.org/10.1109/TGRS.1984.350619.

Cruz, María Caridad, and Roberto Sánchez Medina. 2003. *Agriculture in the City: A Key to Sustainability in Havana, Cuba*. Ottawa, ON, Canada; Kingston, Jamaica: Ian Randle Publishers.

Debbage, Neil, and J. Marshall Shepherd. 2015. "The Urban Heat Island Effect and City Contiguity." *Computers, Environment and Urban Systems* 54 (November): 181–94. https://doi.org/10.1016/j.compenvurbsys.2015.08.002.

Deng, Yu, Wei Qi, Bojie Fu, and Kevin Wang. 2019. "Geographical Transformations of Urban Sprawl: Exploring the Spatial Heterogeneity across Cities in China 1992–2015." *Cities*, July, 102415. https://doi.org/10.1016/j.cities.2019.102415.

Diaz-Briquets, Sergio, and Jorge F. Pérez-López. 2000. *Conquering Nature: The Environmental Legacy of Socialism in Cuba*. Pittsburgh, Pa: University of Pittsburgh Press.

Dinerstein, Eric, David Olson, Anup Joshi, Carly Vynne, Neil D. Burgess, Eric Wikramanayake, Nathan Hahn, et al. 2017. "An Ecoregion-Based Approach to Protecting Half the Terrestrial Realm." *BioScience* 67 (6): 534–45. https://doi.org/10.1093/biosci/bix014.

Dobbs, Richard, and Shirish Sankhe. 2010. "Opinion: India vs China." *Financial Times*, May 18, 2010, sec. Emerging Markets. https://www.ft.com/content/4298b79e-6263-11df-991f-00144feab49a.

Dramstad, Wenche E. 2009. “Spatial Metrics – Useful Indicators for Society or Mainly Fun Tools for Landscape Ecologists?” *Norsk Geografisk Tidsskrift - Norwegian Journal of Geography* 63 (4): 246–54. https://doi.org/10.1080/00291950903368359.

Dramstad, Wenche E., James D. Olson, and Richard T. T. Forman. 1996. *Landscape Ecology Principles in Landscape Architecture and Land-Use Planning*. S.l: Island Press.

Dunning, John B., Rene Borgella, Krista Clements, and Gary K. Meffe. 1995. “Patch Isolation, Corridor Effects, and Colonization by a Resident Sparrow in a Managed Pine Woodland.” *Conservation Biology* 9 (3): 542–50.

Eakin, Hallie, Alexandra Winkels, and Jan Sendzimir. 2009. “Nested Vulnerability: Exploring Cross-Scale Linkages and Vulnerability Teleconnections in Mexican and Vietnamese Coffee Systems.” *Environmental Science & Policy*, Special Issue: Food Security and Environmental ChangeFood Security and Environmental Change: Linking Science, Development and Policy for Adaptation, 12 (4): 398–412. https://doi.org/10.1016/j.envsci.2008.09.003.

Edelemann, Ernesto Marcos. 1981. *Instrucción No. 99: Aclaración del Art. 24 de la Constitución, sobre la succesión de la Tierra de los pequenos agricultores*.

Elmore, James. 1995. Rio Salado Project Update, 1995. https://repository.asu.edu/attachments/167990/content/Elmore-RioSalado%20Proj.%20Update-10%EF%80%A295.mov.

Elvidge, Christopher D., Daniel Ziskin, Kimberly E. Baugh, Benjamin T. Tuttle, Tilottama Ghosh, Dee W. Pack, Edward H. Erwin, and Mikhail Zhizhin. 2009. “A Fifteen Year Record of Global Natural Gas Flaring Derived from Satellite Data.” *Energies* 2 (3): 595–622. https://doi.org/10.3390/en20300595.

European Space Agency, and Université Catholique de Louvain. 2010. “GlobCover 2009 (Global Land Cover Map)” V2.3 (December). http://due.esrin.esa.int/page_globcover.php.

Ewing, Reid, Shima Hamidi, James B. Grace, and Yehua Dennis Wei. 2016. “Does Urban Sprawl Hold down Upward Mobility?” *Landscape and Urban Planning* 148 (April): 80–88. https://doi.org/10.1016/j.landurbplan.2015.11.012.

Fan, Chao, Wenwen Li, Levi J. Wolf, and Soe W. Myint. 2015. “A Spatiotemporal Compactness Pattern Analysis of Congressional Districts to Assess Partisan Gerrymandering: A Case Study with California and North Carolina.” *Annals of the Association of American Geographers* 105 (4): 736–53. https://doi.org/10.1080/00045608.2015.1039109.

Fan, Chao, and Soe Myint. 2014. “A Comparison of Spatial Autocorrelation Indices and Landscape Metrics in Measuring Urban Landscape Fragmentation.” *Landscape and Urban Planning* 121: 117–128.

Fan, Chao, Soe W. Myint, and Baojuan Zheng. 2015. “Measuring the Spatial Arrangement of Urban Vegetation and Its Impacts on Seasonal Surface Temperatures.” *Progress in Physical Geography: Earth and Environment* 39 (2): 199–219. https://doi.org/10.1177/0309133314567583.

Farr, Tom G., Paul A. Rosen, Edward Caro, Robert Crippen, Riley Duren, Scott Hensley, Michael Kobrick, et al. 2007. “The Shuttle Radar Topography Mission.” *Reviews of Geophysics* 45 (2). https://doi.org/10.1029/2005RG000183.

Febles-González, J.M., A. Tolón-Becerra, X. Lastra-Bravo, and X. Acosta-Valdés. 2011. “Cuban Agricultural Policy in the Last 25 Years. From Conventional to Organic Agriculture.” *Land Use Policy* 28 (4): 723–35. https://doi.org/10.1016/j.landusepol.2010.12.008.

Filatova, Tatiana, Peter H. Verburg, Dawn Cassandra Parker, and Carol Ann Stannard. 2013. “Spatial Agent-Based Models for Socio-Ecological Systems: Challenges and Prospects.” *Environmental Modelling & Software*, Thematic Issue on Spatial Agent-Based Models for Socio-Ecological Systems, 45 (July): 1–7. https://doi.org/10.1016/j.envsoft.2013.03.017.

Foody, Giles M. 2017. “Impacts of Sample Design for Validation Data on the Accuracy of Feedforward Neural Network Classification.” *Applied Sciences* 7 (9): 888. https://doi.org/10.3390/app7090888.

Forman, Richard T. T. 1995. “Some General Principles of Landscape and Regional Ecology.” *Landscape Ecology* 10 (3): 133–42. https://doi.org/10.1007/BF00133027.

Forman, Richard T. T. 2008. *Urban Regions : Ecology and Planning Beyond the City*. Cambridge University Press.

———. 2014. *Urban Ecology: Science of Cities*. Cambridge, UK: Cambridge University Press.

Forman, Richard T. T., and M. Godron. 1986. *Landscape Ecology*. New York: John Wiley & Sons, Ltd.

Frazier, Amy E. 2019. “Landscape Metrics.” In *The Geographic Information Science & Technology Body of Knowledge*, 2nd Quarter 2019 Edition. https://gistbok.ucgis.org/bok-topics/landscape-metrics.

Frazier, Amy E., and Peter Kedron. 2017. “Landscape Metrics: Past Progress and Future Directions.” *Current Landscape Ecology Reports* 2 (3): 63–72. https://doi.org/10.1007/s40823-017-0026-0.

Frazier, Amy E., Jacqueline M. Vadjunec, Peter Kedron, and Todd Fagin. 2019. “Linking Landscape Ecology and Land System Architecture for Land System Science: An Introduction to the Special Issue.” *Journal of Land Use Science* 14 (2): 123–34. https://doi.org/10.1080/1747423X.2019.1660728.

Friedl, Mark A., and D. Sulla-Menashe. 2019. “MCD12Q1 MODIS/Terra+Aqua Land Cover Type Yearly L3 Global 500m SIN Grid V006.” *NASA EOSDIS Land Processes DAAC*.

Galletti, Christopher S., Xiaoxiao Li, and John Patrick Connors. 2019. “Establishing the Relationship between Urban Land-Cover Configuration and Night Time Land-Surface Temperature Using Spatial Regression.” *International Journal of Remote Sensing* 40 (17): 6752–74. https://doi.org/10.1080/01431161.2019.1594432.

Gebelein, Jennifer. 2012. “Historical Background of Cuban Land Cover Change.” In , 1–22. A Geographic Perspective of Cuban Landscapes. Springer.

Georgescu, M., M. Moustaoui, A. Mahalov, and J. Dudhia. 2013. “Summer-Time Climate Impacts of Projected Megapolitan Expansion in Arizona.” *Nature Climate Change* 3 (1): 37–41. https://doi.org/10.1038/nclimate1656.

Georgescu, Matei, Philip E. Morefield, Britta G. Bierwagen, and Christopher P. Weaver. 2014. “Urban Adaptation Can Roll Back Warming of Emerging Megapolitan Regions.” *Proceedings of the National Academy of Sciences* 111 (8): 2909–14. https://doi.org/10.1073/pnas.1322280111.

Gerszewski, Alyssa, Philip Vandermeer, Nancy Dallett, Victoria Thompson, and Arizona State University. 2014. “Continuity, Change, and Coming of Age: Redevelopment and Revitalization in Downtown Tempe, Arizona, 1960-2012.” In *ASU Electronic Theses and Dissertations*. Arizona State University. http://hdl.handle.net/2286/R.I.25076.

Golany, Gideon S. 1996. “Urban Design Morphology and Thermal Performance.” *Atmospheric Environment*, Conference on the Urban Thermal Environment Studies in Tohwa, 30 (3): 455–65. https://doi.org/10.1016/1352-2310(95)00266-9.

Goldblatt, Ran, Michelle F. Stuhlmacher, Beth Tellman, Nicholas Clinton, Gordon Hanson, Matei Georgescu, Chuyuan Wang, et al. 2018. “Using Landsat and Nighttime Lights for Supervised Pixel-Based Image Classification of Urban Land Cover.” *Remote Sensing of Environment* 205 (February): 253–75. https://doi.org/10.1016/j.rse.2017.11.026.

Goldblatt, Ran, Wei You, Gordon Hanson, and Amit K. Khandelwal. 2016. “Detecting the Boundaries of Urban Areas in India: A Dataset for Pixel-Based Image Classification in Google Earth Engine.” *Remote Sensing* 8 (8): 634. https://doi.org/10.3390/rs8080634.

Golley, Frank B., and Juan Bellot. 1991. “Interactions of Landscape Ecology, Planning and Design.” *Landscape and Urban Planning* 21 (1–2): 3–11.

Goodchild, Michael F. 2010. “Towards Geodesign: Repurposing Cartography and GIS?” *Cartographic Perspectives*, no. 66 (Fall): 7–21.

Gorelick, Noel, Matt Hancher, Mike Dixon, Simon Ilyushchenko, David Thau, and Rebecca Moore. 2017. “Google Earth Engine: Planetary-Scale Geospatial Analysis for Everyone.” *Remote Sensing of Environment*, Big Remotely Sensed Data: tools, applications and experiences, 202 (December): 18–27. https://doi.org/10.1016/j.rse.2017.06.031.

Gott, Richard. 2004. *Cuba: A New History*. New Haven, Conn; London: Yale University Press.

Grimm, Nancy B., Elizabeth M. Cook, Rebecca L. Hale, and David M. Iwaniec. 2015. *A Broader Framing of Ecosystem Services in Cities*. Routledge Handbooks Online. https://doi.org/10.4324/9781315849256.ch14.

Grimm, Nancy B., Stanley H. Faeth, Nancy E. Golubiewski, Charles L. Redman, Jianguo Wu, Xuemei Bai, and John M. Briggs. 2008. “Global Change and the Ecology of Cities.” *Science* 319 (5864): 756–60.

Groffman, Peter M., Mary L. Cadenasso, Jeannine Cavender-Bares, Daniel L. Childers, Nancy B. Grimm, J. Morgan Grove, Sarah E. Hobbie, et al. 2017. “Moving Towards a New Urban Systems Science.” *Ecosystems* 20 (1): 38–43. https://doi.org/10.1007/s10021-016-0053-4.

Groffman, Peter M., Jeannine Cavender-Bares, Neil D. Bettez, J. Morgan Grove, Sharon J. Hall, James B. Heffernan, Sarah E. Hobbie, et al. 2014. “Ecological Homogenization of Urban USA.” *Frontiers in Ecology and the Environment* 12 (1): 74–81. https://doi.org/10.1890/120374.

Güneralp, Burak, Meredith Reba, Billy U. Hales, Elizabeth A. Wentz, and Karen C. Seto. 2020. “Trends in Urban Land Expansion, Density, and Land Transitions from 1970 to 2010: A Global Synthesis.” *Environmental Research Letters* 15 (4): 044015.

Gustafson, Eric J. 1998. “Quantifying Landscape Spatial Pattern: What Is the State of the Art?” *Ecosystems* 1 (2): 143–56. https://doi.org/10.1007/s100219900011.

Gutman, Garik, Anthony C. Janetos, Christopher O. Justice, Emilio F. Moran, John F. Mustard, Ronald R. Rindfuss, David Skole, Billy Lee Turner II, and Mark A. Cochrane. 2004. *Land Change Science: Observing, Monitoring and Understanding Trajectories of Change on the Earth's Surface*. Vol. 6. Springer Science & Business Media.

Hager, A., M. F. Otarola, M. F. Stuhlmacher, R. A. Castillo, and A. C. Arias. 2015. "Effects of Management and Landscape Composition on the Diversity and Structure of Tree Species Assemblages in Coffee Agroforests." *AGRICULTURE ECOSYSTEMS & ENVIRONMENT* 199: 43–51.

Hahs, Amy K., Mark J. McDonnell, Michael A. McCarthy, Peter A. Vesk, Richard T. Corlett, Briony A. Norton, Steven E. Clemants, et al. 2009. "A Global Synthesis of Plant Extinction Rates in Urban Areas." *Ecology Letters* 12 (11): 1165–73. https://doi.org/10.1111/j.1461-0248.2009.01372.x.

Haralick, Robert M., K. Shanmugam, and Its'Hak Dinstein. 1973. "Textural Features for Image Classification." *IEEE Transactions on Systems, Man, and Cybernetics* SMC-3 (6): 610–21. https://doi.org/10.1109/TSMC.1973.4309314.

Harrison, Paul, and Fred Pearce. 2000. *AAAS Atlas of Population & Environment*. Edited by Victoria Dompka Markham. American Association for the Advancement of Science: Univ of California Press. http://atlas.aaas.org/.

Hausmann, Ricardo, César Hidalgo, Sebastián Bustos, Michele Coscia, Sarah Chung, Juan Jimenez, Alexander Simoes, and Muhammed A. Yildirim. 2012. "The Atlas of Economic Complexity." Media Lab: MIT. https://oec.world/en/.

Hesselbarth, M.H.K., M. Sciaini, K. Wiegand, and J. Nowosad. 2019. *Landscapemetrics: An Open-source R Tool to Calculate Landscape Metrics* (version 1.2.1). Ecography, 42: 1648-1657. https://r-spatialecology.github.io/landscapemetrics/.

Holling, C. S. 2001. "Understanding the Complexity of Economic, Ecological, and Social Systems." *Ecosystems* 4 (5): 390–405.

Hondula, David M., Matei Georgescu, and Robert C. Balling. 2014. "Challenges Associated with Projecting Urbanization-Induced Heat-Related Mortality." *Science of The Total Environment* 490 (August): 538–44. https://doi.org/10.1016/j.scitotenv.2014.04.130.

Houck, Oliver A. 2000. "Environmental Law in Cuba." *Journal of Land Use & Environmental Law* 16: 82.

Huang, Ganlin, and M. L. Cadenasso. 2016. “People, Landscape, and Urban Heat Island: Dynamics among Neighborhood Social Conditions, Land Cover and Surface Temperatures.” *Landscape Ecology* 31 (10): 2507–2515.

Huang, Lu, Weining Xiang, Jianguo Wu, Christoph Traxler, and Jingzhou Huang. 2019. “Integrating GeoDesign with Landscape Sustainability Science.” *Sustainability* 11 (3): 833.

Hurkmans, R. T. W. L., W. Terink, R. Uijlenhoet, E. J. Moors, P. A. Troch, and P. H. Verburg. 2009. “Effects of Land Use Changes on Streamflow Generation in the Rhine Basin.” *Water Resources Research* 45 (6): W06405. https://doi.org/10.1029/2008WR007574.

Iknayan, Kelly J., and Steven R. Beissinger. 2018. “Collapse of a Desert Bird Community over the Past Century Driven by Climate Change.” *Proceedings of the National Academy of Sciences* 115 (34): 8597–8602. https://doi.org/10.1073/pnas.1805123115.

Imhoff, Marc L., Ping Zhang, Robert E. Wolfe, and Lahouari Bounoua. 2010. “Remote Sensing of the Urban Heat Island Effect across Biomes in the Continental USA.” *Remote Sensing of Environment* 114 (3): 504–13. https://doi.org/10.1016/j.rse.2009.10.008.

IPCC. 2014. “Climate Change 2014: Mitigation of Climate Change.” Contribution of Working Group III to the Fifth Assessment Report of the Intergovernmental Panel on Climate Change. Cambridge University Press, Cambridge, United Kingdom and New York, NY, USA. https://www.ipcc.ch/report/ar5/wg3/.

Jenerette, G. Darrel, and David Potere. 2010. “Global Analysis and Simulation of Land-Use Change Associated with Urbanization.” *Landscape Ecology* 25 (5): 657–70. https://doi.org/10.1007/s10980-010-9457-2.

Kalnay, Eugenia, and Ming Cai. 2003. “Impact of Urbanization and Land-Use Change on Climate.” *Nature* 423 (6939): 528–31. https://doi.org/10.1038/nature01675.

Kamarianakis, Yiannis, Xiaoxiao Li, B. L. Turner, and Anthony J. Brazel. 2017. “On the Effects of Landscape Configuration on Summer Diurnal Temperatures in Urban Residential Areas: Application in Phoenix, AZ.” *Frontiers of Earth Science* 13 (3): 445–63. https://doi.org/10.1007/s11707-017-0678-4.

Kedron, Peter, Yun Zhao, and Amy E. Frazier. 2019. “Three Dimensional (3D) Spatial Metrics for Objects.” *Landscape Ecology*, June. https://doi.org/10.1007/s10980-019-00861-4.

Kong, Fanhua, Haiwei Yin, Nobukazu Nakagoshi, and Yueguang Zong. 2010. "Urban Green Space Network Development for Biodiversity Conservation: Identification Based on Graph Theory and Gravity Modeling." *Landscape and Urban Planning* 95 (1): 16–27. https://doi.org/10.1016/j.landurbplan.2009.11.001.

Koont, Sinan. 2011. *Sustainable Urban Agriculture in Cuba*. 1st ed. Gainesville: University Press of Florida.

Kuemmerle, T., P. Hostert, V. St-Louis, and V. C. Radeloff. 2009. "Using Image Texture to Map Farmland Field Size: A Case Study in Eastern Europe." *Journal of Land Use Science* 4 (1–2): 85–107. https://doi.org/10.1080/17474230802648786.

Kupfer, John A. 2012. "Landscape Ecology and Biogeography: Rethinking Landscape Metrics in a Post-FRAGSTATS Landscape." *Progress in Physical Geography: Earth and Environment* 36 (3): 400–420. https://doi.org/10.1177/0309133312439594.

Laaidi, Karine, Abdelkrim Zeghnoun, Bénédicte Dousset, Philippe Bretin, Stéphanie Vandentorren, Emmanuel Giraudet, and Pascal Beaudeau. 2012. "The Impact of Heat Islands on Mortality in Paris during the August 2003 Heat Wave." *Environmental Health Perspectives* 120 (2): 254–59. https://doi.org/10.1289/ehp.1103532.

Lambin, Eric F., B. L. Turner, Helmut J. Geist, Samuel B. Agbola, Arild Angelsen, John W. Bruce, Oliver T. Coomes, et al. 2001. "The Causes of Land-Use and Land-Cover Change: Moving beyond the Myths." *Global Environmental Change* 11 (4): 261–69.

Lamy, T., K. N. Liss, A. Gonzalez, and E. M. Bennett. 2016. "Landscape Structure Affects the Provision of Multiple Ecosystem Services." *Environ. Res. Lett* 11 (12): 124017.

Lebel, L., J. Anderies, B. Campbell, C. Folke, S. Hatfield-Dodds, T. Hughes, and James Wilson. 2006. "Governance and the Capacity to Manage Resilience in Regional Social-Ecological Systems." *Ecology and Society*, June. http://digitalcommons.library.umaine.edu/sms_facpub/52.

Leemans, R., and de Groot. 2003. *Millennium Ecosystem Assessment: Ecosystems and Human Well-Being: A Framework for Assessment*. Island Press. http://library.wur.nl/WebQuery/wurpubs/326575.

Leitao, Andre Botequilha, Joseph Miller, Jack Ahern, and Kevin Mcgarigal. 2006. *Measuring Landscapes: A Planner's Handbook*. Washington, DC: Island Press.

Li, Junxiang, Conghe Song, Lu Cao, Feige Zhu, Xianlei Meng, and Jianguo Wu. 2011. "Impacts of Landscape Structure on Surface Urban Heat Islands: A Case Study of Shanghai, China." *Remote Sensing of Environment* 115 (12): 3249–3263.

Li, Xiaoma, Weiqi Zhou, Zhiyun Ouyang, Weihua Xu, and Hua Zheng. 2012. "Spatial Pattern of Greenspace Affects Land Surface Temperature: Evidence from the Heavily Urbanized Beijing Metropolitan Area, China." *Landscape Ecology* 27 (6): 887–98. https://doi.org/10.1007/s10980-012-9731-6.

Li, Xiaoxiao, Yiannis Kamarianakis, Yun Ouyang, Billie L. Turner II, and Anthony Brazel. 2017. "On the Association between Land System Architecture and Land Surface Temperatures: Evidence from a Desert Metropolis—Phoenix, Arizona, U.S.A." *Landscape and Urban Planning* 163: 107–20. https://doi.org/10.1016/j.landurbplan.2017.02.009.

Li, Xiaoxiao, Wenwen Li, A. Middel, S. L. Harlan, A. J. Brazel, and B. L. Turner II. 2016. "Remote Sensing of the Surface Urban Heat Island and Land Architecture in Phoenix, Arizona: Combined Effects of Land Composition and Configuration and Cadastral–Demographic–Economic Factors." *Remote Sensing of Environment* 174 (March): 233–43. https://doi.org/10.1016/j.rse.2015.12.022.

Lin, Tao, Valerie Gibson, Shenghui Cui, Chang-Ping Yu, Shaohua Chen, Zhilong Ye, and Yong-Guan Zhu. 2014. "Managing Urban Nutrient Biogeochemistry for Sustainable Urbanization." *Environmental Pollution* 192 (September): 244–50. https://doi.org/10.1016/j.envpol.2014.03.038.

Liu, Xiaoping, Guohua Hu, Yimin Chen, Xia Li, Xiaocong Xu, Shaoying Li, Fengsong Pei, and Shaojian Wang. 2018. "High-Resolution Multi-Temporal Mapping of Global Urban Land Using Landsat Images Based on the Google Earth Engine Platform." *Remote Sensing of Environment* 209 (May): 227–39. https://doi.org/10.1016/j.rse.2018.02.055.

Liu, Zhifeng, Chunyang He, Yuyu Zhou, and Jianguo Wu. 2014. "How Much of the World's Land Has Been Urbanized, Really? A Hierarchical Framework for Avoiding Confusion." *Landscape Ecology* 29 (5): 763–71. https://doi.org/10.1007/s10980-014-0034-y.

Luck, Matthew, and Jianguo Wu. 2002. "A Gradient Analysis of Urban Landscape Pattern: A Case Study from the Phoenix Metropolitan Region, Arizona, USA." *Landscape Ecology* 17 (4): 327–39. https://doi.org/10.1023/A:1020512723753.

Maal-Bared, Rasha. 2006. "Comparing Environmental Issues in Cuba before and after the Special Period: Balancing Sustainable Development and Survival." *Environment International* 32 (3): 349–58. https://doi.org/10.1016/j.envint.2005.08.002.

Machado, Mario Reinaldo. 2017. “Alternative to What? Agroecology, Food Sovereignty, and Cuba’s Agricultural Revolution.” *Human Geography* 10 (3): 7–21. https://doi.org/10.1177/194277861701000302.

———. 2018. “What’s Going on with Land-Use in Cuba?: Disparate Data Sets and the Cuban Agricultural Transition.” *Journal of Land Use Science* 13 (4): 439–46. https://doi.org/10.1080/1747423X.2018.1533044.

Martin, Carlos, and Sara McTarnaghan. 2018. “Institutionalizing Urban Resilience: A Midterm Monitoring and Evaluation Reportof 100 Resilient Cities.” 2100 M Street NWWashington, DC 20037: Urban Institute. https://assets.rockefellerfoundation.org/app/uploads/20181205162438/Institutionalizing-Urban-Resilience-A-Midterm-Monitoring-and-Evaluation-Report-of-100-Resilient-Cities.pdf.

Marusich, Laura R., and Jonathan Z. Bakdash. 2018. *Rmcorr* (version 0.3.0). R. https://cran.r-project.org/web/packages/rmcorr/rmcorr.pdf.

McCune, Bruce, and James B. Grace. 2002. *Analysis of Ecological Communities*. Gleneden Beach, OR: MjM Software Design.

McGarigal, Kevin, Samuel A. Cushman, and E Ene. 2012. “FRAGSTATS v4: Spatial Pattern Analysis Program for Categorical and Continuous Maps.” Computer Software Program Produced by the Authors at the University of Massachusetts, Amherst. 2012. http://www.umass.edu/landeco/research/fragstats/fragstats.html.

McGarigal, Kevin, and Barbara J. Marks. 1995. “FRAGSTATS: Spatial Pattern Analysis Program for Quantifying Landscape Structure.” http://www.treesearch.fs.fed.us/pubs/3064.

McGarigal, Kevin, Sermin Tagil, and Samuel A. Cushman. 2009. “Surface Metrics: An Alternative to Patch Metrics for the Quantification of Landscape Structure.” *Landscape Ecology* 24 (3): 433–50. https://doi.org/10.1007/s10980-009-9327-y.

McHarg, Ian L. 1992. *Design with Nature*. New York: JWiley.

McIntyre, S., and G. W. Barrett. 1992. “Habitat Variegation, An Alternative to Fragmentation.” *Conservation Biology* 6 (1): 146–47. https://doi.org/10.1046/j.1523-1739.1992.610146.x.

McKibben, Bill. 2005. “The Cuba Diet.” *Harper’s Magazine* 310 (1859): 61–69.

McPhearson, Timon, Steward T. A. Pickett, Nancy B. Grimm, Jari Niemelä, Marina Alberti, Thomas Elmqvist, Christiane Weber, Dagmar Haase, Jürgen Breuste, and

Salman Qureshi. 2016. “Advancing Urban Ecology toward a Science of Cities.” *BioScience* 66 (3): 198–212. https://doi.org/10.1093/biosci/biw002.

McPhillips, L. E., S. R. Earl, R. L. Hale, and N. B. Grimm. 2019. “Urbanization in Arid Central Arizona Watersheds Results in Decreased Stream Flashiness.” *Water Resources Research* 55 (11). https://doi.org/10.1029/2019WR025835.

McSweeney, Kendra, Nazih Richani, Zoe Pearson, Jennifer Devine, and David J. Wrathall. 2017. “Why Do Narcos Invest in Rural Land?” *Journal of Latin American Geography* 16 (2): 3–29. https://doi.org/10.1353/lag.2017.0019.

Medina, Hanoi, Quirijn de Jong van Lier, Jorge García, and María Elena Ruiz. 2017. “Regional-Scale Variability of Soil Properties in Western Cuba.” *Soil and Tillage Research* 166 (March): 84–99. https://doi.org/10.1016/j.still.2016.10.009.

Meerow, Sara, Joshua P. Newell, and Melissa Stults. 2016. “Defining Urban Resilience: A Review.” *Landscape and Urban Planning* 147 (March): 38–49. https://doi.org/10.1016/j.landurbplan.2015.11.011.

Meng, Dan, Siyao Yang, Huili Gong, Xiaojuan Li, and Jing Zhang. 2016. “Assessment of Thermal Environment Landscape over Five Megacities in China Based on Landsat 8.” *Journal of Applied Remote Sensing* 10 (June): 026034. https://doi.org/10.1117/1.JRS.10.026034.

Menne, Matthew J., Imke Durre, Bryant Korzeniewski, Shelley McNeal, Kristy Thomas, Xungang Yin, Steven Anthony, et al. 2012. “Global Historical Climatology Network - Daily (GHCN-Daily), Version 3.” *NOAA National Climatic Data Center*. https://doi.org/10.7289/V5D21VHZ.

Menne, Matthew J., Imke Durre, Russell S. Vose, Byron E. Gleason, and Tamara G. Houston. 2012. “An Overview of the Global Historical Climatology Network-Daily Database.” *Journal of Atmospheric and Oceanic Technology* 29 (7): 897–910. https://doi.org/10.1175/JTECH-D-11-00103.1.

Meyfroidt, P., R. Roy Chowdhury, A. de Bremond, E. C. Ellis, K. -H. Erb, T. Filatova, R. D. Garrett, et al. 2018. “Middle-Range Theories of Land System Change.” *Global Environmental Change* 53 (November): 52–67. https://doi.org/10.1016/j.gloenvcha.2018.08.006.

Midlarsky, Manus I. 1998. “Democracy and the Environment: An Empirical Assessment.” *Journal of Peace Research* 35 (3): 341–61.

Migurski, Michal. 2018. *Compactr*. gerrymandr/compactr: Metric Geometry and Gerrymandering Group. https://github.com/gerrymandr/compactr.

Mora, Camilo, Bénédicte Dousset, Iain R. Caldwell, Farrah E. Powell, Rollan C. Geronimo, Coral R. Bielecki, Chelsie W. W. Counsell, et al. 2017. "Global Risk of Deadly Heat." *Nature Climate Change* 7 (7): 501–6. https://doi.org/10.1038/nclimate3322.

Moran, Emilio F. 2016. *People and Nature: An Introduction to Human Ecological Relations*. Chichester, West Sussex, UK: John Wiley & Sons.

Munroe, Darla K., and Kendra McSweeney. 2019. "Addressing Root Drivers of Land-Climate Dynamics." *One Earth* 1 (2): 181–84. https://doi.org/10.1016/j.oneear.2019.10.001.

Munteanu, C., T. Kuemmerle, M. Boltiziar, V. Butsic, U. Gimmi, Halada Lúboš, D. Kaim, et al. 2014. "Forest and Agricultural Land Change in the Carpathian Region-A Meta-Analysis of Long-Term Patterns and Drivers of Change." *Land Use Policy* 38: 685–97. https://doi.org/10.1016/j.landusepol.2014.01.012.

Myint, Soe Win, Baojuan Zheng, Emily Talen, Chao Fan, Shai Kaplan, Ariane Middel, Martin Smith, Huei-Ping Huang, and Anthony Brazel. 2015. "Does the Spatial Arrangement of Urban Landscape Matter? Examples of Urban Warming and Cooling in Phoenix and Las Vegas." *Ecosystem Health and Sustainability* 1 (4): 1–15. https://doi.org/10.1890/EHS14-0028.1.

Nassauer, Joan Iverson. 2012. "Landscape as Medium and Method for Synthesis in Urban Ecological Design." *Landscape and Urban Planning* 106 (3): 221–29. https://doi.org/10.1016/j.landurbplan.2012.03.014.

Nassauer, Joan Iverson, and Paul Opdam. 2008. "Design in Science: Extending the Landscape Ecology Paradigm." *Landscape Ecology* 23 (6): 633–44. https://doi.org/10.1007/s10980-008-9226-7.

Nechyba, Thomas J., and Randall P. Walsh. 2004. "Urban Sprawl." *The Journal of Economic Perspectives; Nashville* 18 (4): 177–200.

Neumayer, Eric. 2002. "Do Democracies Exhibit Stronger International Environmental Commitment? A Cross-Country Analysis." *Journal of Peace Research* 39 (2): 139–64.

Ng, Hui-Fuang. 2006. "Automatic Thresholding for Defect Detection." *Pattern Recognition Letters* 27 (14): 1644–49. https://doi.org/10.1016/j.patrec.2006.03.009.

Noss, Reed F. 1987. "From Plant Communities to Landscapes in Conservation Inventories: A Look at The Nature Conservancy (USA)." *Biological Conservation* 41 (1): 11–37.

Oke, T. R. 1984. “Towards a Prescription for the Greater Use of Climatic Principles in Settlement Planning.” *Energy and Buildings* 7 (1): 1–10. https://doi.org/10.1016/0378-7788(84)90040-9.

———. 1988. “Street Design and Urban Canopy Layer Climate.” *Energy and Buildings* 11 (1): 103–13. https://doi.org/10.1016/0378-7788(88)90026-6.

Oke, T. R., G. Mills, A. Christen, and J. A Voogt. 2017. *Urban Climates*. Cambridge University Press. http://www.cambridge.org/us/academic/subjects/earth-and-environmental-science/climatology-and-climate-change/urban-climates.

Oksanen, Jari, F. Guillaume Blanchet, Michael Friendly, Roeland Kindt, Pierre Legendre, Dan McGlinn, Peter R. Minchin, et al. 2018. *Vegan: Community Ecology Package* (version R package version 2.4-6). https://CRAN.R-project.org/package=vegan.

Oliveira, Erneson A., José S. Andrade, and Hernán A. Makse. 2014. “Large Cities Are Less Green.” *Scientific Reports* 4 (February): 4235. https://doi.org/10.1038/srep04235.

Osborne, Lewis L., and David A. Kovacic. 1993. “Riparian Vegetated Buffer Strips in Water-Quality Restoration and Stream Management.” *Freshwater Biology* 29 (2): 243–58. https://doi.org/10.1111/j.1365-2427.1993.tb00761.x.

Ostrom, Elinor. 2009. “A General Framework for Analyzing Sustainability of Social-Ecological Systems.” *Science* 325 (5939): 419–22.

Ostrom, Elinor, Marco A. Janssen, and John M. Anderies. 2007. “Going beyond Panaceas.” *Proceedings of the National Academy of Sciences* 104 (39): 15176–78. https://doi.org/10.1073/pnas.0701886104.

Otsu, N. 1979. “A Threshold Selection Method from Gray-Level Histograms.” *IEEE Transactions on Systems, Man, and Cybernetics* 9 (1): 62–66. https://doi.org/10.1109/TSMC.1979.4310076.

Pardo, Flavio Bravo. 1982. *Ley No. 36: Cooperativas Agropecuarias*.

Peng, Shushi, Shilong Piao, Philippe Ciais, Pierre Friedlingstein, Catherine Ottle, François-Marie Bréon, Huijuan Nan, Liming Zhou, and Ranga B. Myneni. 2012. “Surface Urban Heat Island across 419 Global Big Cities.” *Environmental Science & Technology* 46 (2): 696–703. https://doi.org/10.1021/es2030438.

Perez, Danai Fernandez, Ricardo Remond Noa, and Jose Damian Ruiz Sinoga. 2010. “An Analysis of the Spatial Colonization of Scrubland Intrusive Species in the Itabo and Guanabo Watershed, Cuba.” *Remote Sensing* 2 (3): 740–57.

Peterson, L. K., K. M. Bergen, D. G. Brown, L. Vashchuk, and Y. Blam. 2009. "Forested Land-Cover Patterns and Trends over Changing Forest Management Eras in the Siberian Baikal Region." *Forest Ecology and Management* 257 (3): 911–22. https://doi.org/10.1016/j.foreco.2008.10.037.

Pickett, S. T. A., M. L. Cadenasso, and J. M. Grove. 2004. "Resilient Cities: Meaning, Models, and Metaphor for Integrating the Ecological, Socio-Economic, and Planning Realms." *Landscape and Urban Planning* 69 (4): 369–84. https://doi.org/10.1016/j.landurbplan.2003.10.035.

Pickett, Steward TA, and Mary L. Cadenasso. 2008. "Linking Ecological and Built Components of Urban Mosaics: An Open Cycle of Ecological Design." *Journal of Ecology* 96 (1): 8–12.

Pierer, Carl, and Felix Creutzig. 2019. "Star-Shaped Cities Alleviate Trade-off between Climate Change Mitigation and Adaptation." *Environmental Research Letters* 14 (8): 085011. https://doi.org/10.1088/1748-9326/ab2081.

Polsky, Colin, J. Morgan Grove, Chris Knudson, Peter M. Groffman, Neil Bettez, Jeannine Cavender-Bares, Sharon J. Hall, et al. 2014. "Assessing the Homogenization of Urban Land Management with an Application to US Residential Lawn Care." *Proceedings of the National Academy of Sciences* 111 (12): 4432–37. https://doi.org/10.1073/pnas.1323995111.

Pope, Cynthia, and John C. Finn. 2017. "Editors' Introduction: Geographies of Contemporary Cuba:" *Human Geography*, November. https://doi.org/10.1177/194277861701000301.

Premat, Adriana. 2012. *Sowing Change: The Making of Havana's Urban Agriculture*.

Qin, Yuanwei, Xiangming Xiao, Jinwei Dong, Bangqian Chen, Fang Liu, Geli Zhang, Yao Zhang, Jie Wang, and Xiaocui Wu. 2017. "Quantifying Annual Changes in Built-up Area in Complex Urban-Rural Landscapes from Analyses of PALSAR and Landsat Images." *ISPRS Journal of Photogrammetry and Remote Sensing* 124 (February): 89–105. https://doi.org/10.1016/j.isprsjprs.2016.12.011.

Rahman, Atiqur, Shiv Prashad Aggarwal, Maik Netzband, and Shahab Fazal. 2011. "Monitoring Urban Sprawl Using Remote Sensing and GIS Techniques of a Fast Growing Urban Centre, India." *IEEE Journal of Selected Topics in Applied Earth Observations and Remote Sensing* 4 (1): 56–64. https://doi.org/10.1109/JSTARS.2010.2084072.

Reock, Ernest C. 1961. "A Note: Measuring Compactness as a Requirement of Legislative Apportionment." *Midwest Journal of Political Science* 5 (1): 70–74. https://doi.org/10.2307/2109043.

Roa García, Raúl. 1980. *Ley No. 27: Gran Parque Nacional Sierra Maestra*.

Robinson, Derek, Alan Di Vittorio, Peter Alexander, Almut Arneth, C. Michael Barton, Daniel Brown, Albert Kettner, Carsten Lemmen, Brian O'Neill, and Marco Janssen. 2018. "Modelling Feedbacks between Human and Natural Processes in the Land System." *Earth System Dynamics* 9: 895–914.

Rodríguez-Ojea, Arturo, Santa Jiménez, Antonio Berdasco, and Mercedes Esquivel. 2002. "The Nutrition Transition in Cuba in the Nineties: An Overview." *Public Health Nutrition* 5 (1a): 129–33.

Rosenberg, Kenneth V., Adriaan M. Dokter, Peter J. Blancher, John R. Sauer, Adam C. Smith, Paul A. Smith, Jessica C. Stanton, et al. 2019. "Decline of the North American Avifauna." *Science* 366 (6461): 120–24. https://doi.org/10.1126/science.aaw1313.

Rosenzweig, Cynthia, and William Solecki. 2015. "New York City Panel on Climate Change 2015 Report Introduction." *Annals of the New York Academy of Sciences* 1336 (1): 3–5. https://doi.org/10.1111/nyas.12625.

Roy Chowdhury, R., and B. L. Turner. 2019. "The Parallel Trajectories and Increasing Integration of Landscape Ecology and Land System Science." *Journal of Land Use Science*, 1–20.

Rozenfeld, Hernán D., Diego Rybski, José S. Andrade, Michael Batty, H. Eugene Stanley, and Hernán A. Makse. 2008. "Laws of Population Growth." *Proceedings of the National Academy of Sciences* 105 (48): 18702–7. https://doi.org/10.1073/pnas.0807435105.

Ruddiman, William F. 2013. "The Anthropocene." *Annual Review of Earth and Planetary Sciences* 41 (1): 45–68. https://doi.org/10.1146/annurev-earth-050212-123944.

Sassen, Saskia. 2008. "Re-Assembling the Urban." *Urban Geography* 29 (2): 113–26. https://doi.org/10.2747/0272-3638.29.2.113.

Schneider, A., and C. M. Mertes. 2014. "Expansion and Growth in Chinese Cities, 1978–2010." *Environmental Research Letters* 9 (2): 024008. https://doi.org/10.1088/1748-9326/9/2/024008.

Schumaker, Nathan H. 1996. "Using Landscape Indices to Predict Habitat Connectivity." *Ecology* 77 (4): 1210–25. https://doi.org/10.2307/2265590.

Seto, Karen C., and Michail Fragkias. 2005. "Quantifying Spatiotemporal Patterns of Urban Land-Use Change in Four Cities of China with Time Series Landscape

Metrics." *Landscape Ecology* 20 (7): 871–88. https://doi.org/10.1007/s10980-005-5238-8.

Seto, Karen C., Michail Fragkias, Burak Güneralp, and Michael K. Reilly. 2011. "A Meta-Analysis of Global Urban Land Expansion." *PLOS ONE* 6 (8): e23777. https://doi.org/10.1371/journal.pone.0023777.

Seto, Karen C., Burak Güneralp, and Lucy R. Hutyra. 2012. "Global Forecasts of Urban Expansion to 2030 and Direct Impacts on Biodiversity and Carbon Pools." *Proceedings of the National Academy of Sciences* 109 (40): 16083–88. https://doi.org/10.1073/pnas.1211658109.

Seto, Karen C., Anette Reenberg, Christopher G. Boone, Michail Fragkias, Dagmar Haase, Tobias Langanke, Peter Marcotullio, Darla K. Munroe, Branislav Olah, and David Simon. 2012. "Urban Land Teleconnections and Sustainability." *Proceedings of the National Academy of Sciences of the United States of America* 109 (20): 7687–92. https://doi.org/10.1073/pnas.1117622109.

Shadish, William R., Thomas D. Cook, and Donald T. Campbell. 2002. *Experimental and Quasi-Experimental Designes for Generalized Causal Inference*. Belmont, CA: Wadsworth: Cengage Learning.

Shastri, Hiteshri, Beas Barik, Subimal Ghosh, Chandra Venkataraman, and Pankaj Sadavarte. 2017. "Flip Flop of Day-Night and Summer-Winter Surface Urban Heat Island Intensity in India." *Scientific Reports* 7 (1): 1–8. https://doi.org/10.1038/srep40178.

Shen, Huanfeng, Liwen Huang, Liangpei Zhang, Penghai Wu, and Chao Zeng. 2016. "Long-Term and Fine-Scale Satellite Monitoring of the Urban Heat Island Effect by the Fusion of Multi-Temporal and Multi-Sensor Remote Sensed Data: A 26-Year Case Study of the City of Wuhan in China." *Remote Sensing of Environment* 172 (January): 109–25. https://doi.org/10.1016/j.rse.2015.11.005.

Smiraglia, D., T. Ceccarelli, S. Bajocco, L. Perini, and L. Salvati. 2015. "Unraveling Landscape Complexity: Land Use/Land Cover Changes and Landscape Pattern Dynamics (1954–2008) in Contrasting Peri-Urban and Agro-Forest Regions of Northern Italy." *Environmental Management* 56 (4): 916–32. https://doi.org/10.1007/s00267-015-0533-x.

Steffen, Will, Åsa Persson, Lisa Deutsch, Jan Zalasiewicz, Mark Williams, Katherine Richardson, Carole Crumley, et al. 2011. "The Anthropocene: From Global Change to Planetary Stewardship." *AMBIO* 40 (7): 739. https://doi.org/10.1007/s13280-011-0185-x.

Steffen, Will, Katherine Richardson, Johan Rockström, Sarah E. Cornell, Ingo Fetzer, Elena M. Bennett, Reinette Biggs, et al. 2015. “Planetary Boundaries: Guiding Human Development on a Changing Planet.” *Science* 347 (6223): 1259855. https://doi.org/10.1126/science.1259855.

Steiner, Frederick. 2014. “Frontiers in Urban Ecological Design and Planning Research.” *Landscape and Urban Planning* 125 (May): 304–11. https://doi.org/10.1016/j.landurbplan.2014.01.023.

Steinitz, Carl. 2012. *A Framework for Geodesign: Changing Geography by Design*. First edition.. Redlands, California: Esri.

Stewart, D., and T. R. Oke. 2012. “Local Climate Zones for Urban Temperature Studies.” *Bulletin of the American Meteorological Society* 93 (12): 1879–1900. https://doi.org/10.1175/BAMS-D-11-000191.

Stricker, Pamela. 2010. “Bringing Social Justice Back in: Cuba Revitalises Sustainable Development.” *Local Environment* 15 (2): 185–97.

Stuhlmacher, Michelle, Riley Andrade, B. L. Turner II, Amy E. Frazier, and Wenwen Li. 2020. “Environmental Outcomes of Urban Land System Change: Comparing Riparian Design Approaches in the Phoenix Metropolitan Area.” *Land Use Policy* in press.

Tellman, Beth, Nicholas R. Magliocca, B. L. Turner, and Peter H. Verburg. 2020. “Understanding the Role of Illicit Transactions in Land-Change Dynamics.” *Nature Sustainability*, January, 1–7. https://doi.org/10.1038/s41893-019-0457-1.

Tian, Yuhong, Chi Yung Jim, Yan Tao, and Tao Shi. 2011. “Landscape Ecological Assessment of Green Space Fragmentation in Hong Kong.” *Urban Forestry & Urban Greening* 10 (2): 79–86.

Trianni, G., G. Lisini, E. Angiuli, E. A. Moreno, P. Dondi, A. Gaggia, and P. Gamba. 2015. “Scaling up to National/Regional Urban Extent Mapping Using Landsat Data.” *IEEE Journal of Selected Topics in Applied Earth Observations and Remote Sensing* 8 (7): 3710–19. https://doi.org/10.1109/JSTARS.2015.2398032.

Turner, B. L. 2002. “Contested Identities: Human-Environment Geography and Disciplinary Implications in a Restructuring Academy.” *Annals of the Association of American Geographers* 92 (1): 52–74.

Turner, B. L. II. 2010. “Sustainability and Forest Transitions in the Southern Yucatan: The Land Architecture Approach.” *Land Use Policy* 27 (2): 170–179.

———. 2016. “Land System Architecture for Urban Sustainability: New Directions for Land System Science Illustrated by Application to the Urban Heat Island Problem.” *Journal of Land Use Science* 11 (6): 689–97. https://doi.org/10.1080/1747423X.2016.1241315.

Turner, B. L., Eric F. Lambin, and Anette Reenberg. 2007. “The Emergence of Land Change Science for Global Environmental Change and Sustainability.” *Proceedings of the National Academy of Sciences of the United States of America* 104 (52): 20666–71. https://doi.org/10.1073/pnas.0704119104.

Turner, B.L., Anthony C. Janetos, Peter H. Verburg, and Alan T. Murray. 2013. “Land System Architecture: Using Land Systems to Adapt and Mitigate Global Environmental Change.” *Global Environmental Change* 23 (2): 395–97. https://doi.org/10.1016/j.gloenvcha.2012.12.009.

Turner, V. Kelly, and Christopher S. Galletti. 2015. “Do Sustainable Urban Designs Generate More Ecosystem Services? A Case Study of Civano in Tucson, Arizona.” *The Professional Geographer* 67 (2): 204–17. https://doi.org/10.1080/00330124.2014.922021.

United Nations. 2018a. “World Urbanization Prospects: 2018 Revision.” SP.URB.TOTL.IN.ZS. United Nations, Population Division. https://www.un.org/development/desa/publications/2018-revision-of-world-urbanization-prospects.html.

———. 2019. “World Urbanization Prospects: 2019 Revision.” ST/ESA/SER.A/423. United Nations, Population Division. https://population.un.org/wpp/Publications/.

United Nations, Department of Economic and Social Affiars, Population Division. 2018b. “World Urbanization Prospects: The 2018 Revision, Key Facts.” Working Paper No. ESA/P/WP.252. New York: United Nations. https://population.un.org/wup/Publications/Files/WUP2018-KeyFacts.pdf.

Vadjunec, Jacqueline M., Amy E. Frazier, Peter Kedron, Todd Fagin, and Yun Zhao. 2018. “A Land Systems Science Framework for Bridging Land System Architecture and Landscape Ecology: A Case Study from the Southern High Plains.” *Land* 7 (1): 27. https://doi.org/10.3390/land7010027.

Veldkamp, Antonie, and Eric F. Lambin. 2001. “Predicting Land-Use Change.” *Agriculture, Ecosystems & Environment* 85 (1): 1–6.

Verburg, Peter H., Peter Alexander, Tom Evans, Nicholas R. Magliocca, Ziga Malek, Mark DA Rounsevell, and Jasper van Vliet. 2019. “Beyond Land Cover Change: Towards a New Generation of Land Use Models.” *Current Opinion in Environmental Sustainability* 38: 77–85.

Verburg, Peter H., Neville Crossman, Erle C. Ellis, Andreas Heinimann, Patrick Hostert, Ole Mertz, Harini Nagendra, et al. 2015. “Land System Science and Sustainable Development of the Earth System: A Global Land Project Perspective.” *Anthropocene* 12 (December): 29–41. https://doi.org/10.1016/j.ancene.2015.09.004.

Verburg, Peter H, Karl-Heinz Erb, Ole Mertz, and Giovana Espindola. 2013. “Land System Science: Between Global Challenges and Local Realities.” *Current Opinion in Environmental Sustainability*, Human settlements and industrial systems, 5 (5): 433–37. https://doi.org/10.1016/j.cosust.2013.08.001.

Wan, Z., S. Hook, and G. Hulley. 2015. “MOD11A2 MODIS/Terra Land Surface Temperature/Emissivity 8-Day L3 Global 1km SIN Grid V006.” *NASA EOSDIS Land Processes DAAC*. https://doi.org/10.5067/MODIS/MOD11A2.006.

Wang, Chuyuan, Soe W. Myint, Peilei Fan, Michelle Stuhlmacher, and Jiachuan Yang. 2018. “The Impact of Urban Expansion on the Regional Environment in Myanmar: A Case Study of Two Capital Cities.” *Landscape Ecology* 33 (5): 765–782.

Warren, Paige S., Susannah B. Lerman, Riley Andrade, Kelli L. Larson, and Heather L. Bateman. 2019. “The More Things Change: Species Losses Detected in Phoenix despite Stability in Bird–Socioeconomic Relationships.” *Ecosphere* 10 (3): e02624.

Whittle, Daniel, and Orlando Rey Santos. 2006. “Protecting Cuba’s Environment: Efforts to Design and Implement Effective Environmental Laws and Policies in Cuba.” *Cuban Studies* 37: 73.

Wickham, Hadley. 2017. *Tidyverse* (version version 1.2.1.). R Package. https://CRAN.R-project.org/package=tidyverse.

Wines, James. 2000. *Green Architecture*. Edited by Philip Jodidio. Köln ; New York: Taschen.

World Bank Group. 2019. “Population Estimates and Projections,” September. https://datacatalog.worldbank.org/dataset/population-estimates-and-projections.

Wright, Julia. 2009. *Sustainable Agriculture and Food Security in an Era of Oil Scarcity: Lessons from Cuba*. Sterling, VA; London: Earthscan.

Wu, Jianguo. 2013. “Landscape Sustainability Science: Ecosystem Services and Human Well-Being in Changing Landscapes.” *Landscape Ecology* 28 (6): 999–1023. https://doi.org/10.1007/s10980-013-9894-9.

———. 2014. “Urban Ecology and Sustainability: The State-of-the-Science and Future Directions.” *Landscape and Urban Planning* 125: 209–221.

———. 2019. “Linking Landscape, Land System and Design Approaches to Achieve Sustainability.” *Journal of Land Use Science*, 1–17.

Wu, Jianguo, and Ye Qi. 2000. “Dealing with Scale in Landscape Analysis: An Overview.” *Geographic Information Sciences* 6 (1): 1–5.

Wulder, Michael A., Steven E. Franklin, Joanne C. White, Julia Linke, and Steen Magnussen. 2006. “An Accuracy Assessment Framework for Large-area Land Cover Classification Products Derived from Medium-resolution Satellite Data.” *International Journal of Remote Sensing* 27 (4): 663–83. https://doi.org/10.1080/01431160500185284.

Xu, Hanqiu. 2006. “Modification of Normalised Difference Water Index (NDWI) to Enhance Open Water Features in Remotely Sensed Imagery.” *International Journal of Remote Sensing* 27 (14): 3025–33. https://doi.org/10.1080/01431160600589179.

Zar, Jerrold H. 2010. *Biostatistical Analysis*. Prentice Hall.

Zhang, Yujia, and Xiaoxiao Li. 2017. “Land Cover Classification of the CAP LTER Study Area at Five-Year Intervals from 1985 to 2010 Using Landsat Imagery.” *Environmental Data Initiative*, October. https://doi.org/10.6073/pasta/dab4db27974f6c8d5b91a91d30c7781d.

Zhang, Yujia, Ariane Middel, and B. L. Turner. 2019. “Evaluating the Effect of 3D Urban Form on Neighborhood Land Surface Temperature Using Google Street View and Geographically Weighted Regression.” *Landscape Ecology* 34 (3): 681–97. https://doi.org/10.1007/s10980-019-00794-y.

Zhang, Yujia, Alan T. Murray, and B. L. Turner. 2017. “Optimizing Green Space Locations to Reduce Daytime and Nighttime Urban Heat Island Effects in Phoenix, Arizona.” *Landscape and Urban Planning* 165 (September): 162–71. https://doi.org/10.1016/j.landurbplan.2017.04.009.

Zheng, Baojuan, Soe W. Myint, and Chao Fan. 2014. “Spatial Configuration of Anthropogenic Land Cover Impacts on Urban Warming.” *Landscape and Urban Planning* 130 (October): 104–11. https://doi.org/10.1016/j.landurbplan.2014.07.001.

Zhou, Bin, Diego Rybski, and Jürgen P. Kropp. 2017. “The Role of City Size and Urban Form in the Surface Urban Heat Island.” *Scientific Reports* 7 (1): 4791. https://doi.org/10.1038/s41598-017-04242-2.

Zhou, Weiqi, Ganlin Huang, and Mary L. Cadenasso. 2011. “Does Spatial Configuration Matter? Understanding the Effects of Land Cover Pattern on Land Surface Temperature in Urban Landscapes.” *Landscape and Urban Planning* 102 (1): 54–63. https://doi.org/10.1016/j.landurbplan.2011.03.009.

Zhou, Weiqi, Jia Wang, and Mary L. Cadenasso. 2017. “Effects of the Spatial Configuration of Trees on Urban Heat Mitigation: A Comparative Study.” *Remote Sensing of Environment* 195 (June): 1–12. https://doi.org/10.1016/j.rse.2017.03.043.

APPENDIX A

PERMISSIONS FROM CO-AUTHORS

All co-authors granted their permission for these first-authored, co-authored works to be used in my dissertation. The names of the co-authors corresponding to each chapter are listed below.

CHAPTER 2:
Riley Andrade, B.L. Turner II, Amy Frazier, and Wenwen Li

CHAPTER 3:
B.L. Turner II, Amy Frazier, Jessica Leffel, and Yushim Kim

CHAPTER 4:
Matei Georgescu, Yina Hu, Ran Goldblatt, Sarthak Gupta, B.L. Turner II, Amy Frazier, Nicholas Clinton, and Robert Balling

APPENDIX B

CHAPTER 2: SUPPLEMENTAL MATERIAL

Bird species seen or heard at the Rio Salado and New River CAP LTER birding sites.

Table 1. Common name, scientific name, and 4-letter alpha code for all bird species in our analysis. The 4-letter alpha codes are the ones used during the CAP LTER data collection—English name 54th AOU Supplement (2013) alpha codes.

4-letter alpha code	Common Name	Scientific Name
ABTO	Abert's Towhee	*Melozone aberti*
AMBI	American Bittern	*Botaurus lentiginosus*
AMCO	American Coot	*Fulica americana*
AMKE	American Kestrel	*Falco sparverius*
ANHU	Anna's Hummingbird	*Calypte anna*
ATFL	Ash-throated Flycatcher	*Myiarchus cinerascens*
AUWA	Audubon's Warbler	*Setophaga coronata auduboni*
BCNH	Black-crowned Night-Heron	*Nycticorax nycticorax*
BEKI	Belted Kingfisher	*Megaceryle alcyon*
BEWR	Bewick's Wren	*Thryomanes bewickii*
BGGN	Blue-gray Gnatcatcher	*Polioptila caerulea*
BHCO	Brown-headed Cowbird	*Molothrus ater*
BLPH	Black Phoebe	*Sayornis nigricans*
BNST	Black-necked Stilt	*Himantopus mexicanus*
BRSP	Brewer's Sparrow	*Spizella breweri*
BTGN	Black-tailed Gnatcatcher	*Polioptila melanura*
BTYW	Black-throated Gray Warbler	*Setophaga nigrescens*
CACW	Cactus Wren	*Campylorhynchus brunneicapillus*
CANG	Canada Goose	*Branta canadensis*
CHSP	Chipping Sparrow	*Spizella passerina*
CITE	Cinnamon Teal	*Spatula cyanoptera*
CLSW	Cliff Swallow	*Petrochelidon pyrrhonota*
COGA	Common gallinule	*Gallinula galeata*
COHU	Costa's Hummingbird	*Calypte costae*
CORA	Common Raven	*Corvus corax*
COYE	Common Yellowthroat	*Geothlypis trichas*
EUCD	Eurasian Collared-Dove	*Streptopelia decaocto*
EUST	European Starling	*Sturnus vulgaris*
GAQU	Gambel's Quail	*Callipepla gambelii*
GBHE	Great Blue Heron	*Ardea herodias*
GIWO	Gila Woodpecker	*Melanerpes uropygialis*
GREG	Great Egret	*Ardea alba*
GRHE	Green Heron	*Butorides virescens*
GRYE	Greater Yellowlegs	*Tringa melanoleuca*
GTGR	Great-tailed Grackle	*Quiscalus mexicanus*

GTTO	Green-tailed Towhee	*Pipilo chlorurus*
HOFI	House Finch	*Haemorhous mexicanus*
HOSP	House Sparrow	*Passer domesticus*
HOWR	House Wren	*Troglodytes aedon*
INDO	Inca Dove	*Columbina inca*
KILL	Killdeer	*Charadrius vociferus*
LBDO	Long-billed Dowitcher	*Limnodromus scolopaceus*
LBWO	Ladder-backed Woodpecker	*Dryobates scalaris*
LEGO	Lesser Goldfinch	*Spinus psaltria*
LESA	Least Sandpiper	*Calidris minutilla*
LISP	Lincoln's Sparrow	*Melospiza lincolnii*
LUWA	Lucy's Warbler	*Leiothlypis luciae*
MALL	Mallard	*Anas platyrhynchos*
MAWR	Marsh Wren	*Cistothorus palustris*
MGWA	MacGillivray's Warbler	*Geothlypis tolmiei*
MODO	Mourning Dove	*Zenaida macroura*
NECO	Neotropic Cormorant	*Phalacrocorax brasilianus*
NOCA	Northern Cardinal	*Cardinalis cardinalis*
NOFL	Northern Flicker	*Colaptes auratus*
NOMO	Northern Mockingbird	*Mimus polyglottos*
NRWS	Northern Rough-winged Swallow	*Stelgidopteryx serripennis*
OCWA	Orange-crowned Warbler	*Leiothlypis celata*
OSPR	Osprey	*Pandion haliaetus*
PBGR	Pied-billed Grebe	*Podilymbus podiceps*
PHAI	Phainopepla	*Phainopepla nitens*
PWWR	Pacific/Winter Wren	*Troglodytes pacificus/ Troglodytes hiemalis*
PYRR	Pyrrhuloxia	*Cardinalis sinuatus*
RCKI	Ruby-crowned Kinglet	*Regulus calendula*
ROPI	Rock Pigeon	*Columba livia*
RWBL	Red-winged Blackbird	*Agelaius phoeniceus*
SAPH	Say's Phoebe	*Sayornis saya*
SOSP	Song Sparrow	*Melospiza melodia*
SPSA	Spotted Sandpiper	*Actitis macularius*
TOWA	Townsend's Warbler	*Setophaga townsendi*
VERD	Verdin	*Auriparus flaviceps*
VIRA	Virginia Rail	*Rallus limicola*
WCSP	White-crowned Sparrow	*Zonotrichia leucophrys*
WEKI	Western Kingbird	*Tyrannus verticalis*
WEME	Western Meadowlark	*Sturnella neglecta*
WESA	Western Sandpiper	*Calidris mauri*

WETA	Western Tanager	*Piranga ludoviciana*
WISN	Wilson's Snipe	*Gallinago delicata*
WIWA	Wilson's Warbler	*Cardellina pusilla*
WWDO	White-winged Dove	*Zenaida asiatica*
YEWA	Yellow Warbler	*Setophaga petechia*
YRWA	Yellow-rumped Warbler	*Setophaga coronata*

APPENDIX C

CHAPTER 3: SUPPLEMENTAL MATERIAL

Figure 1 visualizes the output of the 30 meter land use/land cover classification output for 1985-2010 in five year time steps.

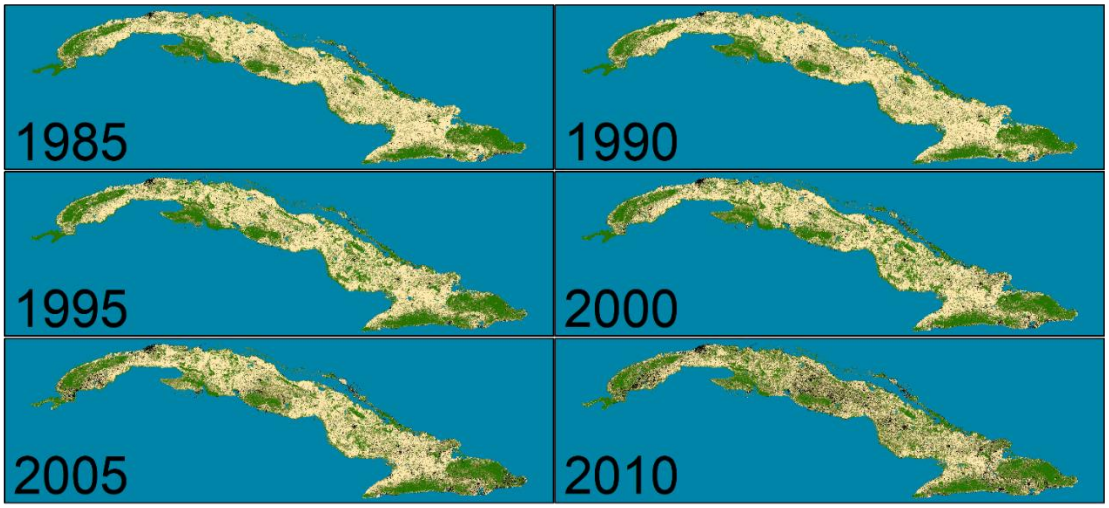

Figure 1. Land use/land cover classification for each year of analysis. Light tan is agricultural lands, olive green is barren/grass/shrublands, fir green is forest lands, black is built-up lands, and blue is water.

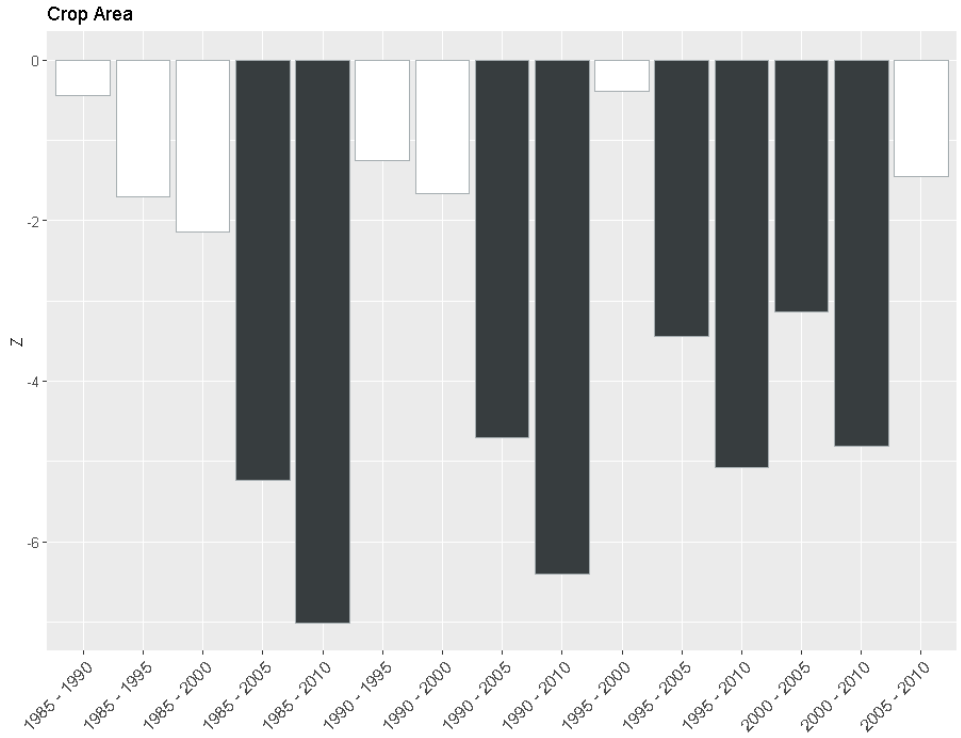

Figure 2. Crop area bar plot of the Dunn test Z value for the year comparison. Positive or negative Z values indicate the direction of the differences. Dark grey bars are statistically significant (p<0.05) and white bars are not.

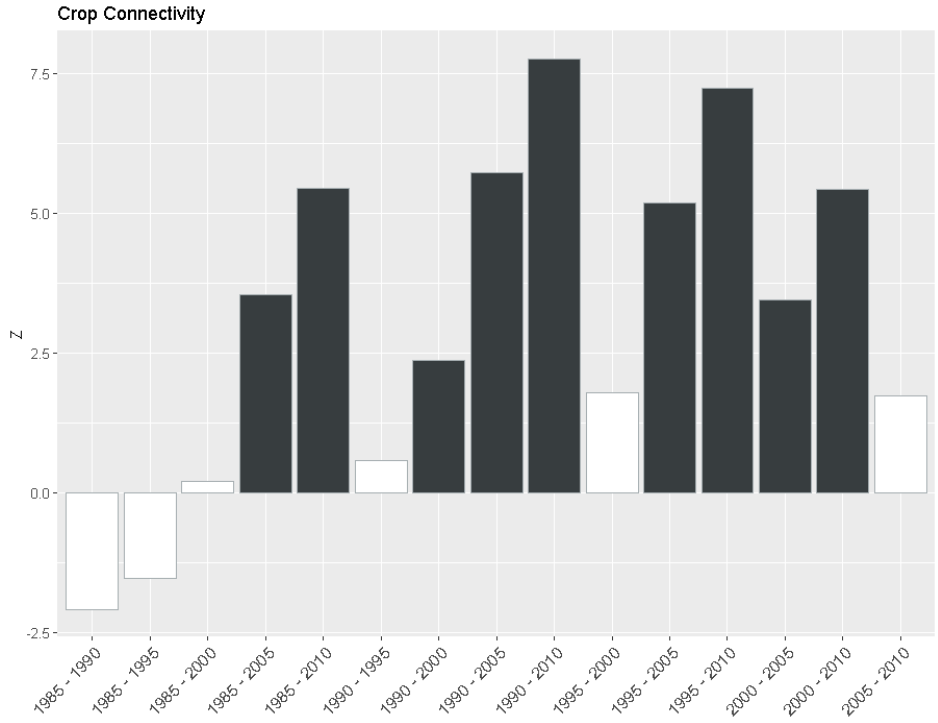

Figure 3. Crop connectivity bar plot of the Dunn test Z value for the year comparison. Positive or negative Z values indicate the direction of the differences. Dark grey bars are statistically significant (p<0.05) and white bars are not.

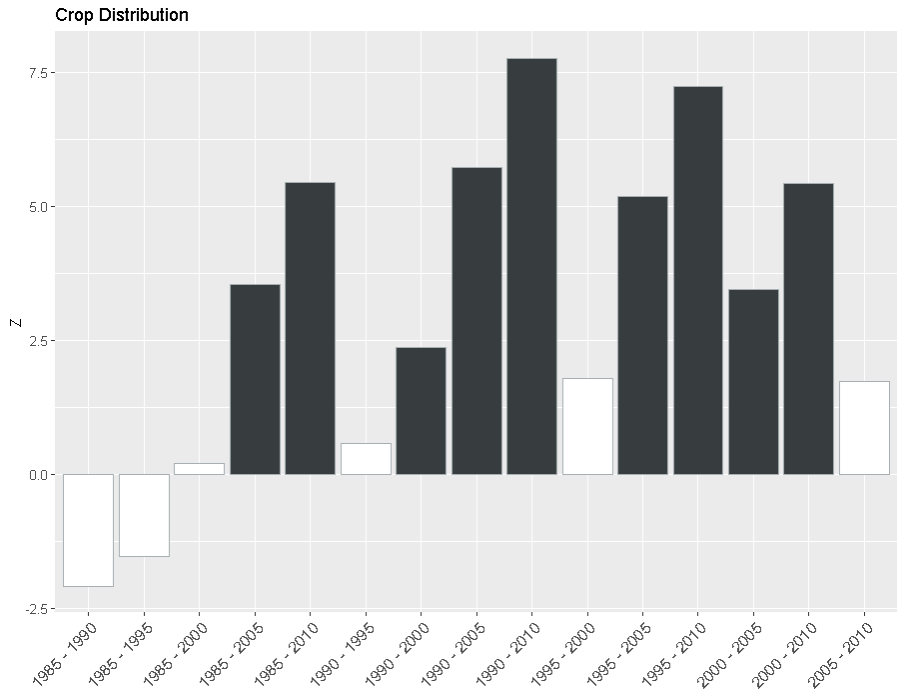

Figure 4. Crop patch distance (distribution) bar plot of the Dunn test Z value for the year comparison. Positive or negative Z values indicate the direction of the differences. Dark grey bars are statistically significant (p<0.05) and white bars are not.

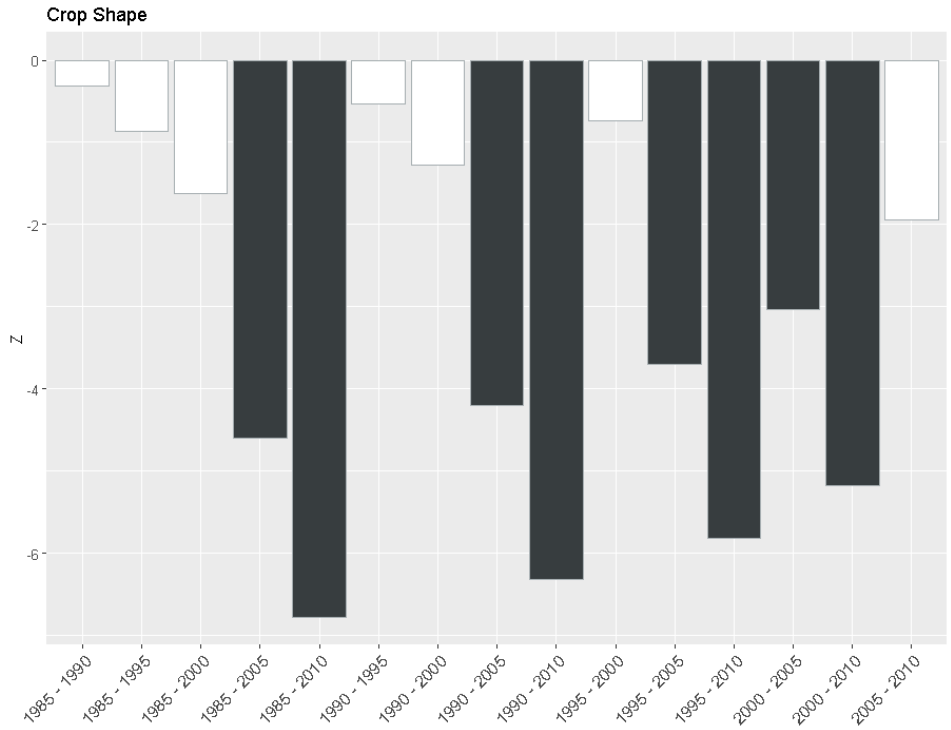

Figure 5. Crop shape bar plot of the Dunn test Z value for the year comparison. Positive or negative Z values indicate the direction of the differences. Dark grey bars are statistically significant (p<0.05) and white bars are not.

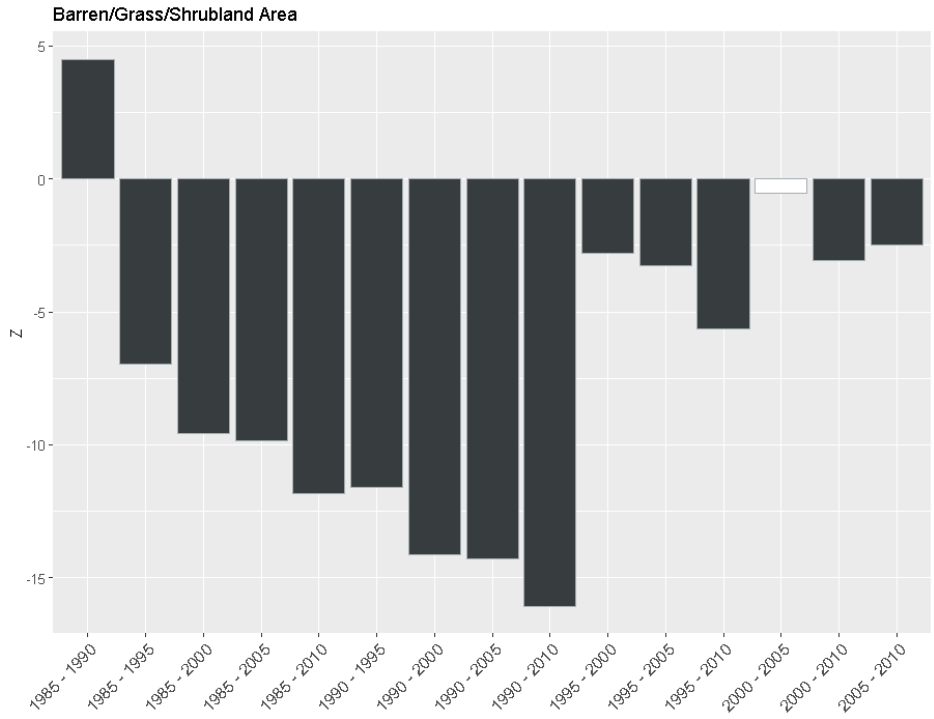

Figure 6. Barren/grass/shrubland area bar plot of the Dunn test Z value for the year comparison. Positive or negative Z values indicate the direction of the differences. Dark grey bars are statistically significant (p<0.05) and white bars are not.

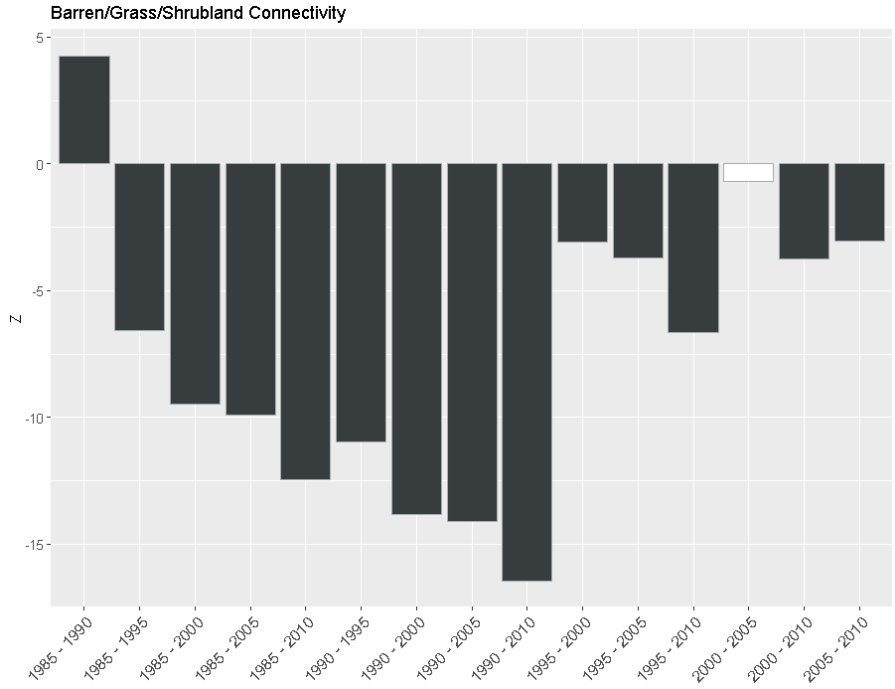

Figure 7. Barren/grass/shrubland connectivity bar plot of the Dunn test Z value for the year comparison. Positive or negative Z values indicate the direction of the differences. Dark grey bars are statistically significant (p<0.05) and white bars are not.

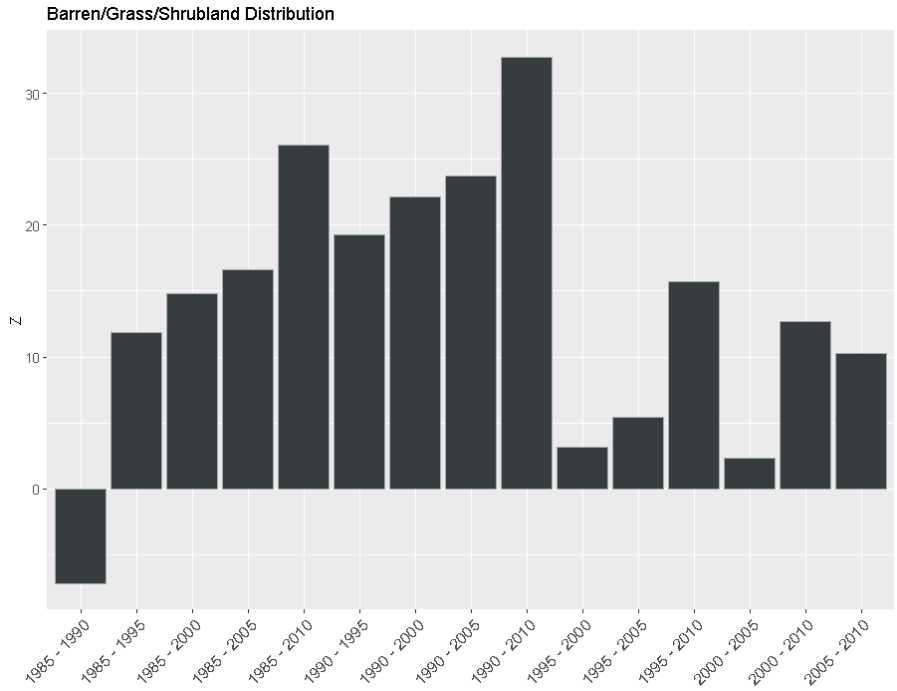

Figure 8. Barren/grass/shrubland patch distance (distribution) bar plot of the Dunn test Z value for the year comparison. Positive or negative Z values indicate the direction of the differences. Dark grey bars are statistically significant (p<0.05) and white bars are not.

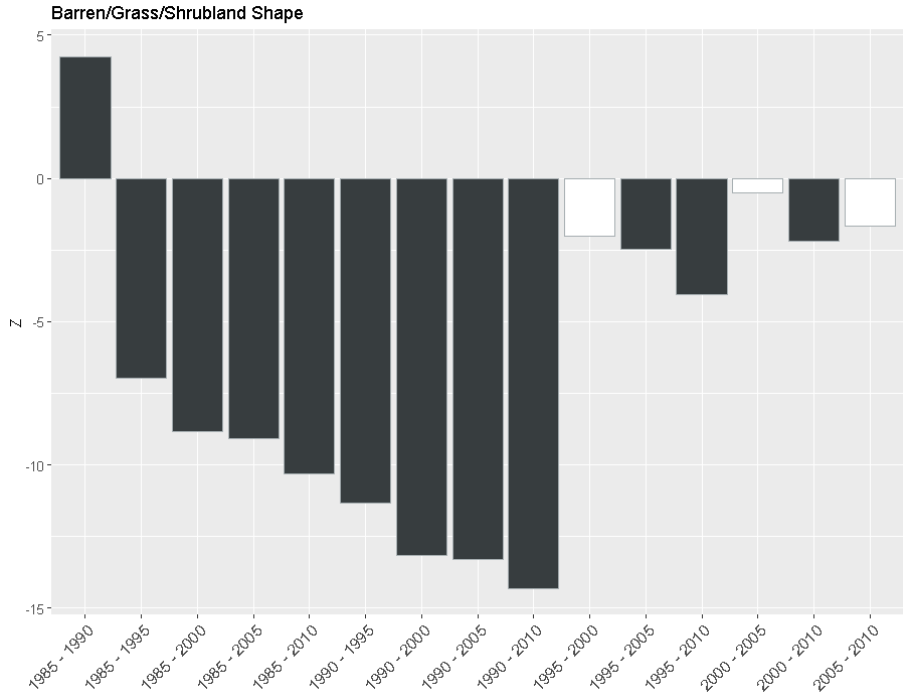

Figure 9. Barren/grass/shrubland shape bar plot of the Dunn test Z value for the year comparison. Positive or negative Z values indicate the direction of the differences. Dark grey bars are statistically significant (p<0.05) and white bars are not.

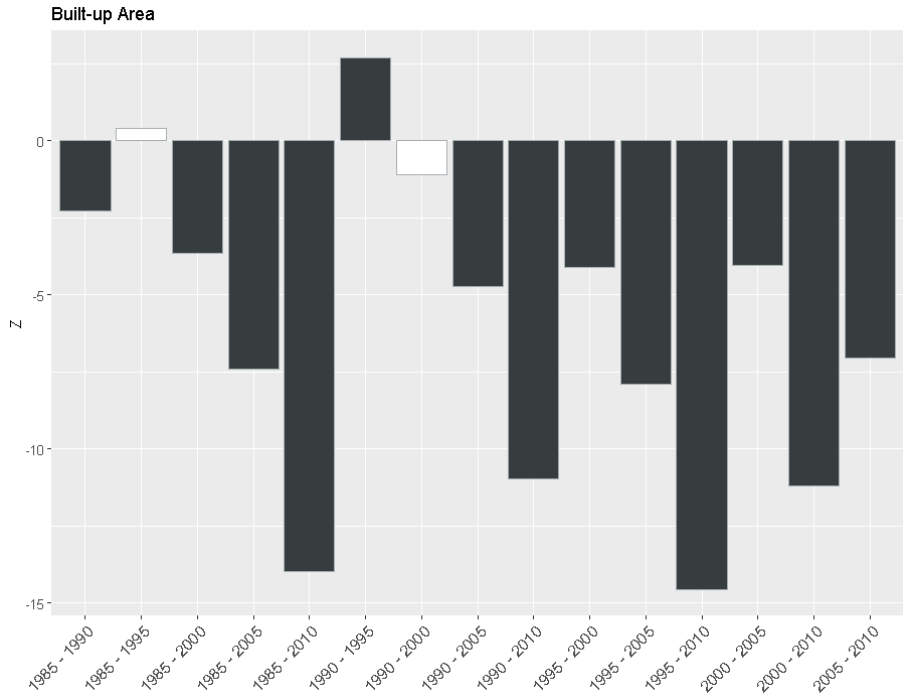

Figure 10. Built-up area bar plot of the Dunn test Z value for the year comparison. Positive or negative Z values indicate the direction of the differences. Dark grey bars are statistically significant (p<0.05) and white bars are not.

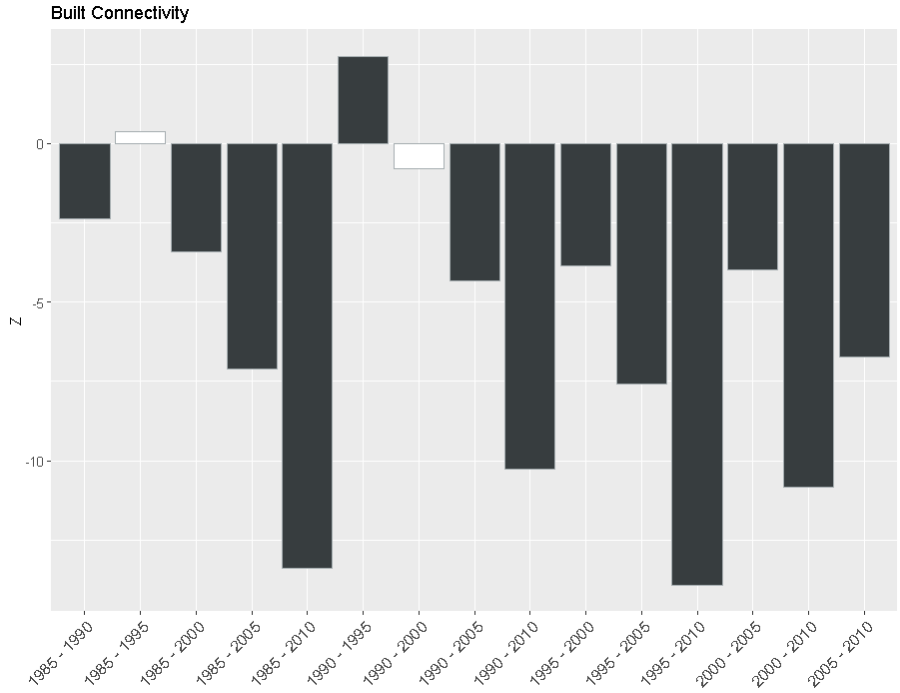

Figure 11. Built-up connectivity bar plot of the Dunn test Z value for the year comparison. Positive or negative Z values indicate the direction of the differences. Dark grey bars are statistically significant (p<0.05) and white bars are not.

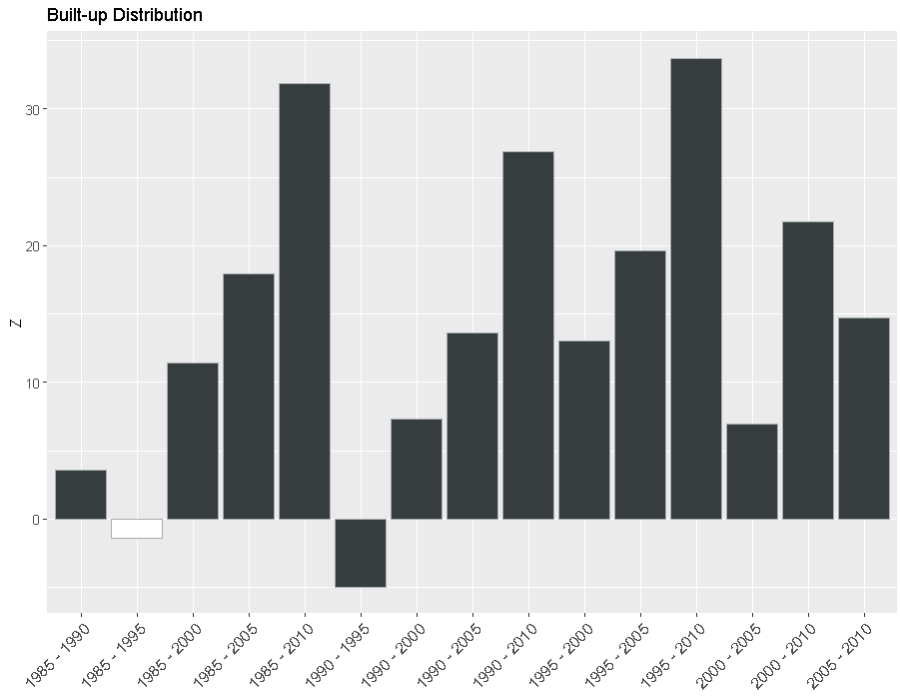

Figure 12. Built-up patch distance (distribution) bar plot of the Dunn test Z value for the year comparison. Positive or negative Z values indicate the direction of the differences. Dark grey bars are statistically significant (p<0.05) and white bars are not.

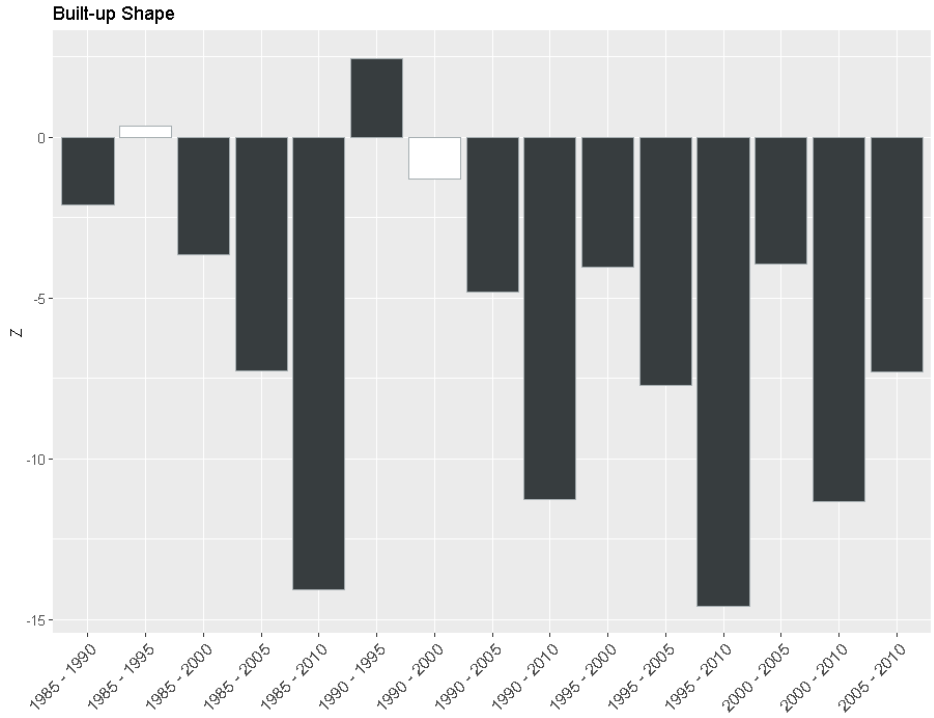

Figure 13. Built-up shape bar plot of the Dunn test Z value for the year comparison. Positive or negative Z values indicate the direction of the differences. Dark grey bars are statistically significant (p<0.05) and white bars are not.

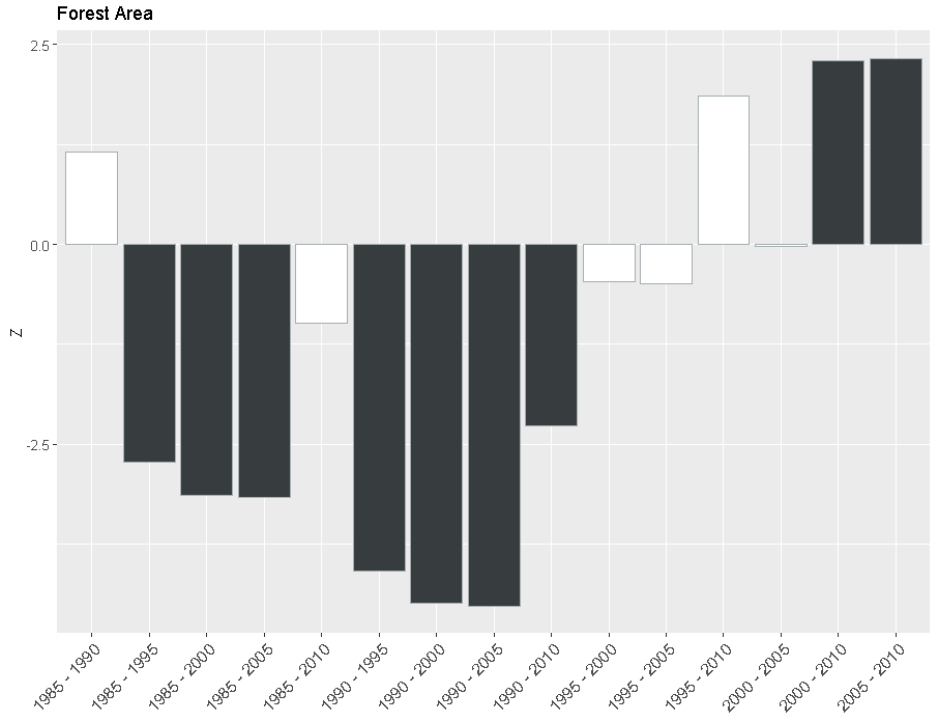

Figure 14. Forest area bar plot of the Dunn test Z value for the year comparison. Positive or negative Z values indicate the direction of the differences. Dark grey bars are statistically significant (p<0.05) and white bars are not.

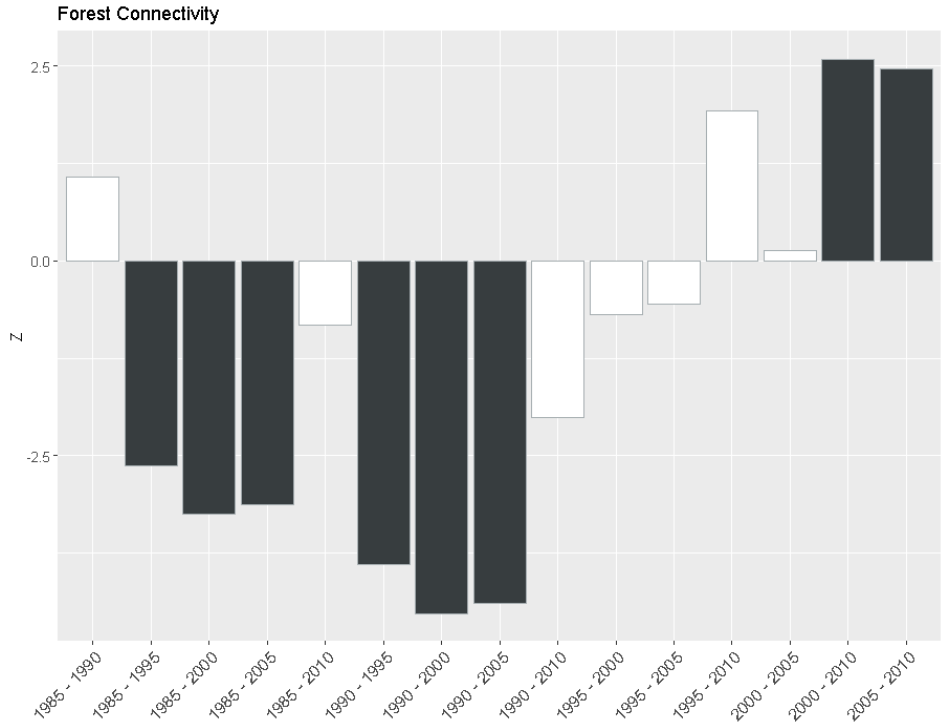

Figure 15. Forest connectivity bar plot of the Dunn test Z value for the year comparison. Positive or negative Z values indicate the direction of the differences. Dark grey bars are statistically significant (p<0.05) and white bars are not.

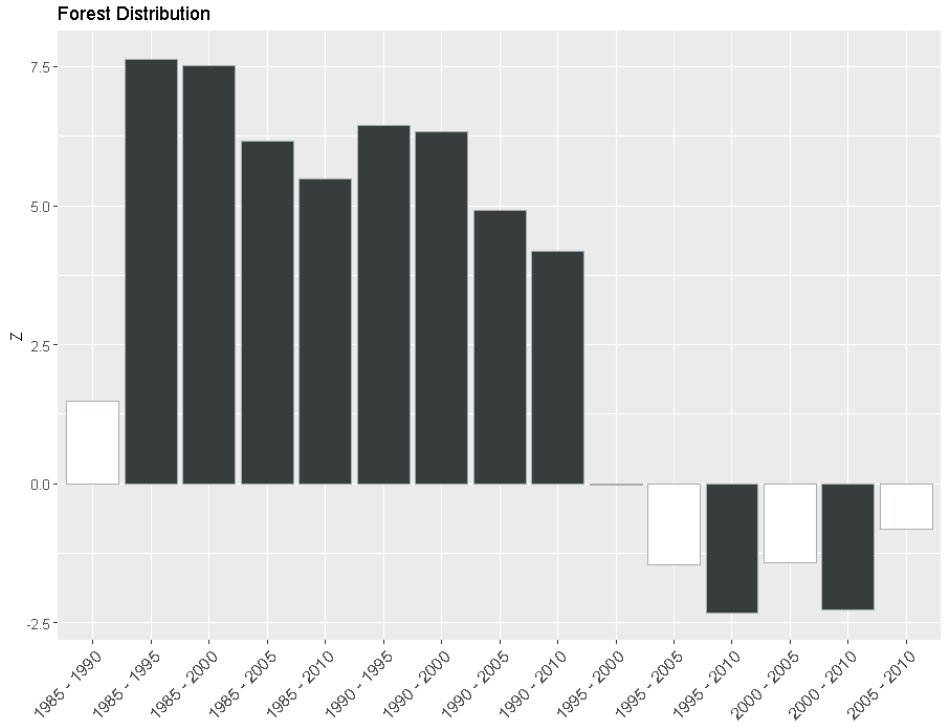

Figure 16. Forest patch distance (distribution) bar plot of the Dunn test Z value for the year comparison. Positive or negative Z values indicate the direction of the differences. Dark grey bars are statistically significant (p<0.05) and white bars are not.

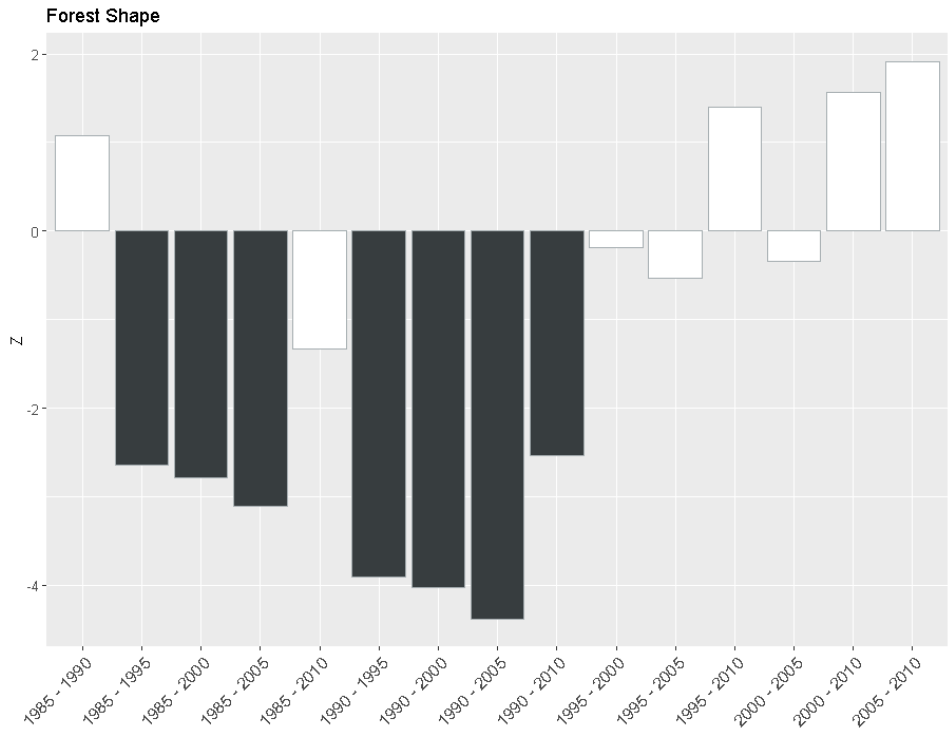

Figure 17. Forest shape bar plot of the Dunn test Z value for the year comparison. Positive or negative Z values indicate the direction of the differences. Dark grey bars are statistically significant (p<0.05) and white bars are not.

APPENDIX D

CHAPTER 4: SUPPLEMENTAL MATERIAL

D.1 Methodology

D.1.1 Threshold Setting

Table 1 presents the balanced accuracies of 2013 classifications done to determine if the method from Goldblatt et al. (2018) could be extended to different sensors.

Table 1. Balanced accuracy of 2013 classifications in India and the United States. 2013 was used to test compatibility because Landsat 5, Landsat 7, DMPS-OLS, and VIIRS were all active that year.

India		United States	
Landsat 7 & DMSP-OLS	Landsat 8 & VIIRS	Landsat 7 & DMSP-OLS	Landsat 8 & VIIRS
76.5%	80.5%	81.9%	81.5%

A variety of thresholds were used to determine where to scatter training points for the classification. Table 2 presents the NDVI, NDWI, and nighttime light threshold for each country and satellite.

Table 2. NDVI, NDWI, and nighttime light thresholds used in the United States, India and China for Landsat 5, Landsat 7, Landsat 8, DMSP-OLS, and VIIRS

		United States	India	China
Landsat 5	NDVI	90th percentile	90th percentile	75th percentile
	NDWI	-0.01	-0.01	0.15
Landsat 7	NDVI	90th percentile	90th percentile	75th percentile
	NDWI	-0.01	-0.01	0.15
Landsat 8	NDVI	90th percentile	90th percentile	75th percentile
	NDWI	-0.01	-0.01	0.15
DMSP-OLS	Highly lit	90th percentile	95th percentile	95th percentile
	Low lit	75th percentile	75th percentile	25th percentile
VIIRS	Highly lit	90th percentile	90th percentile	95th percentile
	Low lit	60th percentile	55th percentile	25th percentile

NDWI does not use a percentile threshold because of minimal regional variation compared to NDVI or nighttime lights. A higher NDWI threshold was used in China because the dense urbanization cast shadows, which required a stricter threshold so that only water would be masked (Xu 2006). Nighttime light thresholds for Landsat 7 and DMSP-OLS were from Goldblatt et al. (2018). Due to the change in sensors in 2015, new thresholds were determined for Landsat 8 and VIIRS using the same methods.

D.1.2 Biome Grouping

Table 3 displays each city in the analysis according to country and biome group. Biome groupings come from Dinerstein et al. (2017) with some biomes combined to increase the number of cities in a given biome grouping. Groupings made up of multiple biomes are noted in parenthesis in the rightmost column.

Table 3**.** List of the 50 cities for each country and the biome they reside in. Rows that are greyed-out are the biomes that are not included in the final analysis.

	India	China	United States
Desert and xeric shrublands	Chandigarh, Guntur, Gurgaon, Ludhiana, Nashik, Tiruchirappalli		El Paso, Las Vegas, Phoenix, Salt Lake City
Wetlands (combination of flooded grasslands & savannas and mangroves)	Surat		Miami
Mediterranean forests, woodlands, and scrub			Los Angeles, San Diego, San Francisco
Montane grasslands and shrublands		Lanzhou	
Temperate forests (combination of temperate conifer forests and temperate broadleaf and mixed forests)		Anshan, Baoding, Beijing, Changchun, Changsha, Chengdu, Chongqing, Dalian, Handan, Hangzhou, Harbin, Hefei, Huaian, Jilin, Jining, Linyi, Luoyang, Nanchang, Nanjing, Nantong, Pingdingshan, Qingdao, Shanghai, Shenyang, Shijiazhuang, Tangshan, Tianjin, Weifang, Wuhan, Xi'an, Xinxiang, Xuzhou, Yantai, Yinchuan, Zhengzhou	Atlanta, Boston, Bridgeport, Buffalo, Charlotte, Cincinnati, Cleveland, Columbus, Detroit, Indianapolis, Louisville, Minneapolis, Nashville, New Orleans, New York, Philadelphia, Pittsburgh, Providence, Raleigh, Seattle, Springfield, Washington DC
Temperate grasslands,		Baotou, Datong, Hohhot	Austin, Chicago, Dallas, Denver, Fort Myers,

savannas and shrublands			Jacksonville, Kansas City, Memphis, Milwaukee, Oklahoma City, Orlando, Portland, Richmond, Sacramento, Saint Louis, San Antonio, Tampa, Virginia Beach
Tropical and subtropical dry broadleaf forests	Ahmadabad, Asansol, Bangalore, Bhopal, Chennai, Dhanbad, Durgapur, Hyderabad, Indore, Jaipur, Jamshedpur, Karagpur, Mysuru, Nagpur, Pune, Ramgarh, Ranchi, Salem, Tiruppur, Vadodara, Vijayawada, Warangal		
Tropical and subtropical grasslands, savannas, and shrublands			Houston, McAllen
Tropical and subtropical moist broadleaf forests	Agartala, Agra, Bhilai, Bhubaneswar, Coimbatore, Delhi, Guwahati, Imphal, Kanpur, Karunagappalli, Kochi, Kolkata, Lucknow, Meerut, Mumbai, Patna, Prayagraj, Rourkela, Thiruvananthapuram, Varanasi, Visakhapatnam	Fuzhou, Guangzhou, Guiyang, Haikou, Jieyang, Kunming, Liuzhou, Nanning, Quanzhou, Taizhou, Wenzhou	

D.2 Results

D.2.1 Accuracy Assessment Comparison

We compared the accuracy of our classification (30m) to similar classifications available for all three countries (Table 4). GlobCover has a 300m resolution and is only available

for 2009. MODIS MCD 12Q2.006 has a 500m resolution and is available from 2001-2015.

Table 4. Balanced accuracies for GlobCover: Global Land Cover Map in 2009 and MODIS MCD12Q2.006 Land Cover Dynamics Yearly Global 500m, Annual International Geosphere-Biosphere Programme (IGBP) classification for 2001, 2005, 2010, and 2015.

Classification / Year	Validation Year	China	India	United States
GlobCover / 2009	2010	76.93%	67.3%	59.3%
MCD12Q2.006 / 2001	2000	88.8%	77.4%	78.2%
MCD12Q2.006 / 2005	2005	89.9%	77.8%	78.7%
MCD12Q2.006 / 2010	2010	90.5%	78.3%	79.0%
MCD12Q2.006 / 2015	2015	91.6%	78.4%	79.1%

D.2.2 Effect of Biome

To test if the climatological conditions of each city affected the strength and direction of the SUHI relationships, the correlations were separated by the biome associated with the climatic type (Fig. 1). Five biomes are home to 142 of the 150 cities in our analysis: 32 in the tropical and subtropical moist broadleaf forest biome; 22 in the tropical and subtropical dry broadleaf forest biome; 57 in the temperate forest biome (which is a combination of the broadleaf, mixed and conifer temperate forest biome); and 21 in the temperate grasslands, savannas, and shrublands biome. The remaining 8 cities reside in biomes for which there are too few cities to conduct a statistically viable analysis.

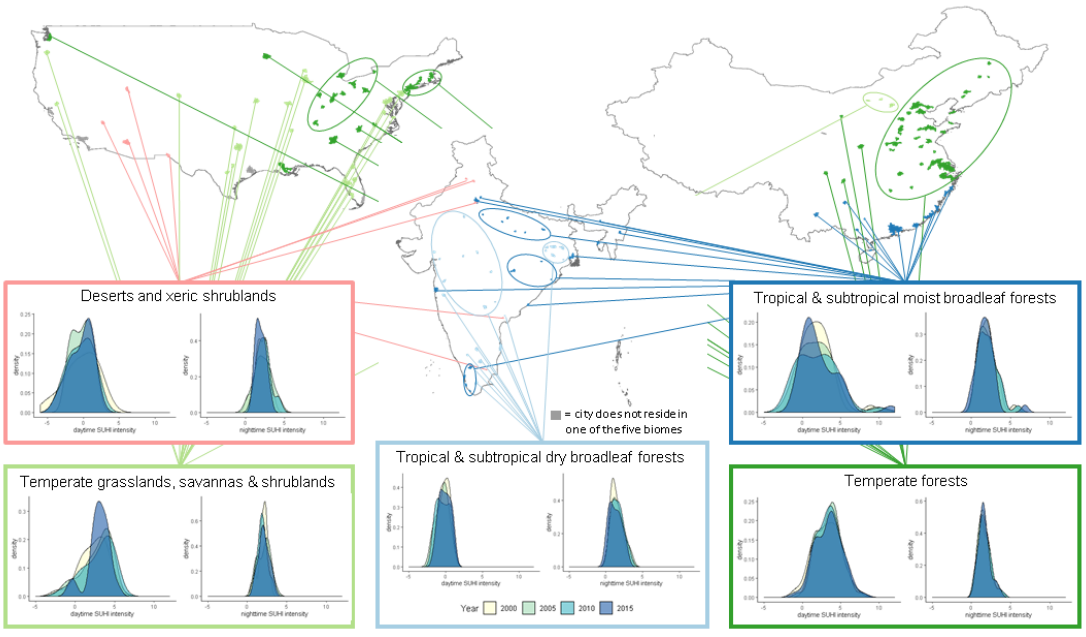

Figure 1. Distribution of yearly daytime and nighttime surface urban heat island intensity by biome. The color of city footprints corresponds to the biome they reside in. 8 cities are grey because they reside in biomes (a. tropical and subtropical grasslands, savannas, and shrublands; b. flooded grasslands and savannas; c. mangrove; d. montane grasslands

and shrublands; and e. Mediterranean forests, woodlands, and scrub) that were excluded because of limited numbers of cities in these biomes.

Cities in tropical and subtropical moist broadleaf forests experienced the whole range of daytime SUHI intensity (-5°C to 10°C) (Fig. 1) Temperate forests had the highest mean daytime SUHI intensity (~3.4°C) and deserts have the lowest (~-0.3°C) with tropical and subtropical dry broadleaf forests close behind (~-0.28°C) (Table 5). Deserts had the highest mean nighttime SUHI intensity (~2.1°C), and tropical and subtropical dry broadleaf forests had the lowest (~ 1.5°C). Along with a narrower range of values, nighttime SUHI effect also had less variation over time.

Temporally, 2000 had a wider spread of values and 2015 was more concentrated, but several biomes (day and night in tropical and subtropical dry broadleaf forests, and night in temperate grasslands, savannas and shrublands) were an exception to this. Cities residing in temperate grasslands, savannas, and shrublands-deserts had the greatest variation over time. Tropical and subtropical dry broadleaf forests and temperate forests had the least variation.

Despite the variation in SUHI intensity across biomes, we see similar relationships with urban form change over time (Fig. 2). For the relationships that are statistically significant across multiple biomes, it was more common for the strength of the relationships to change, not the direction.

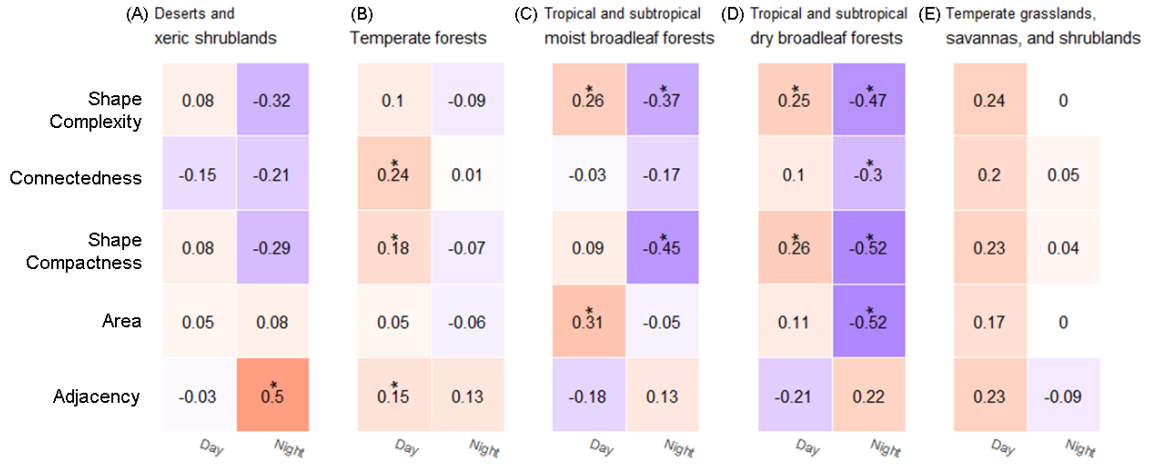

Figure 2. Correlation matrix for the repeated measures correlation results for the five biomes that house the majority of the 150 cities. Color indicates direction and strength of the relationship while asterisks indicate p-values of < 0.05.

Shape complexity and shape compactness have the greatest number of statistically significant relationships with daytime and nighttime SUHI effect across the five biomes (Fig. 2). The moist/dry tropical and subtropical broadleaf forests had the greatest number of statistically significant relationships between urban form and the daytime/nighttime SUHI effect. Collectively, these two biomes contain 54 of the most populous cities in the three countries. Figure 3 shows the raw data (points) and the repeated measures regression slope (dotted lines) between form and daytime/nighttime SUHI in the tropical and subtropical dry broadleaf forest biome. In the tropical and subtropical dry broadleaf forests, the intensity of the daytime and nighttime SUHI effect

exhibited opposite relationships with urban form (Fig 3). For example, increasing shape complexity led to greater daytime SUHI intensity but lower nighttime SUHI intensity (Fig. 3A).

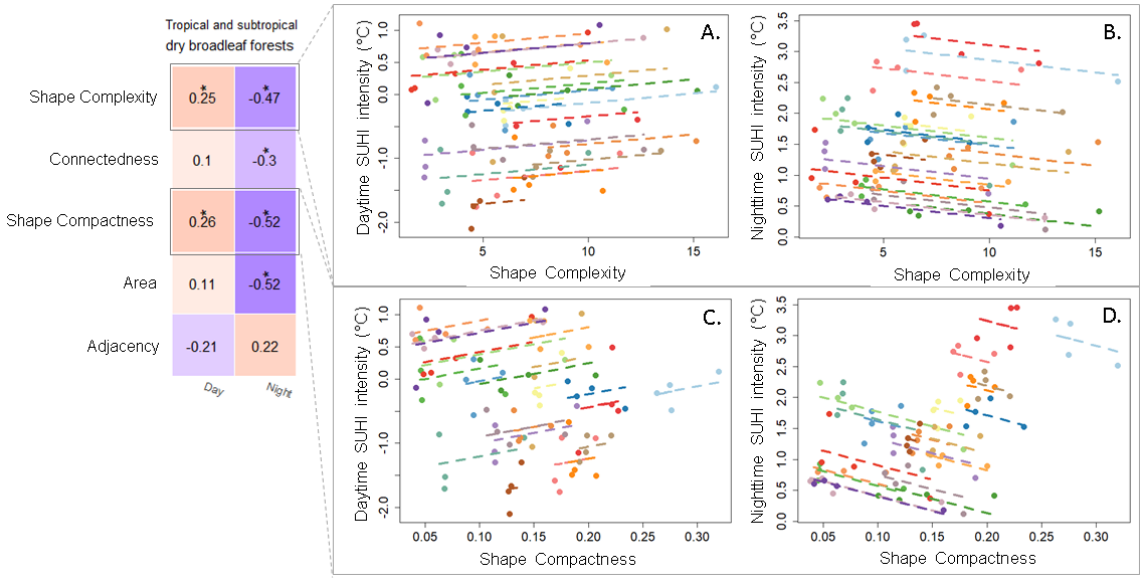

Figure 3. Repeated measures correlation between shape complexity, shape compactness, daytime and nighttime surface urban heat island intensity in the tropical and subtropical dry broadleaf forest biome. Each color corresponds to a different city with the points marking the relationship over time between a given pattern metric and the daytime surface urban heat island intensity. The dashed lines are the common regression slopes for each city in the tropical and subtropical dry broadleaf forest biome over time.

The moist and dry tropical and subtropical broadleaf forest biomes were the biomes with the greatest number of statistically significant relationships between urban form and SUHI intensity (Fig. 2). These two biomes are home to 86% of the cities we examine in India, 22% of Chinese cities, but no US cities (Table 3). The high proportion of large Indian cities residing in these two biomes suggests that purposeful urban form modification in India could make the largest impact on SUHI reduction. Much of the work on urban form and urban heat island has been concentrated in the US and China (Debbage and Shepherd 2015; Fan, Myint, and Zheng 2015; Li et al. 2011; Li et al. 2016; Meng et al. 2016), and India has the least amount of research on the topic (Shastri et al. 2017).163

D.2.3 Repeated Measures Correlation vs. Linear Trends for Individual Cities

To test how representative the relationships found by the repeated measures correlation were, we also calculated the slope over time for the relationship between the landscape metrics and daytime and nighttime SUHI for the full set of 150 cities. Figure 4 is the same daytime and nighttime repeated measures figure as Ch. 4, Fig. 6, but with the addition of the individual slopes of cities as dotted lines.

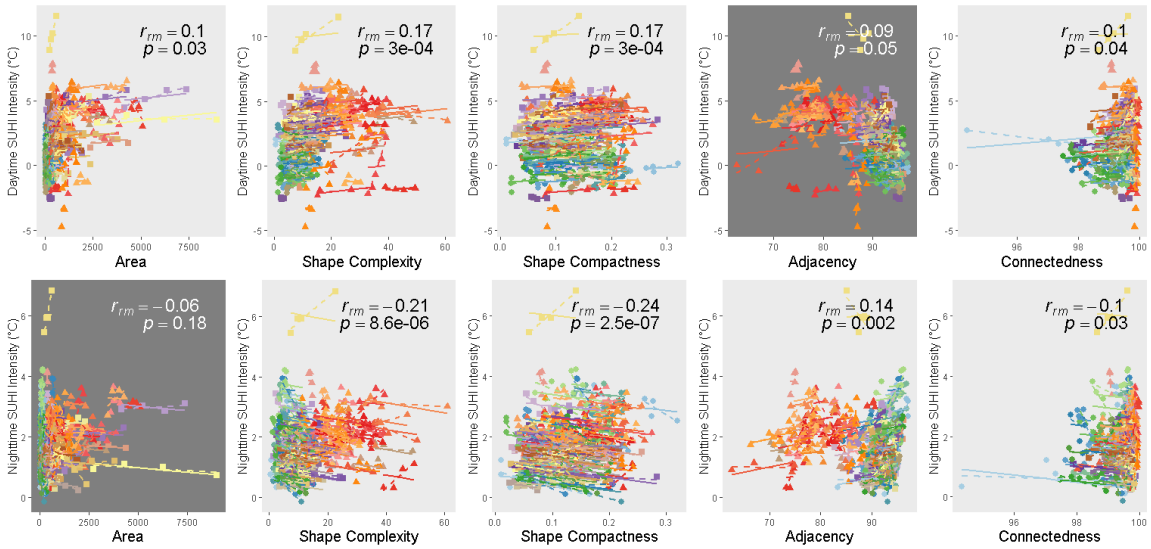

Figure 4. Repeated measures correlation for the 150 cities between area, shape complexity, shape compactness, adjacency, connectedness, daytime (top row), and nighttime (bottom row) surface urban heat island intensity. Each color corresponds to a different city with the points marking the yearly relationship (one point is one year) between a given pattern metric and surface urban heat island intensity. Circular points correspond to Indian cities, triangular points correspond to US cities, and square points correspond to Chinese cities. Solid lines are the common regression slopes for each of the 150 cities over time, while dotted lines are the individual city linear trends. Light grey plots are statistically significant (p<0.05) and dark grey plots are not.

The vast majority of the individual city slopes were not statistically significant, especially those very close to zero. These slopes lie largely in the center of Fig. 6 and are not visible. To show the distribution, Fig. 5 and 6 are histograms of the slopes for the 150 cities for daytime and nighttime, respectively.

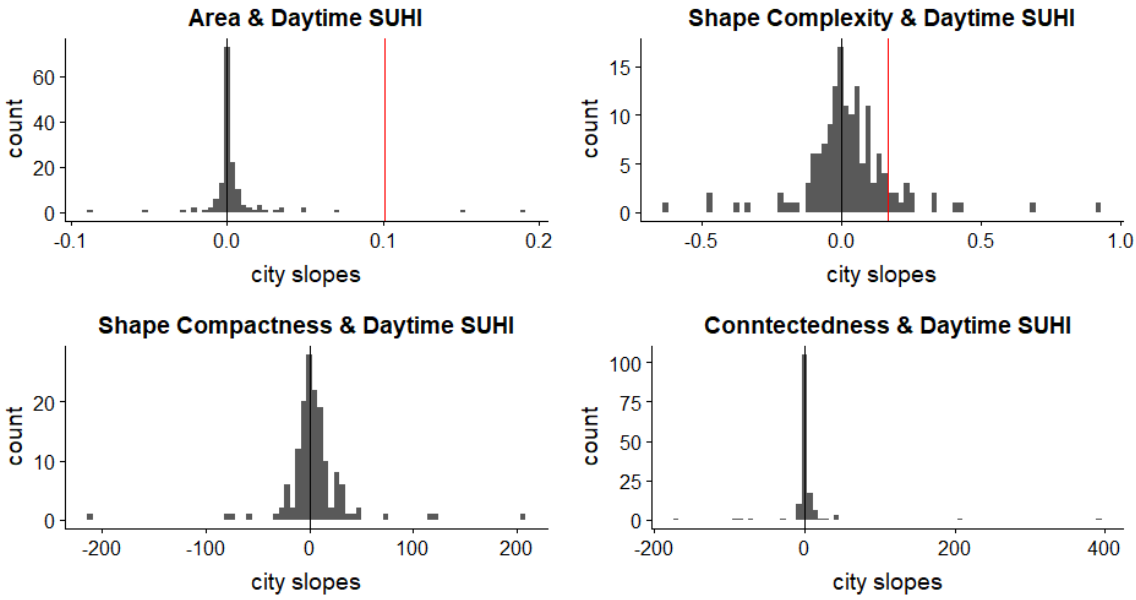

Figure 5. Histograms of individual city slopes for the relationships between landscape metrics (the four that were statistically significant according to the repeated measures correlation) and daytime SUHI intensity. Black line is drawn at zero and the red line is drawn at the slope found by the repeated measures correlation. The red line is not visible on plots where the repeated measures correlation slope is also very close to zero.

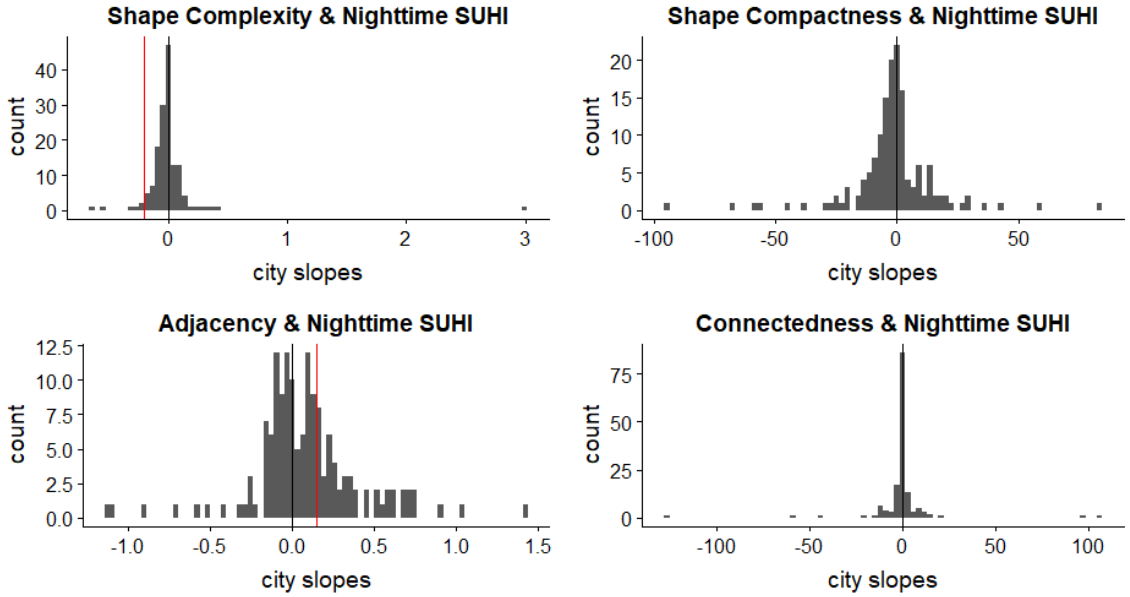

Figure 6. Histograms of individual city slopes for the relationships between landscape metrics (the four that were statistically significant according to the repeated measures correlation) and nighttime SUHI intensity. Black line is drawn at zero and the red line is drawn at the slope found by the repeated measures correlation. The red line is not visible on plots where the repeated measures correlation slope is also very close to zero.

These slopes were used to determine how many cities had opposite relationships between the landscape metrics and SUHI from the relationship determined by the repeated measures correlation. Approximately 40-45% of cities had opposite relationships individually compared to the relationships determined by the whole. Many of these cities, however, had slopes very close to zero (Fig. 5 & 6) and therefore did not exert as much of an influence on the final repeated measures correlation values as did the cities with larger slopes. When the zero and nearly zero slopes were removed (those in the center bin of each histogram), the proportion of cities with opposite relationships dropped to 10-40% depending on the metric. Table 5 presents these values for each metric and SUHI intensity relationship that was statistically significant in the repeated measures correlation.

Table 5. Total number of cities and relative proportion of cities that had opposite slopes from the repeated measures correlation. City totals are presented as well the number of cities once the histogram bin centering around zero is removed from the total count. Greyed out rows are for those that were not statistically significant in the repeated measures correlation.

	Daytime				Nighttime			
	Total		Removed 0		Total		Removed 0	
	#	%	#	%	#	%	#	%
Area	65	43%	28	19%				
Shape Complexity	63	42%	54	36%	63	42%	38	25%
Shape Compactness	63	42%	47	31%	64	43%	51	34%
Adjacency					62	41%	59	39%
Connectedness	62	41%	16	11%	68	45%	29	19%